METATHESIS AND ISOMERIZATION ACTIVITY OF RUTHENIUM CARBENE CATALYSTS IN ACYCLIC DIENE METATHESIS POLYMERIZATION

By

FLORENCE C. COURCHAY

A DISSERTATION PRESENTED TO THE GRADUATE SCHOOL
OF THE UNIVERSITY OF FLORIDA IN PARTIAL FULFILLMENT
OF THE REQUIREMENTS FOR THE DEGREE OF
DOCTOR OF PHILOSOPHY

UNIVERSITY OF FLORIDA

2005

To my parents Elizabeth and Bernard, and grandparents Suzanne, Luce, Aimé, and Yvon

ACKNOWLEDGMENTS

First and foremost, I would like to thank my parents Elizabeth and Bernard, and grandparents, Suzanne, Luce and Yvon. I would have never come this far without them. Their unconditional love and support have meant the world to me. They helped me become the person I am today; there are no words to describe the respect, the love and the gratitude I feel.

These past 4 plus years in graduate school were one of the most rewarding, life-changing experiences I have ever been through, and none of it would have been possible without the help and guidance of my advisor Professor Ken Wagener. Arriving in a foreign country is a scary thing to take on, so I am most thankful for his support and understanding, his words of wisdom, his genuine concern, and his exciting take on science. I would also like to thank all the members of my supervisory committee (Dr. John Reynolds, Dr. Mike Scott, Dr. Dan Talham, and Dr. Tony Brennan), for the time they invested in reading and discussing this document. My work here would not have been completed without the precious help of Dr. Ion Ghiviriga who spent many hours assisting me with NMR spectroscopy. I also wish to thank Dr. Khalil Abboud for his kind help with X-ray crystallography, and Dr. James Boncella for helpful discussions.

At the University of Florida, I thank all my coworkers on the polymer floor; particularly all the Wagener's group members past and present. Among them I would like to thank Dr. Ed Lehman for his expertise in catalysis, and James Leonard for his help with X-ray crystallography and his constant enthusiasm in the lab. Special thanks go to

John Sworen, my mentor and my friend, who helped me get started in the lab and much further. I have learned from a true master, I will be forever indebted to him. I would also like to thank my friends and classmates Travis Baughman and Piotr Matloka, for all the poking, the laughs, and all our discussions, chemistry-related or not. I will never forget our Eurotrip! This experience would not have been the same without Emilie Galand, Sophie Bernard, Merve Ertas, Kornelia Matloka, and Victoria Broadstreet. Their friendship helped me through my ups and downs and I will miss them immensely, along with the shopping extravaganzas, the late-night talks, and the party-dancing. Pauline Anselme, my roommate during my first year here, was also a wonderful support as I was settling into my new life as a graduate student. I also wish to thank Armando Coronado, my undergraduate student, for his tremendous help with all the boring stuff I delegated to him. Finally, I would not have succeeded without the support of Josh McClellan, who has been there for me in the worst and the best of times.

TABLE OF CONTENTS

page

LIST OF TABLES

LIST OF FIGURES

Abstract of Dissertation Presented to the Graduate School
of the University of Florida in Partial Fulfillment of the
Requirements for the Degree of Doctor of Philosophy

METATHESIS AND ISOMERIZATION ACTIVITY
OF RUTHENIUM CARBENE CATALYSTS
FOR ACYCLIC DIENE METATHESIS POLYMERIZATION

By

Florence C. Courchay

December 2005

Chair: Kenneth Wagener
Major Department: Chemistry

Acyclic diene metathesis (ADMET) polymerization being a step condensation, the catalyst requires long lifetimes and a robustness that allows its reactivity at high temperatures. Accordingly, several novel ruthenium metathesis catalysts were investigated through a kinetic study conducted under ADMET polymerization conditions. Their kinetic behavior was compared to the classical 1st and 2nd generation Grubbs' complexes (**[Ru]1** and **[Ru]4**, respectively) at various temperatures. Among the catalysts tested, Hoveyda-type systems were sterically and electronically modified. The complexes containing bulkier N-heterocyclic carbene (NHC) ligands consistently result in faster initial ADMET rates than any other existing phosphine or Hoveyda complexes. Electronic modifications are mostly dominated by the steric effect of the NHC ligand, especially at low temperatures. Although these complexes show promising longevity and stability in small molecule chemistry, they do not produce higher molecular weight polymer than catalyst **[Ru]4**.

Soon after, olefin isomerization emerged as an undesirable side reaction induced by NHC-containing catalysts during metathesis processes. With fast initiators, isomerization occurs after the metathesis reaction, while it becomes competitive with slower initiators. After several attempts to reduce isomerization by designing new catalytic systems featuring different phosphine, carbene, or NHC ligands, a comprehensive mechanistic study was undertaken. From a deuterium labeling experiment monitored by NMR spectroscopy, olefin isomerization promoted by catalyst **[Ru]4** under metathesis conditions was determined to operate via a metal-hydride addition-elimination pathway. Further deuteration of the catalyst itself, by synthesis of analogue **[Ru]23**, revealed the existence of an exchange process between the NHC ligand and the substrate, suggesting the presence of a ruthenium dihydride. However, the active species could not be identified spectroscopically.

Finally, **[Ru]1**, **[Ru]4** and Schrock's molybdenum catalyst **[Mo]1** were individually examined during the metathesis of olefins containing allylic methyls. Conversions in cross-metathesis were limited to 50% with all catalysts, while ADMET only produced the dimer of the corresponding diene. These results are directly correlated to the orientation of the substrate's bulk during the metallacyclobutane formation, the alkyl branch being adjacent to the metal center in the case of the molybdenum catalyst **[Mo]1**, and opposite to it in the case of ruthenium catalyst **[Ru]1** and **[Ru]4**.

CHAPTER 1
INTRODUCTION

Introduction to Metathesis

Olefin metathesis has become a powerful tool for the formation of carbon-carbon bonds.[1,2] Discovered inadvertently in the mid-1950s,[3,4] it was not until 1967 that Calderon[5,6] recognized the term "olefin metathesis", which is understood as the metal-catalyzed redistribution of carbon-carbon double bonds. In 2005, the metathesis reaction was distinguished by the Nobel prize in chemistry, awarded to Prof. Yves Chauvin who unveiled the mechanism, and Prof. Richard Schrock and Prof. Bob Grubbs who developed the catalysts that expanded the versatility of the reaction. This transformation enjoys a variety of applications (Figure 1-1). Ring-closing metathesis (RCM) is the intramolecular reaction of an acyclic diene into an unsaturated ring. This reaction has particularly been taken advantage of in the pharmaceutical industry, where the synthesis of complex cyclic systems used to require several, often tedious steps.[7-11] The cross-metathesis (CM) reaction involves the scrambling of substituent groups between two olefins to form two new products.[12-15] The extensive use of cross-metathesis in organic synthesis has also been applied to green chemistry to convert oleochemical feedstocks into valuable chemical products. Ring-opening metathesis is the opening of an unsaturated cycle by cross-coupling with a mono-olefin, to form a substituted acyclic diene.[16-18] Metathesis has also been actively used in the production of polymer molecules, either through ring-opening metathesis polymerization (ROMP)[19,20] or acyclic diene metathesis (ADMET) polymerization.[21,22] While ROMP is a chain-addition type of

polymerization driven by the release of ring-strain in the cyclic monomer, ADMET is a step-condensation whose equilibrium is driven by the release of a small molecule, ethylene.

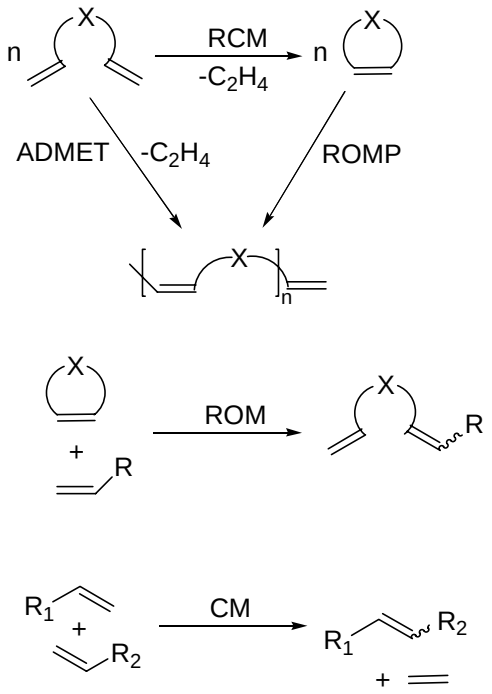

Figure 1-1. Olefin metathesis

Early Catalyst Developments

For a long time, the scope of the reaction was limited by its insufficient catalyst performance, using multicomponent homogeneous and heterogeneous systems such as WCl_6/Bu_4Sn, $WOCl_4/EtAlCl_2$, MoO_3/SiO_2, and Re_2O7/Al_2O_3. It was not until Hérisson and Chauvin[23] proposed that the mechanism involved the interconversion of an olefin and a metal alkylidene through a metallacyclobutane intermediate that well-defined catalysts were developed, considerably expanding the range of metathesis applications (Figure 1-2). His work in metathesis was awarded the Nobel Prize of Chemistry in 2005.

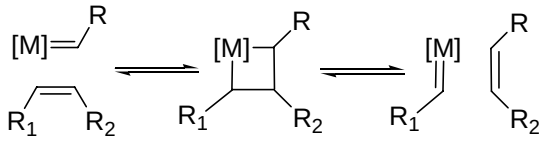

Figure 1-2. Mechanism of olefin metathesis

The first tantalum[24,25] and tungsten alkylidenes[26] led to the development of the highly active molybdenum and tungsten alkylidenes of the general formula $(NAr)(OR')_2M{=}CHR$, where the most widely used is better known as molybdenum Schrock catalyst **[Mo]1** with Ar=2,6-$^{i}Pr_2$-C_6H_3, R=CMe_2-Ph, and R'=$C(CH_3)(CF_3)_2$ (Figure 1-3).[27,28]

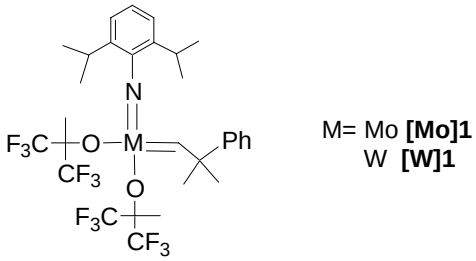

Figure 1-3. Schrock's alkylidene catalyst

These catalysts were referred to as "well-defined" in contrast to the "ill-defined" classical catalysts since the catalytically active species is spectroscopically identifiable. Molybdenum complexes are actually more active than their tungsten analog that tend to be trapped into a metallacyclobutane form. Catalyst **[Mo]1** allowed the metathesis of terminal and internal olefins, the ROMP of low-strain monomers, as well as the RCM of sterically demanding and eletron-poor substrates.[27-30] Schrock carbenes are regarded as X_2 ligands that render the metal of these complexes in its higher oxidation state (+VI). Thus, these early transition-metal catalysts have moderate-to-poor functional group tolerance because of the high oxophilicity of the metal centers, which also renders them extremely sensitive to oxygen and moisture.

Well-Defined Ruthenium Catalysts $X_2L(PR_3)Ru=CHR$'[31]

The impetus for developing olefin metathesis catalysts of the late-transition metals was to make less electrophilic complexes that would preferentially react with olefins in the presence of heteroatomic functionalities. With this in mind, ruthenium was introduced to metathesis chemistry as $RuCl_3$(hydrate), which effectively promoted the ROMP of norbornene in aqueous solution, albeit at low initiation rates.[32] Further catalyst screening revealed that $Ru(H_2O)_6(tos)_2$ (tos=*p*-toluenesulfonate) had even shorter initiation times and could ring-open functionalized norbornene.[33] However, these ill-defined ruthenium complexes were limited to the ring-opening of strained olefins, and therefore did not work for ADMET.

First-Generation Grubbs Catalysts

The real breakthrough came in 1992, with the synthesis of the first, well-defined, metathesis active ruthenium alkylidene complex $Cl_2(PPh_3)_2Ru=CHCHCPh_2$, based on the same methodology as their tungsten analogs, starting with $RuCl_2(PPh_3)_3$ and 3,3-diphenylcyclopropene (Figure 1-4).[34] The alkylidene proton is visible by ^{1}H NMR as two overlapping triplets at δ 17.94 ppm. In contrast with Schrock's catalysts, the carbene unit is considered a neutral L-type ligand that renders the metal center in a second oxidation state, although it is sometimes shown as a Ru(IV). The carbene moiety is believed to be an intermediate between a Schrock and a Fisher type carbene.

Phosphine exchange with the larger and more basic PCy_3 further enhanced activity as complex $Cl_2(PPh_3)_2Ru=CHCHCPh_2$ was able to promote the ROMP of lower strain monomers and the metathesis of acyclic olefins.[35] Even though the catalytic activity was far lower compared to the early transition metal carbene complexes, the ease of use and the newly-found functional group tolerance of this first generation of ruthenium catalysts

rendered them attractive for a variety of applications. Of 250 publications on olefin metathesis that appeared between 1990 and 1999, 75% reported using ruthenium metathesis catalysts. Their synthesis was industrialized by using diazoalkanes as the alkylidene precursor, which also produced complex **[Ru]1** after phosphine exchange, the most widely used catalyst of this series and better known as "1st generation Grubbs' catalyst" (Figure 1-4).[36,37] The key to this synthesis is the insolubility of **[Ru]1** in acetone, which allows for a simple and convenient wash of the crude product right out of the reaction pot. The use of rather explosive diazo compounds can be bypassed through the rearrangement of vinyl or propargyl halides in the presence of $Ru(H)(H_2)Cl(PR_3)_2$ (Figure 1-5).

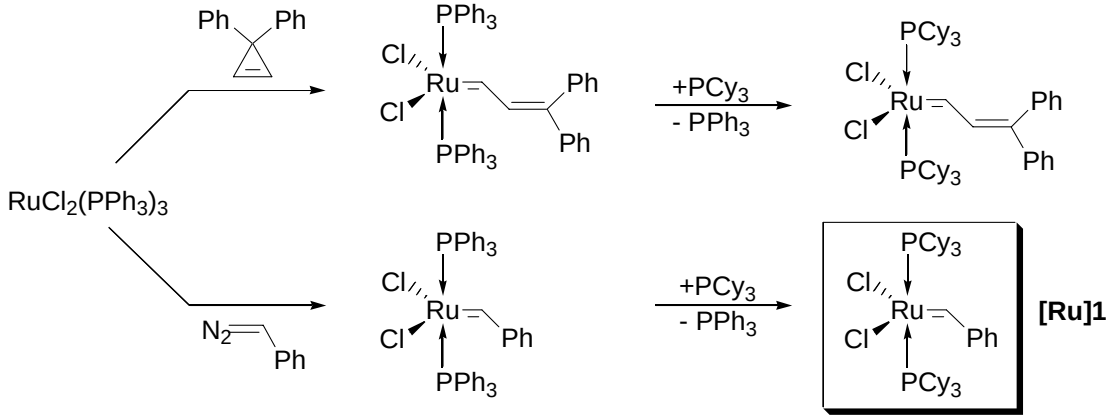

Figure 1-4. Synthesis of the first generation ruthenium carbene catalysts

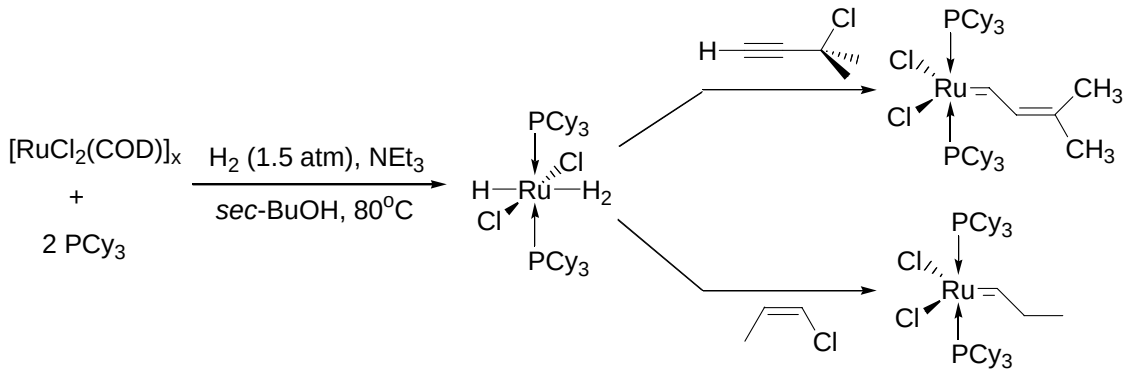

Figure 1-5. Alternative route to ruthenium carbene catalysts

These $(PR'_3)_2Cl_2Ru=CHR$ complexes typically exhibit a distorted square-pyramidal geometry with the alkylidene moiety in the apical position, and a trans bi(phosphine) ligand arrangement at the base of the square pyramid. Although in most cases the carbene is coplanar to the P-Ru-P plane, in the case of bulky phosphine, it is twisted away, almost perpendicular to the P-Ru-P plane.

The remarkable tolerance of these catalysts allowed scientists to apply a variety of modifications to the ligand sphere for specific conditions. Hence, their use was extended to ROMP and RCM in aqueous media by substituting the PCy_3 ligands to water-soluble phosphine such as $Cy_2P(CH_2)_2NMe_3^+Cl^-$.[38-40] Several supported models were also introduced for heterogeneous catalysis.[41-45] Other variations have been reported, including heterobimetallic complexes[46] and multidentate ligands, such as Shiff bases,[47-48] arenes,[49-52] and bidentate phosphines,[53,54] in an attempt to tune in activity and/or stability (Complexes **[Ru]A-D** in Figure 1-6). Pyridine coordinated complex **[Ru]E** features a remarkably high activity but a short lifetime,[55] while the alkoxy-chelated complex **[Ru]F**, better known as Hoveyda catalyst, shows exceptional stability, which allow its use in reagent grade solvents and/or in air.[56]

These first-generation of ruthenium catalyst are air stable and can be handled on the benchtop without significant loss of activity. Solutions prepared in reagent-grade solvents decompose slowly (over several hours) through different unclear processes, the primary pathway involving a bimolecular decomposition. Several mechanistic studies that suggested the formation of a highly active mono(phosphine) intermediate during the catalytic cycle triggered the development of second-generation ruthenium catalysts.[57-63]

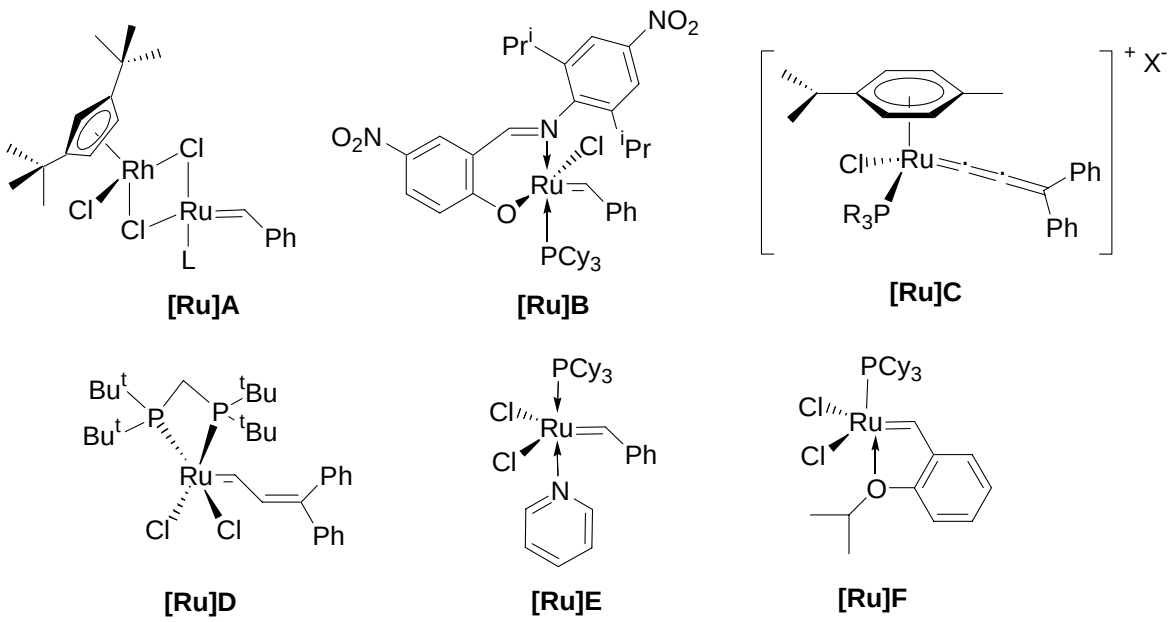

Figure 1-6. Other well-defined, metathesis-active $L_2X_2Ru=CHR$ ruthenium carbene catalysts

Second-Generation Grubbs Catalysts

Attempts to increase the concentration of the monophosphine complex by addition of phosphine traps (such as HCl or CuCl) only led to fast decomposition of the catalyst. Even though the activity was greatly enhanced, increasing the concentration of the monophosphine complex was not the way to improve catalytic efficiency. After Herrmann *et al.*[64] reported complex **[Ru]2** (Figure 1-7), researchers turned to N-heterocyclic carbene (NHC) ligands, sometimes referred to as "phosphine mimics" for their strong σ-donor and weak π-acceptor characteristics. Unlike most organic carbenes, these NHC ligands, pioneered by Arduengo[65-68] and now used extensively in organometallic chemistry, are ground-state singlets, although this electronic structure is not fully understood. In any case, these NHC ligands are stronger σ-donors and much less labile than phosphines. So, while complex **[Ru]2** showed little improvement in activity, a mixed ligand complex would overcome the problem both ways: promote

phosphine dissociation by *trans* effect, and stabilize the electron-deficient intermediate through the steric bulk and electron donation of the remaining NHC ligand. Indeed, complex **[Ru]3** containing a mesityl-substituted NHC ligand (IMes) exhibited greatly enhanced metathesis activity and stability toward air and a variety of functional groups (Figure 1-7).[69,70] Soon after, the saturated version **[Ru]4** was discovered by the Grubbs[71] group to be even more reactive, albeit less stable than **[Ru]3**. The 1,3-dimesityl-4,5-dihydroimidazol-2-ylidene ($IMesH_2$) ligand was thought to be more basic than its C-C unsaturated counterpart because of the reduced conjugation throughout the NHC ring. However, this carbene is not stable in air, and must be formed in situ, either from the imidazolium salt and a base, or through the chloroform adduct. Complex **[Ru]3** can then be isolated after a methanol wash and column chromatography, if further purification is desired. The methanol wash, which sometimes contaminates the catalyst with hydrides, can be avoided by running the reaction in anhydrous hexanes.[72]

These NHC-containing complexes exhibit the same distorted square-pyramidal geometry. But while two carbene fragments are present, they display different Ru-C distances (e.g. in **[Ru]2** Ru-C(carbene)=1.841(11), Ru-C(L)= 2.069(11) Å).These important metrical parameters clearly distinguish two metal-carbene interactions: a covalently bound benzylidene and a datively bound N-heterocyclic carbene, the latter acting as a two-electron donor, also reflecting their very poor π-acceptor character. The NHC group also appear to be more sterically demanding than PCy_3.[73] Finally, this new class of catalysts combines the activity of early transition metal complexes and the functional group tolerance of **[Ru]1**.

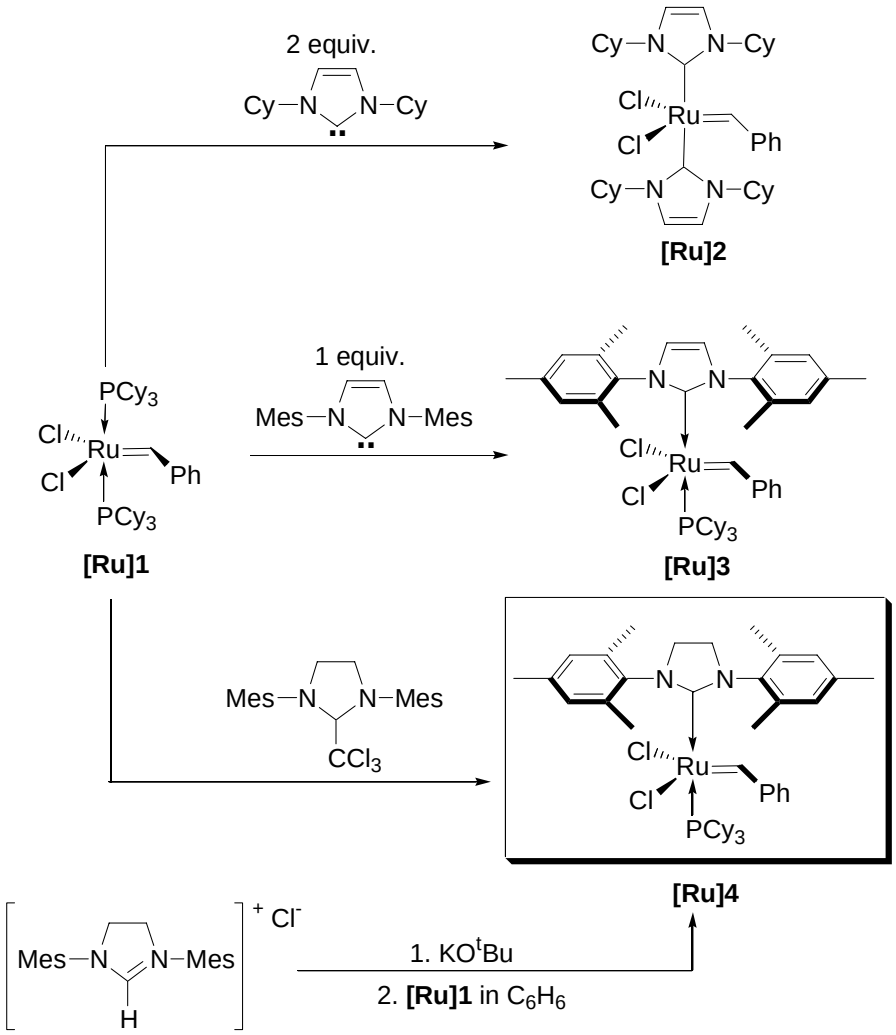

Figure 1-7. Synthesis of 2nd generation ruthenium metathesis catalysts

Mechanistic Considerations

Mechanistic studies started shortly after the discovery of the first ruthenium alkylidene $Cl_2(PPh_3)_2Ru{=}CHCPh_2$ and played a major role in the development of the 2nd generation of catalysts. For a while, scientists believed in an associative mechanism where the olefin first coordinated to the metal center to form a stable 18 e^- complex, followed by phosphine dissociation and subsequent formation of the metallacyclobutane.[57] Yet, Grubbs *et al.* reported in 2001[74,75] that the substitution of a phosphine ligand with and olefinic substrate actually proceeds in a dissociative fashion to

generate the four-coordinate 14 e$^-$ species $X_2LRu{=}CHR'$ (**IB**) (Figure 1-8). The recoordination of free phosphine is competitive with substrate binding and the catalytic turnovers that the active species carries out before being "quenched" with free PR_3 depends on a variety of factors, detailed below.

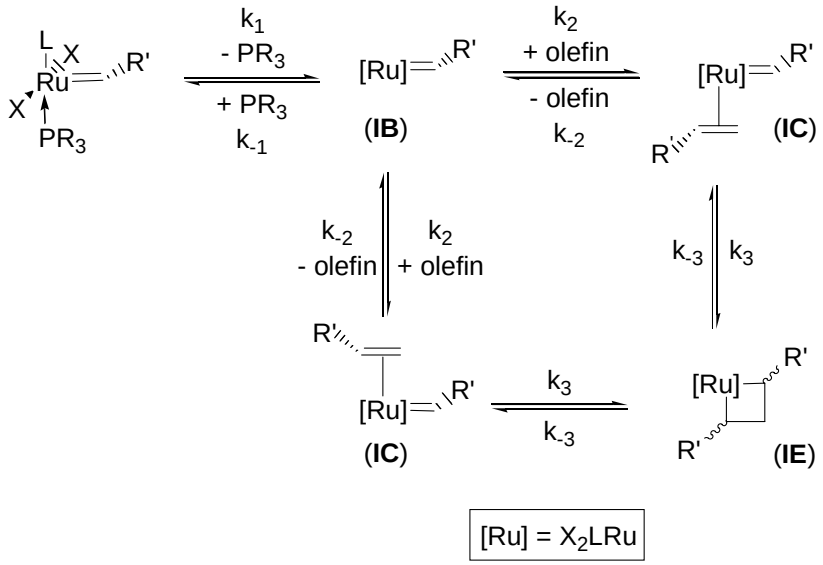

Figure 1-8. Mechanism of metathesis catalyzed by ruthenium alkylidene

Role of the L-type ligand

Conversely to the general idea spread at the time when NHC-containing catalysts were developed, phosphine dissociation is much slower than with the bis-phosphine systems. The high activity of **[Ru]4** over **[Ru]1**, for example, can be understood by considering the ratio of phosphine rebinding to olefin binding rates (k_{-1}/k_2), which virtually indicates metathesis activity, the smaller ratio, the more active catalyst. Data show that the $IMesH_2$ ligand increases selectivity for binding olefinic substrates over free phosphine by 4 orders of magnitude.[75] This increase in selectivity is due to the excellent electron donation and weak π-acidity of NHCs, which promotes and stabilizes metal-to-olefin back-bonding to a greater extent than the phosphine ligand, and therefore favors

the formation of intermediate **IC**.[76] For example, **[Ru]4** is more active than **[Ru]3** in the ROMP of COD, $IMesH_2$ being a better σ donor than IMes.[77,78] In addition, the electron donation of NHC ligands is expected to accelerate the oxidative addition required for the metallacyclobutane formation.

The reason for the dramatic decrease in initiation exhibited by these NHC-containing catalysts is still debated. Although both PCy_3 and $IMesH_2$ are large ligands, this could be due to a steric effect, as the distribution of the steric bulk is dramatically different in each case.[78] The differential steric distribution could be the source of stabilizing or destabilizing interactions that would change the activation energy required for phosphine loss. An electronic effect could also explain these rates difference by considering the weaker π-acidity of NHCs compared to phosphines. While the two phosphine ligands have to compete for Ru-P π-back bonding in the bis-phosphine complex, the ruthenium-phosphine bond is reinforced in the NHC-containing complex by stronger π-backbonding. Unfortunately this is not reflected by the crystal structures where Ru-PCy_3 bond distances barely change upon substitution of one PCy_3 with IMes (Ru-P= 2.4097(6) and 2.4221(6)Å in **[Ru]1** and Ru-P= 2.419(3)Å in **[Ru]3**).[70]

Role of the phosphine ligand (PR_3)

Changing the phosphine ligand has a dramatic effect on both catalyst initiation and catalyst activity. However, the effect is inverted from the first generation to the second generation of catalysts. Indeed, bis-phosphines complexes are rendered more active by larger and more electron donating phosphines, whether it promotes dissociation by *trans* effect or it helps stabilize the 14 e^- metallacyclobutane.[57,79] On the other hand, less

electron donating phosphines, hence more labile, tend to increase the activity of NHC-containing systems by accelerating the dissociation step.[75]

Role of the halide ligand (X)

While larger halides increase initiation rates by forcing phosphine dissociation, the overall activity suffers from the increased bulk around the metal center. For example, with both **[Ru]1** and **[Ru]4**, moving from the di-chloride to the di-iodide complex results in a 100-fold increase in k_{-1}/k_2.[75] Because the conformation of intermediates **B** and **C** are still unclear at this point, the reasons behind this large shift remain speculative. One possible explanation involves the suggestion that olefin coordination requires a trans isomerization of the X-type ligands, which would be less favorable with larger X-ligands.[57]

Role of the carbene ligand (R')

The effect of the carbene ligand is significant because , unlike the other ligands, it can change throughout the metathesis reaction. For example ROMP reactions produce an alkylidene complex that becomes the propagating species, while RCM, CM and ADMET generate a methylidene after the first turnover. Sterically bulky and electron-donating R^1 groups (e.g. alkyls) lead to higher initiation rates because they more effectively promote phosphine dissociation.[75] In contrast, small and electronically neutral groups (e.g. H) are less effective at labilizing the phosphine ligand.[80] Indeed, the methylidene complexes, especially those containing NHC ligands, are extremely poor initiators at room temperature. While the methylidene of **[Ru]4** remain an active metathesis catalyst in its phosphine-free form, it is virtually incapable of re-entering the metathesis cycle once trapped with free-PCy_3.

Stereochemical aspects

As mentioned above the conformation of the olefin-bound complex is still unidentified because these intermediate are not isolable or observable spectroscopically. Until recently, the nature of the metallacyclobutane was the subject of a theoretical debate, whether it was a reaction intermediate[61] or a transition state,[81-83] when Piers *et al.*[84] finally isolated a ruthenacyclobutane as a C_{2v} structure. Grubbs and others[61,85] have shown that the olefin may bind either *trans* to a halide (X), which necessitates a rearrangement (**IC-a** and **IC-b** in Figure 1-9), or *trans* to the L-type ligand (**IC-c**). Although in some cases there seems to be more evidence for intermediate **IC-a**,[86] the symmetrical C_{2v} structure of the metallacyclobutane suggests that **IC-c** is the correct conformation.

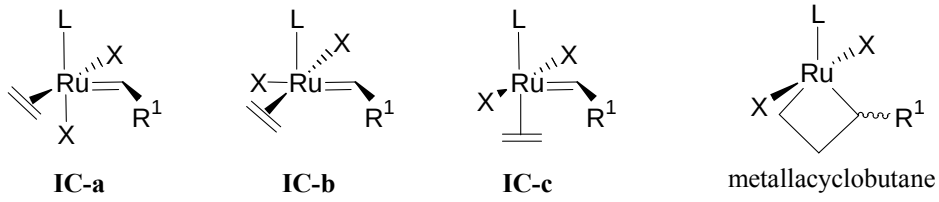

Figure 1-9. Proposed conformations for olefin-bound Grubbs catalyst intermediate

In the case of monosubstituted dienes, and probably as a general rule, α,α'-disubstituted metallacyclobutane seem to be kinetically favored, within the limits of non-sterically demanding olefins (Figure 1-10).[80] This preference is more likely the result of the greater stabilization of the metal center by electron-donating substituents in an α-position rather than in a β-position. Conversely, this conformation only leads to non-productive metathesis suggesting that the energy difference between the 2 metallacyclobutane is not enough to prevent the metathesis reaction. However, this may not apply in the case of sterically demanding olefins.

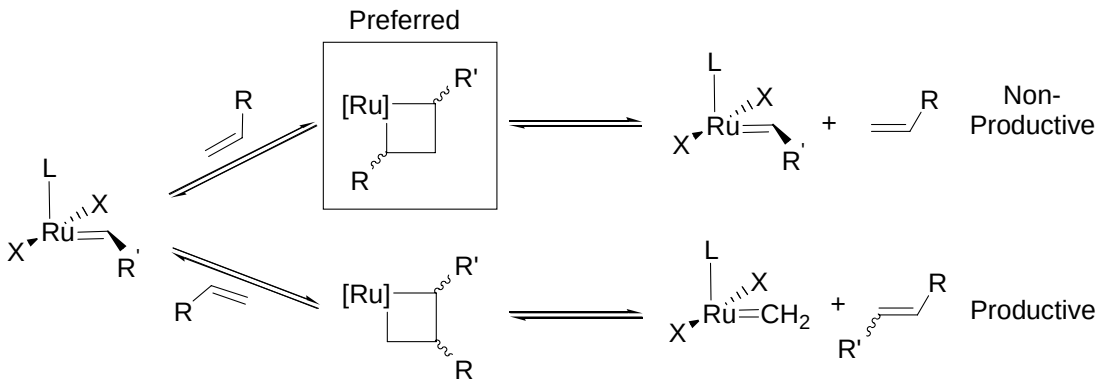

Figure 1-10. Stereochemical preference of the α,α'-disubstituted metallacyclobutane

Catalyst Decomposition

Even though a substantial amount of effort has been devoted to the understanding of decomposition pathways in solution and under metathesis conditions, this area still comports many unanswered questions. The thermal decomposition of **[Ru]1** has been proposed to occur via phosphine dissociation followed by bimolecular coupling of two 4-coordinate ruthenium fragments, the addition of phosphine slowing down the decomposition rate.[87] Conversely, the decomposition of the methylidene follows first-order kinetics which could be the result of an intramolecular C-H activation of an L-ligand. In general, NHC-containing complexes exhibit significantly improved thermal stabilities compared to their bis-phosphine counterparts. For example, **[Ru]3** shows no sign of decomposition after 1h at 100°C in toluene, while in the same conditions 75% of **[Ru]1** has already decomposed.[88] This increased stability is a combination of the stabilizing effect of the NHC ligand on the 14e- intermediate and of the reduced extent of phosphine dissociation. Nevertheless, only one compound has been identified so far, bimetallic hydride complex **[Ru]5**, from the thermal decomposition of **[Ru]4** methylidene analog.[89]

Others have studied the behavior of these catalyst under different conditions and isolated other decomposition products. For example, carbonyl hydrides **[Ru]6** and **[Ru]7** (Figure 1-11) first isolated during the decomposition of alkoxycarbene complexes,[90,91] were identified as products of the reaction of **[Ru]1** and **[Ru]4** with primary alcohols in the presence of a base.[72,92-94] However, the mechanism is still at a speculative stage. Noteworthy, **[Ru]8**, product of the C-H activation of a mesityl group, was isolated during the synthesis of **[Ru]4** but was never observed as a proper decomposition product of **[Ru]4**.[72]

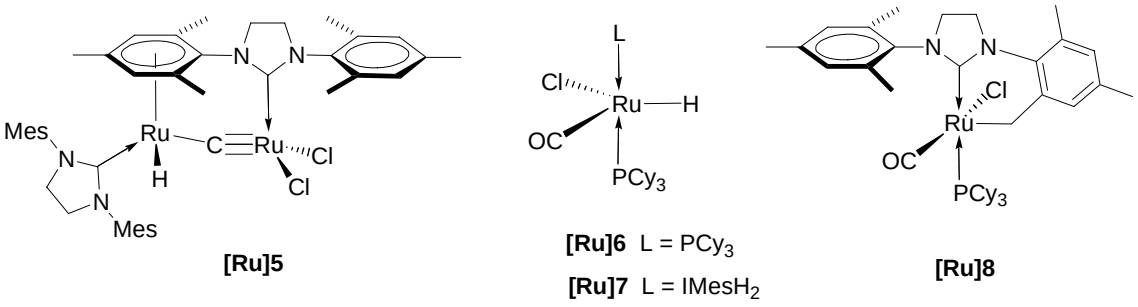

Figure 1-11. Decomposition products of ruthenium carbene complexes

Other Second-Generation Ruthenium Catalysts

A variety of related second-generation catalysts have been investigated in olefin metathesis. Hoveyda *et al.*[95] reported a second-generation tethered catalyst **[Ru]9**, which turns out to be a faster initiator than **[Ru]4** (Figure 1-12). Even though **[Ru]4** and **[Ru]9** generate the same propagating species after a single turnover, **[Ru]9** afford considerably higher yields with electron-deficient olefins, which is probably due to the absence of a strong donor ligand.[96-98] This observation emphasizes the importance of ligand rebinding during the metathesis cycle. Bis-pyridine complexes provides similar results, and is often used as an intermediate for phosphine exchange.[99]

Several modifications of the NHC ligands have also been implemented. Among those **[Ru]10** was reported to catalyze terminal olefins much faster than **[Ru]4**, thanks to the increased bulk of its NHC ligand exerting a stronger steric pressure on the carbene and therefore prompting phosphine dissociation.[100,101]

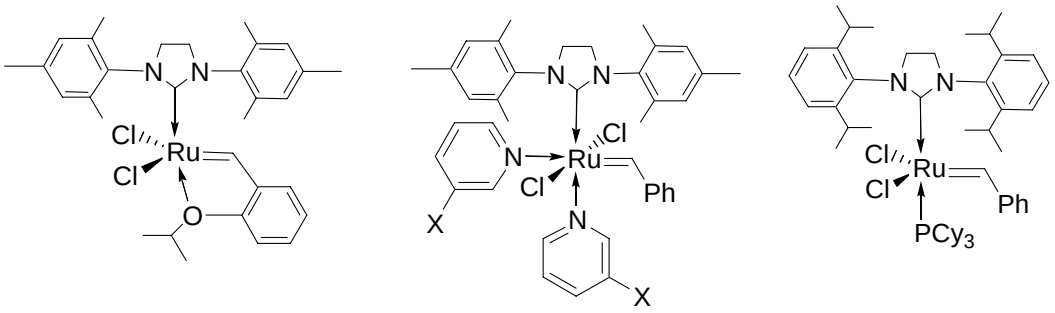

Figure 1-12. Other second-generation catalysts

The isopropoxystyrene ligand of **[Ru]9** represents an ideal anchor for heterogeneous catalysis applications,[102-107] and further ligand modification by substitution of electronic and steric groups.[108,109] In addition to their extreme stability towards air and moisture, the release-return mechanism of these Hoveyda-type catalysts confers them an interesting recyclability (Figure 1-13).[95]

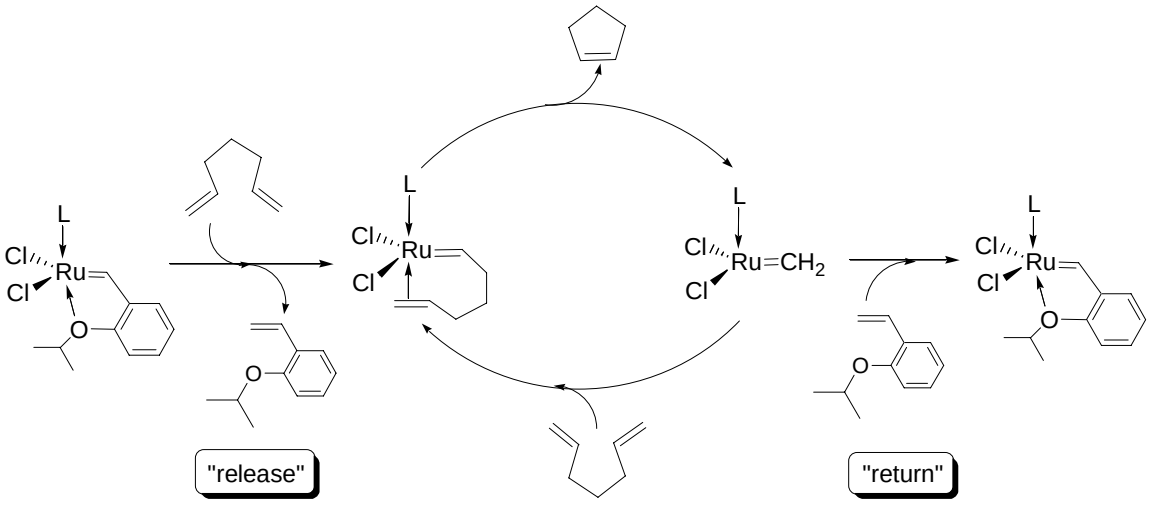

Figure 1-13. Hoveyda's "release-return" mechanism

Introduction to ADMET Polycondensation

Before continuing into catalyst considerations, it is important to understand the requirements of a polycondensation type of reaction, such as ADMET. This next section will focus on ADMET polymerization, its characteristics and requirements for catalyst modeling, and its applications for polymer synthesis following the development of ruthenium carbene catalysts.

Catalytic Cycle

ADMET is essentially the self metathesis of a diene to form high polymer, and therefore operates through the Chauvin mechanism. The precatalyst goes through a first turnover to generate the active alkylidene complex **A1**. Upon coordination of a second monomer molecule, an α,β-metallacyclobutane (**M2**) is formed to produce a dimer and the methylidene complex **A3**. A substantial amount of the α,α-metallacyclobutane probably also forms but only leads to non-productive metathesis. The methylidene **A3** then reacts with another monomer molecule, which upon formation of the α-metallacyclobutane (**M4**) releases a molecule of ethylene and the "starting" alkylidene complex. The cycle then goes on to form trimer, tetramer, etc. until reaching high molecular weigh polymer. For each "coupling" reaction one molecule of ethylene is formed. However, reaction of a polymer chain with ethylene will result in depolymerization. To drive ADMET equilibrium onto a productive pathway and achieve high molecular weigh polymer, ethylene gas is usually eliminated from the reaction vessel as the polymerization proceeds.

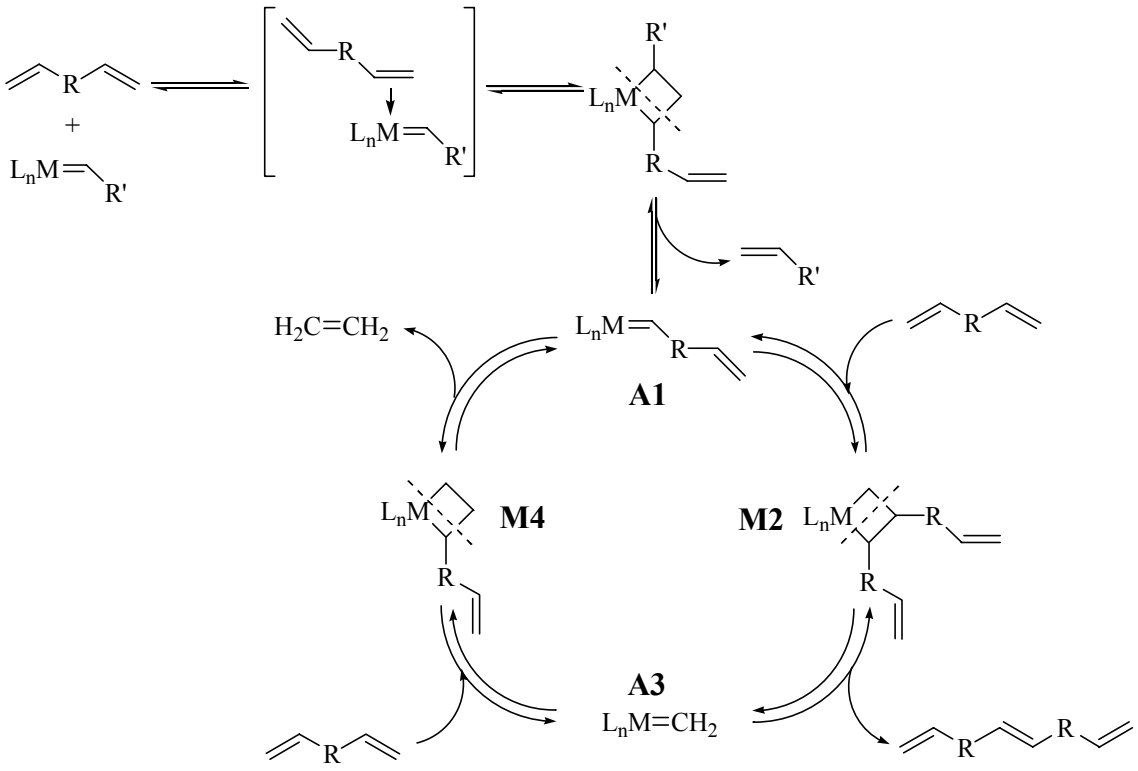

Figure 1-14. Mechanism of productive ADMET

Kinetics and Equilibrium Considerations

From a kinetic viewpoint, ADMET is a step-growth condensation reaction, meaning that it proceeds by the stepwise reaction between the functional groups of reactants, in this case the olefinic double bond, to produce dimer, trimer, tetramer, and so on until eventually large polymer molecules are formed.[110] The size of the polymer molecules continuously increases with time (conversion) at a relatively slow rate. Therefore, high conversions are required to reach high molecular weight polymer as expressed by the Carothers equation where $\overline{X}_n$ is the number-average degree of polymerization, or the average number of structural units per polymer chain, and p is the extent of reaction or conversion of the diene monomer (Equation 1-1). In other words,

$\overline{X}_n$ is simply given as the total number of monomer molecules M initially present divided by the total number of molecules present at time *t*.

$$\overline{X}_n = \frac{1}{1-p} = \frac{[M]}{[M]_0} \qquad (1\text{-}1)$$

Step-polymerizations are characterized by the disappearance of monomer very early in the reaction. For example in most step polymerizations, there is less than 1% of monomer left when the average polymer chain contains about 10 monomer units. High-molecular-weight polymer is obtained only near the end of the reaction (>98% conversion). Passed these high conversions, each connection that is made involves two high molecular weight molecules, and the average degree of polymerization increases exponentially at this point, as illustrated by Figure 1-15. the catalyst therefore needs to remain highly active throughout the entire polymerization, which sometimes require long reaction times.

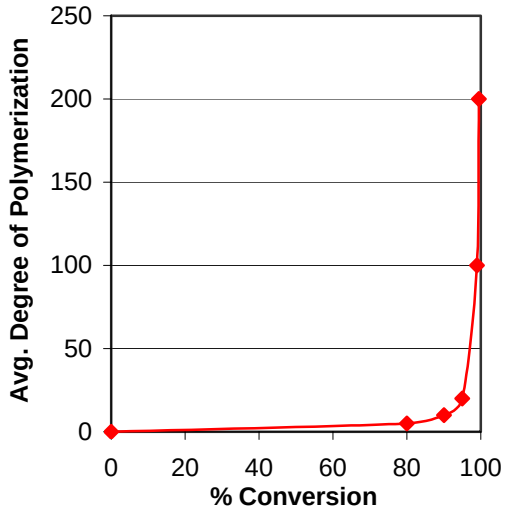

Figure 1-15. Variation of molecular weight with conversion in step polymerization

Most metathesis catalysts are more reactive towards terminal olefin than unstrained internal olefins, mostly because of the reduced steric hindrance of terminal olefins. For this reason, ADMET is conducted with α,ω-diene monomers to achieve the highest conversions possible. Incidentally, this generates methylidene complexes, which in the case of ruthenium hinders the rate of metathesis. This point will be further developed in the next section. Of course, any mono-olefin impurity should avoided at all times, since they will act as end-capping reagents, therefore limiting the molecular weight of the polymer. However, in some instances, mono-olefins can be used as chain transfer agents to reach a target molecular weight.

Condensation reactions are usually equilibrium processes that require the removal of the condensate molecule to shift the equilibrium towards high conversions, i.e. high molecular weights polymers. Industrially, the synthesis of commercial condensation polymers, such as polyesters, polyamides and polycarbonates, liberate molecules a such as water, alcohols or even HCl that often require heat and vacuum to be evacuated.[111] In ADMET, the condensate molecule is ethylene gas, which is conveniently removed at room temperature. For this reason, most ADMET polymerizations are run under vacuum, without a solvent, which also minimizes cyclization.

Cyclization versus Linear Polymerization

The production of linear polymers by step polymerization is sometimes complicated by the competitive occurrence of intramolecular cyclization reactions.[112] This phenomenon depends on thermodynamics and kinetic considerations of the size of the ring structure that may be formed. Thermodynamically, the stability of the ring decreases under 4 and over 8 atoms. Kinetically, the probability of ring formation

decreases as the possibility of the 2 functional groups encountering each other decreases. Oligomeric cyclics has been observed in ADMET; however, the amount and the form of cyclics were impossible to identify.[113] The metathesis reaction allowing the ring-closing of acyclic dienes (RCM), the use of monomers able to form 5-,6-, and 7-membered rings should be avoided in ADMET (Figure 1-16). Cyclization can also be limited by carrying out the polymerization at high concentrations of reactants. Linear polymerization being a bimolecular (intermolecular) process, the reaction rate increases as the concentration of reactants increase. Typically, ADMET polymerization is run in the bulk, at high temperatures to lower the viscosity as it increases with the polymer molecular weight. Similarly, the synthesis of large rings (more than 20 atoms) has been achieved in high dilution conditions.[114]

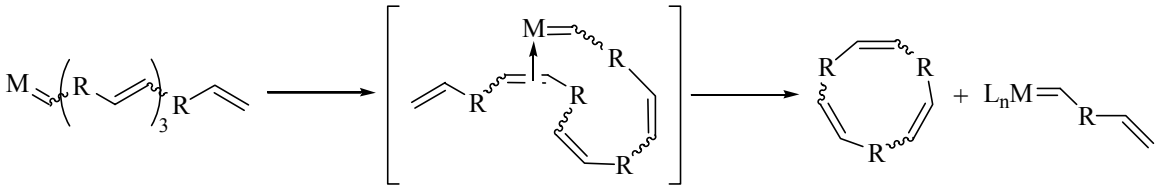

Figure 1-16. Formation of cyclics in ADMET

Interchange Reactions and Molecular-Weight Distribution

Interchange involves reactions between the terminal functional group of one polymer molecule with the interunit repeating linkage of another polymer molecule. These interchange reactions are quite common in condensation polymers, such as polyamides and polyesters.[115] Two polymer chains react to yield one shorter and one longer chain, which does not affect the average molecular weight of the polymer. In ADMET, the carbon-carbon double bonds of the polymer backbone are still metathesis active and can react with either a polymeric alkylidene complex or a methylidene

complex formed from a productive metathesis cycle (Figure 1-17). This phenomenon is often referred as *trans-metathesis* and will go on until the system reaches a thermodynamic equilibrium. It allows the perfect randomization of copolymers synthesized by ADMET, whether the two monomers are mixed together or one monomer is incorporated into a different homopolymer.[116]

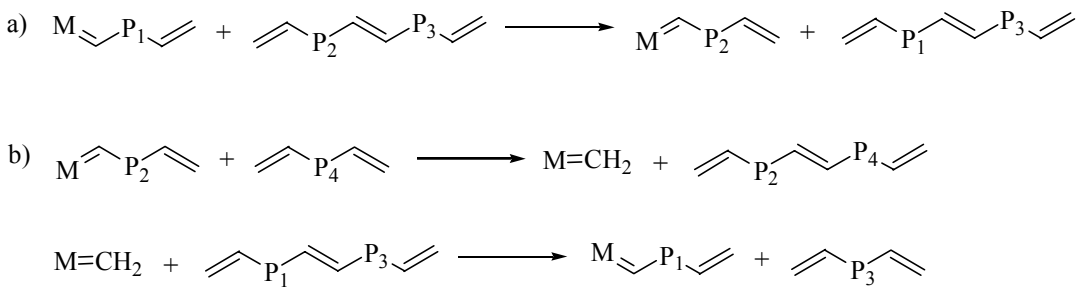

Figure 1-17. *Trans-metathesis* in ADMET: a) Interchange with a polymeric alkylidene; b) Interchange with the methylidene from a productive step

The product of a polymerization is a mixture of polymers molecules of different molecular weights. The polydispersity index (PDI) is a measure of the breadth of this molecular weight distribution, defined as the weight average molecular weight M_w divided by the number average molecular weight M_n.[117] Hence, a high PDI will be the indicative of a broad molecular weight distribution, which will have various impacts on the polymer mechanical properties. The molecular weight distribution has been derived by Flory[118] through a statistical approach which predicts that for step polymerization, the PDI should be close to 2 when the conversions approach 100%. As a matter of fact, most ADMET polymers exhibit a PDI of 2.0, thanks to trans-metathesis. Lower PDIs indicate the presence of competitive mechanisms such as cyclization followed by ROMP.

Utility of ADMET

Although ADMET is limited by the catalyst lifetime and therefore does not reach molecular weights higher than 80,000 g/mol, the polymers obtained present sufficiently

interesting material properties for application. Actually, many commercial polymers, such as polyesters and polyimides present most interesting properties at molecular weights ranging between 15,000 and 30,000g/mol.

The clean mechanism of ADMET has often allowed to bypass some of the most puzzling challenges in the polymer community. For example, the random or alternated copolymerization of ethylene with polar monomers is complicated by the reactivity differences of the 2 monomers, often producing block copolymers through standard polymerization procedures. ADMET provides a unique method to synthesize completely linear polymer analogous to sequence specific or statistical copolymers of ethylene and polar monomers in a wide variety of comonomer compositions. This is achieved by polymerization of the appropriate functionalized diene followed by exhaustive hydrogenation. The design of the diene monomer can therefore lead to virtually any polymer via ADMET, whether it is used for modeling known structures or developing new materials, such as amino-acid containing polymers and polysiloxanes (Figure 1-18).

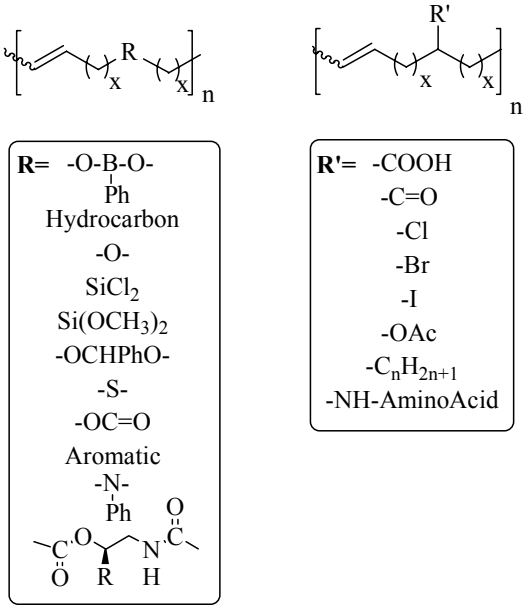

Figure 1-18. Examples of polymeric structures obtained via ADMET polymerization

In addition, the ADMET polymerization of different alkyl branched dienes has provided a family of model ethylene/α-olefin copolymers and allowed the study of the effects of regular microstructures on polymer properties. The structure-property relationships of various ethylene copolymers can be clarified using these model systems, by comparing T_m as a function of the functional group or by examining crystal packing.

Ruthenium Catalysis Applied to ADMET

The development of ruthenium Grubbs catalysts greatly expanded the scope of ADMET by allowing the polymerization of functionalized dienes that are not tolerated by Schrock's catalysts and by easing polymerization procedures. Even though the first generation of catalysts require higher catalyst loadings and afford generally lower molecular weights, it never necessitate absolute dryness of monomer or oxygen-free conditions as Schrock catalysts do.

A polymer formed via ruthenium-catalyzed ADMET has a typical *trans* content of about 80%., whereas Schrock's catalysts produce 90 to 95% *trans* polymer. The preferred *trans* configuration is not only a correlation of the metallacyclobutane conformation but is also a thermodynamic reflection of the *trans* metathesis equilibrium. The difference between the two types of catalysts is more likely the result of a sterically less flexible metallacyclobutane in the case of Schrock's catalysts due to its bulky ligand sphere.

Ruthenium 1st Generation

It was not until the introduction of **[Ru]1** that ruthenium became extensively used in ADMET. Indeed, its triphenylphosphine and vinylidene analogs only promotes ADMET at a very slow rate at normal catalyst loadings (0.1 to 1.0 mol%).[119] Typically, the polymers produced with **[Ru]1** have a molecular weight range of 25 to 35 kg/mol and

an 80% trans ratio, at optimal catalyst loadings of 0.25 mol%.[119] This catalyst allows the polymerization of monomers containing acetals, alcohols,[119] aromatic groups,[120] esters both in the main chain[121] and as pendant group, ketones,[122] ethers,[123] boronates,[124] germanium,[125] silyl chlorides and siloxanes,[126] in addition to a variety of alkyl branched monomers.[127-130] Amine[131] and carboxylic acid[132] containing olefins can also be polymerized via ADMET but require to be protected prior polymerization. However, in the case of hydrocarbon polymers, the molecular weights reached with **[Ru]1** are still much lower than what can be obtained with Schrock's catalysts. For example, an ADMET ethylene-propylene copolymer, with the same methyl branch content, has a M_n of 17,400 g/mol with **[Ru]1**, versus M_n of 72,000 g/mol with **[Mo]1**.[128] Other model ethylene copolymers, such as ethylene-vinyl chloride,[121] ethylene-vinyl acetate,[122] ethylene-acrylate,[133] and ethylene-styrene copolymers[133] were also successfully synthesized with **[Ru]1**, some even exhibiting unique thermal characteristics. Other useful structures include various cyclolinear phosphazene polymers,[134,135] and liquid crystalline polyesters.[136]

Numerous block copolymer architectures have also been devised using functionalized polyoctenamer telechelics via ADMET polycondensation,[121,137] for example in the synthesis of novel poly(γ-benzyl-$_L$-glutamate)-*b*-polyoctenamer-*b*-(γ-benzyl-$_L$-glutamate) triblock copolymers. In this case, the functional group tolerance of **[Ru]1** allowed the end-capping of ADMET polymerized polyoctenamer with phtalimido groups, as the first step towards a potentially bioactive triblock copolymer.[138]

The only requirement for the monomers is to place the functionality at least 2 carbons away from the double-bond to limit cyclization and/or catalyst deactivation by

intramolecular coordination leading to the formation of a stable chelate.[60] The polymerization of 1,5-hexadiene and polyethylene glycol (PEG) grafted copolymers have been limited to oligomeric structures for this reason.[119,139-141]

Because these catalysts react rapidly and quantitatively with vinyl ethers to form Fisher carbenes that are relatively metathesis inactive,[74,91] this provides a convenient way to quench most ADMET reactions by addition of ethyl vinyl ether. This also insures that the ADMET polymer has well-defined olefinic end-groups.

Depolymerization of commercial polybutadiene by ADMET can be achieved by applying high pressures of ethylene in the presence of **[Ru]1** to yield 1,5-hexadiene.[142] In the absence of ethylene and solvent the depolymerization only produces cyclics.[143] The results are much better than with Schrock's catalyst thanks to the lesser sensitivity of the ruthenium catalysts.

Ruthenium 2nd Generation

Complex **[Ru]4** has been used extensively for ADMET, for it yields polymers of higher molecular weight than **[Ru]1**. Overall, the reactivity of **[Ru]4** falls in between that of **[Ru]1** and **[Mo]2**.[144] For example, the polymerization of 1,9-decadiene with **[Ru]4** using the same catalyst loadings (0.25 mol%) affords polyoctenamer with a M_n of 75,000 g/mol, compared to only 25,000 g/mol with **[Ru]1**.[145] However, all polymers obtained using second-generation catalysts exhibit irregular microstructures as evidenced by a depreciation of the melting temperature T_m. This is due to a competitive isomerization reaction that disturbs the molecular structure by migration of the double-bond along the olefin backbone. Therefore these catalysts are not suitable for the modeling of precise polymer architectures.

On the other hand, the second generation of catalysts has allowed the ADMET polymerization of amino-acid containing dienes.[146] These reactions need to be conducted in THF solution because of the solid nature of the monomers. The polymers produced have molecular weights of up to 30,000 g/mol and represent ideal candidates for biological applications.[147]

Imperfect comb graft copolymers of polyethylene (PE) and PEG were synthesized with **[Ru]4** in higher molecular weights than with **[Ru]1** (12,000 vs. 5,500 g/mol), albeit as irregular microstructures.[141] Tandem ADMET/ATRP polymerization was used for the preparation of polyethylene grafted polystyrene copolymers; however, only low molecular weight materials were obtainable because of the steric hindrance of the polystyrene grafted diene interacting with the catalyst.[148] For this particular class of copolymers, ROMP followed by ATRP polymerization was able to afford higher molecular weights.[149,150]

The use of 2nd generation ruthenium catalysts for the synthesis of conjugated polymers has hardly been explored, and would not be expected to promote the vinyl addition reactions that have been problematic in ADMET of electron-rich monomers with the more electrophilic molybdenum complexes. Attempts to polymerize 1,4-divinylbenzene only resulted in dimers and trimers because the mixture solidified passed a DP of 3.[151]

Depolymerization reactions with **[Ru]4** also affords better results than **[Ru]1** or **[Mo]1** for polyisoprene and polybutadiene blocks of triblock copolymers of the type polystyrene-polyene-polystyrene.[152] Complex **[Ru]4** is also able to depolymerize sulfur crosslinked polyisoprene into oligomers (DP=10). This field represents a potentially

useful recycling technique especially if the robustness and the cost of the catalysts can be improved.

Limitations

These late-transition metal catalysts are not immune to interaction with functional groups, as exampled by the isolation of multiple chelates of functionalized olefins with ruthenium olefin metathesis catalysts.[60,153,154] Hoveyda-type catalysts are an example of this phenomenon that retains high catalytic reactivity. Concerning the nature of the functional group tolerance the coordination of the heteroatom to the metal is of central focus. Reversible coordinations will only delay or slow down the metathesis reaction and maybe prevent high conversions while irreversible coordination will simply deactivate the catalyst towards ADMET.[60] A typical example is the case of thioethers, which are polymerizable with Schrock's molybdenum, but not with the **[Ru]1**.[155] A stable Ru-S chelate complex is formed as evidenced by the appearance of a new alkylidene by ^{31}P NMR. The Ru-S bond is expected to be stronger than the Mo-S bond according to the size and polarizability of the two metals. Even though the ruthenium is tolerant towards a greater variety of functional groups than **[Mo]1**, kinetically, coordinating functionalities such as ethers and sulfides, influence the rate of polymerization to a much greater extent with **[Ru]1** than with **[Mo]1**.[155] Indeed, after phosphine dissociation, heteroatoms can compete with olefins for the open coordination site and thus retard the rate of metathesis. Reversible coordination probably occurs both intra and intermolecularly in ADMET due to the high monomer concentrations in bulk conditions. This effect is not as significant in the case of molybdenum catalysts probably because of the steric influence of the bulky ligand sphere.

Hydrogenation

The ruthenium catalysts feature the possibility to be converted into hydrogenation catalysts, which can be attractive for the one-pot synthesis of branched polyethylene by sequenced ADMET polymerization-hydrogenation. Heterogeneous hydrogenation could be performed by simple addition of chromatographic silica to the diluted polymerization mixture under 200-500 psi of hydrogen.[121] Copolymers of ethylene-styrene, ethylene-vinyl chloride and ethylene-acrylate were prepared this way.[133] Even though many examples have shown that ruthenium carbenes **[Ru]1** and **[Ru]4** could be transformed into homogeneous hydrogenation catalysts, this strategy has not been tested during ADMET polymerization.[156-159] The homogeneous catalyst could then be washed away by precipitation of the saturated polymer.

Kinetics

Kinetics in ADMET can hardly be monitored by NMR since ADMET requires bulk conditions (to limit cyclization) while NMR operates in diluted solution of deuterated solvents. So the best way, so far, to measure ADMET kinetics is to measure the volume of ethylene released, which is directly correlated to the degree of polymerization. Even though this method does not reflect ADMET kinetics under vacuum, it allows the comparative study of different catalysts, which was first implemented with **[Mo]1** and **[Ru]1** by Brzezinska *et al.*[155] At early conversions, i.e. before the viscosity grew so high that the rate becomes diffusion controlled, ADMET follows a quasi-second order rate. **[Mo]1** was found to catalyze ADMET of 1,9-decadiene about 50 times faster than **[Ru]1**. Nevertheless, **[Ru]4** promotes ADMET faster than **[Ru]1** at temperatures of 45 and higher.[144] An induction period marks the slow phosphine dissociation of this NHC containing catalyst; however, the greater affinity of the $14e^-$ complex for π-olefinic

substrates combined with a slower phosphine rebinding allow for higher molecular weights polymers. Hence, phosphine dissociation/rebinding plays a major role in the ADMET mechanism, the ultimate concern being the molecular weight of the polymer, not the initial metathesis rate.

Olefin Isomerization

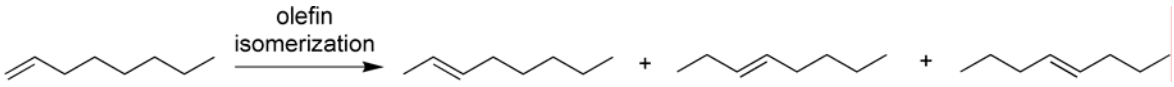

Figure 1-19. Structural olefin isomerization of 1-octene.

In spite of their high reactivity in metathesis chemistry, these ruthenium catalysts were suspected to undergo non-metathesis transformations.[160-165] Among them, alkene isomerization has emerged as an important side reaction of ruthenium catalyzed metathesis, disturbing the product's microstructure by apparent migration of the double bond along the alkyl chain (Figure 1-19).[166] First observed on substrates containing allylic functionalities in combination with first generation catalysts,[167-171] double bond isomerization has since been reported with 2nd generation catalysts on a broad variety of substrates competitively and sometimes prior to olefin metathesis.[114,173-176] More recently, olefin isomerization was evidenced in ADMET catalyzed by **[Ru]4**, by the MALDI-TOF analysis of an amino-acid branched polymer.[177] Whether it occurs on the monomer, or on the polymer followed by trans-metathesis, isomerization during ADMET results in irregular microstructures presenting altered properties (Figure 1-20). Noteworthy, under ADMET conditions, first-generation **[Ru]1** was found not to isomerize olefins.[178]

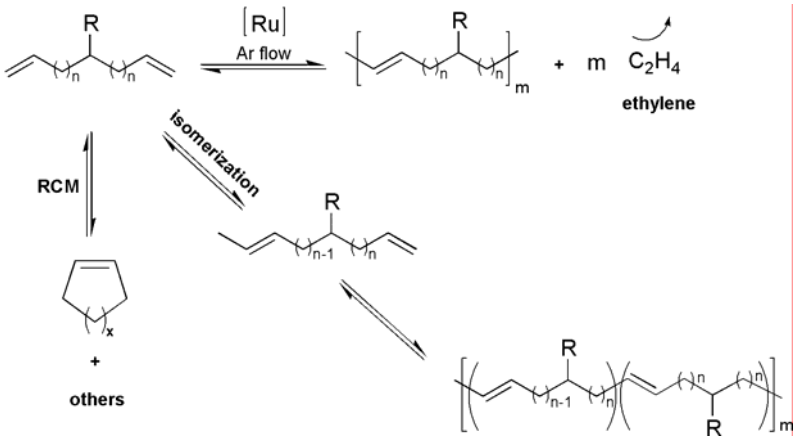

Figure 1-20. Olefin isomerization during ADMET polymerization

Olefin isomerization is promoted by a variety of metal complexes and has been known to operate via two distinctive pathways: the π-allyl hydride mechanism involves a metal in a low oxidation state that forms an η^3-allyl intermediate upon coordination of the olefin, while the metal hydride addition-elimination involves a long-lived metal hydride that forms an alkyl intermediate (Figure 1-21).[179] However, in the case of ruthenium metathesis catalysts, the intermediate responsible for this undesirable reaction has not been identified yet, although it is often attributed to the formation of a ruthenium hydride in situ, as a decomposition product of the original carbene catalyst.[180,181]

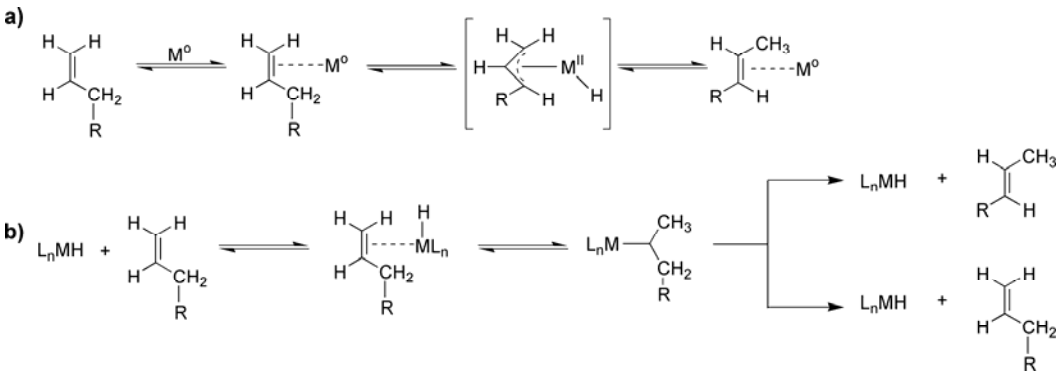

Figure 1-21. Olefin isomerization mechanism: a) π-allyl mechanism. b) metal-hydride addition-elimination mechanism

CHAPTER 2
METATHESIS ACTIVITY AND STABILITY OF NEW GENERATION RUTHENIUM POLYMERIZATION CATALYSTS

Reproduced in part with permission from: Courchay, F. C.; Sworen, J. C.; Wagener, K. B. *Macromolecules* **2003**, *36*, 8231-8239.

Introduction

The recent development of ruthenium carbene complexes (Figure 2-1) has increased considerably the utility of olefin metathesis both in the fields of organic synthesis and polymer chemistry. The introduction of the well-defined, functional-group tolerant complex $(PCy_3)_2(Cl)_2Ru{=}CHPh$ **[Ru]1** by Grubbs and coworkers[37,57,80,87] stimulated researchers' interest towards late-transition metal-catalyzed metathesis chemistry, for it is a useful catalyst in a variety of ring-closing metathesis (RCM), cross-metathesis (CM), acyclic diene metathesis polymerization (ADMET) and ring-opening metathesis polymerization (ROMP) reactions.[7-10,20,31] Improvements on this "first generation" ruthenium structure have been reported by many groups in recent times. For example, the Grubbs research group reported that incorporation of the more bulky and strongly sigma-donating imidazolylidene ligand leads to higher activity and thermal stability,[71] enabling the preparation of α-functionalized, di-, tri- and tetrasubstituted olefins.[12] These imidazolylidene based catalysts behave in a manner similar to that of early transition metal catalysts such as Schrock's molybdenum catalyst **[Mo]1**,[27,28] and remain active at loadings as low as 0.05 mol% for RCM and 0.0001 mol% for ROMP.[71]

Additional ligand variations have led to further improvements in both catalytic activity and stability. For example, Mol and coworkers[101] reported improved turnovers during the cross metathesis of terminal olefins with a modified version of the imidazolylidene ligand, catalyst $(IPrH_2)(PCy_3)(Cl)_2Ru{=}CHPh$ **[Ru]10**, first synthesized by Fürstner.[100] Also, Hoveyda *et al.*[95] have developed the complex $(H_2IMes)(Cl)_2Ru{=}CH(o\text{-}i PrOC_6H_4)$ **[Ru]9** which promotes olefin metathesis by a unique "release-return" mechanism, allowing efficient metal recovery without significant loss of activity. In fact, complex **[Ru]9** can readily be used in combinatorial synthesis in air with reagent-grade solvents. This Ru-complex offers reactivity, chemo- and stereoselectivity profiles differing from both catalysts **[Ru]1** and **[Ru]4**, notably during the metathesis of electron-deficient olefins.[96-98] The robustness of this complex also allows its use in solid-supported heterogeneous catalysis.[102-107,181]

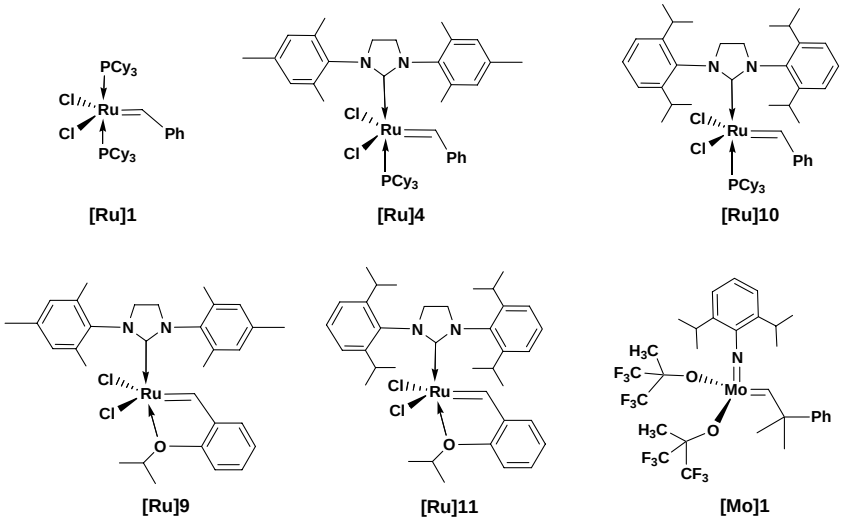

Figure 2-1. Metathesis catalysts

Acyclic diene metathesis (ADMET) chemistry has enjoyed the benefit of this metathesis catalyst research, resulting in the synthesis of unique architectures and new functionalized materials,[121-133,141-143] such as perfectly branched polyethylene,[127,128,130]

and amino acid containing polyolefins.[146,147] The choice of catalyst to perform these transformations is dictated by the monomer structure and the reaction conditions. For example, Schrock's catalyst is best used for hydrocarbon dienes and some functionalized olefins, whereas Grubbs' catalysts are preferred with highly-functionalized monomers and at higher temperatures. ADMET, CM and RCM require longer reaction times than ROMP chemistry, and so catalyst entities with longer lives are preferred. Consequently, our group has a particular interest in complexes that exhibit both long lifetimes and high turnovers ratios. A new catalyst structure (complex **[Ru]11**) was prepared by combining the thinking that yielded the Grubbs, Hoveyda and Mol complexes, and was found to exhibit improvements in terms of stability under ADMET conditions.

A kinetic approach was used to investigate the activity and utility of these ruthenium complexes during ADMET polymerization, work which has led to the design of more efficient ADMET catalyst systems.[155] Previously, Lehman and Wagener[144] reported a comparative kinetic study of Grubbs' catalysts **[Ru]1** and **[Ru]4** during the ADMET polymerization of the benchmark monomer, 1,9-decadiene, research that showed the effect of temperature on activity and initiation rates. Catalyst **[Ru]4** is clearly more active if used at temperatures of 45 °C and above. The olefin isomerization activity of catalysts **[Ru]1** and **[Ru]4** was investigated as well,[176] where catalyst **[Ru]4** was found to isomerize both external and internal olefins if used at its optimal temperature for ADMET, 60 °C. This observation is important to consider when building precise polymer microstructures.

Herein the early kinetic work is expanded to include complexes **[Ru]10, [Ru]9** and the new complex **[Ru]11**, comparing them with the 1st and 2nd generation Grubbs'

catalysts.[144] Initial rates of ADMET polymerization were measured at different temperatures, and the stability and activity of these complexes were examined at longer reaction times. Finally, their propensity to induce olefin isomerization was investigated under polycondensation conditions.

Results and Discussion

Kinetic Assessment of Catalyst Activity.

ADMET polycondensation of α, ω-dienes releases ethylene as the condensate, the volume of which can be measured and used to calculate the average degree of polymerization (DP) of the monomer as a function of time. The kinetic experiments were run for approximately an hour, focusing on the oligomerization (not polymerization) of the monomer. The monomer 1,9-decadiene was chosen in this study because of its well-understood behavior during ADMET chemistry. Monitoring oligomerization by plotting DP versus time allows for an efficient method to compare the catalytic activity for various complexes. Table 1 displays the initial rates of 1,9-decadiene ADMET chemistry, calculated as the initial slope (DP vs. time) of each kinetic curve during the average dimerization (DP=2) of the monomer.

Table 2-1. Initial rates for complexes **[Ru]1-[Ru]11** during the ADMET oligomerization of 1,9-decadiene

Catalyst	Monomer:Catalyst Ratio	Initial Rate (10^{-3} DP s^{-1})		
		30 °C	45 °C	60 °C
[Ru]1[a]	450:1	1.0 ± 0.5	2.3 ± 0.4	5.1 ± 0.6
[Ru]4[a]	450:1	0.42 ± 0.05	4.4 ± 0.7	23 ± 3
[Ru]10	450:1	36 ± 1	39 ± 7	55 ± 10
[Ru]10	900:1	8.8 ± 4.0	39 ± 1	78 ± 10
[Ru]9	450:1	4.8 ± 3	18 ± 5	-
[Ru]11	450:1	12 ± 2	42 ± 4	68 ± 10

[a] Data obtained from reference 144.

Catalytic activity was measured at three temperatures (30 °C, 45 °C and 60 °C) and two catalyst loadings (450:1 and 900:1 monomer:catalyst), providing a broad basis set to evaluate the catalyst systems tested. This activity was compared to the widely used 1st and 2nd generation ruthenium catalysts, previously examined in ADMET conversions by our group.[144]

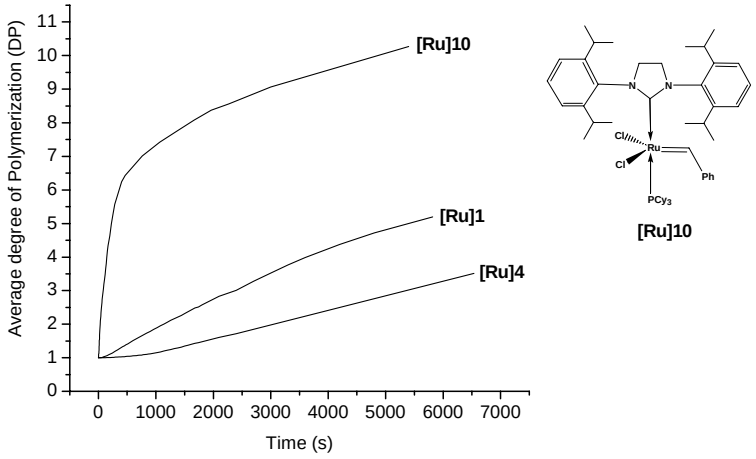

Figure 2-2. Degree of polymerization (DP) vs. time curves for complex **[Ru]1**, **[Ru]4** and **[Ru]10** using 450:1 monomer:catalyst ratio at 30°C

The kinetic runs at 30 °C show that the Mol catalyst, complex **[Ru]10,** exhibits the highest activity of any ruthenium complex to date in the dimerization of 1,9-decadiene. Figure 2-2 illustrates these data. When compared to the benchmark catalyst **[Ru]1**, complex **[Ru]10** shows a 36-fold increase in activity at 30 °C (see Table 1). This low temperature activity makes catalyst **[Ru]10** an ideal candidate for controlled organic synthesis and polymerization applications. Further, the initial dimerization rate when using complex **[Ru]10** is greater than either complex **[Ru]1** or **[Ru]4** at both 45 and 60 °C. For example, complex **[Ru]10** affords a dimerization rate of $55x10^{-3}$ DP s^{-1}, twice that when using complex **[Ru]4** at 60 °C; in fact, the high activity of complex **[Ru]10** at

60 °C makes it difficult to accurately measure the evolution of ethylene, resulting in a large error in the measured DP.

This higher activity of complex **[Ru]10** most likely originates from the increased steric bulk around the ruthenium center, a result of the isopropyl groups present on the ligand. Apparently, the interaction of the isopropyl groups with the carbene fragment and/or the chloro groups allows for faster and earlier dissociation of the tricyclohexyl phosphine, which has been commonly accepted as the initial rate-determining step of the metathesis reaction. This statement can be confirmed by comparing the ^{31}P NMR spectrum of complex **[Ru]10** versus either complex **[Ru]1** or **[Ru]4**. The phosphine resonance is shifted from 32 ppm for **[Ru]4** to 28.1 ppm for **[Ru]10**, where this upfield shift indicates a weaker Ru-P bond, implying an easier dissociation of the phosphine. Also, the induction period observed with **[Ru]4** is not observed with **[Ru]10**, which is consistent with complex **[Ru]10**'s faster phosphine dissociation. The induction period is thought to correspond to the initial dissociation of phosphine before the steady-state concentration of the 14 electron (e^-) ruthenium alkylidene complex is reached.

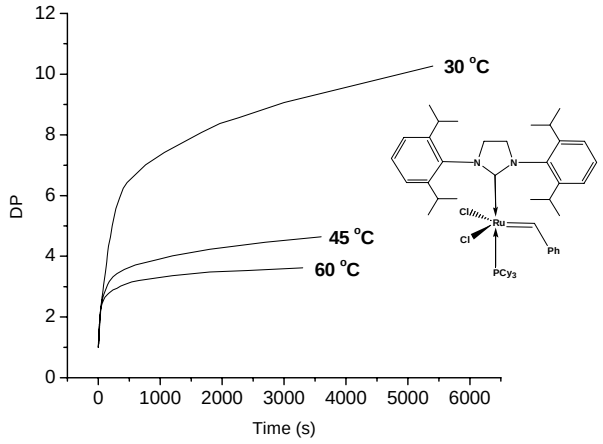

Figure 2-3. Comparison of the activity of complex **[Ru]10** at three different temperatures using a 450:1 monomer:catalyst ratio

While complex **[Ru]10** shows the largest decadiene dimerization rate for any complex to date, increasing temperature has an adverse effect on the lifetime of the catalyst (Figure 2-3). Complex **[Ru]10** no longer competes with either **[Ru]1** or **[Ru]4** at temperatures above 45 °C beyond trimerization of 1,9-decadiene. Figure 2-4 further illustrates this phenomenon; these lower turnovers were also reported by Mol at elevated temperature.[100,101] This decrease in conversion likely is due to the thermal decomposition of the complex as observed with Grubbs' catalysts,[87] or by way of C-H and/or C-C activation pathways.[182,183] Decomposition may occur faster with complex **[Ru]10** for 2 reasons: 1) the rate increase in phosphine dissociation is known to affect the catalyst stability by generating too many unstable 14 e^- species; 2) the presence of an electron rich methine proton on the isopropyl groups makes it more likely to undergo C-H activation than the methyl protons of complex **[Ru]4**. Moreover, the additional carbons on each isopropyl group may increase the probability of ruthenium insertion into the C-C bond.

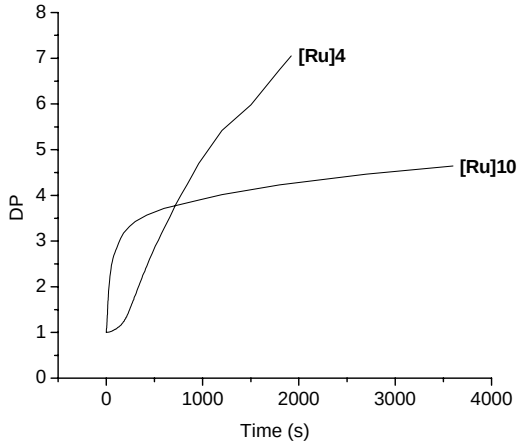

Figure 2-4. Degree of polymerization (DP) vs. time curves for complexes **[Ru]4** and **[Ru]10** using 450:1 monomer:catalyst ratio at 45 °C

On the other hand, this temperature trend is inverted when the monomer-to-catalyst ratio is doubled (Figure 2-5). Indeed, higher conversions are reported when the

temperature is increased from 30 to 60 °C with its average DP reaching 4 and 5.8, respectively. In addition, complex **[Ru]10** is more active initially at 60 °C when using lower catalyst ratios; the data are reported in Table 1. For example, when the catalyst concentration is decreased by a factor of two, the respective rate increases from $55x10^{-3}$ to $78x10^{-3}$ DP s^{-1}. The increase in the overall activity observed at high temperature when lower catalyst concentrations are used may correspond to a decrease in the catalyst decomposition rate, which would in turn support a bimolecular decomposition pathway.[87] However, at this point the possibility of an internal decomposition as outlined above cannot be ruled out. More likely, this would prove the coexistence of both mechanisms. Further, the reaction rate for complex **[Ru]10** at 30°C is decreased by a factor of 4, which is consistent with the lower catalyst ratio as little decomposition should occur at such low temperatures. Besides, this activity trend has been reported by Mol[101] as well in the dimerization of terminal olefins.

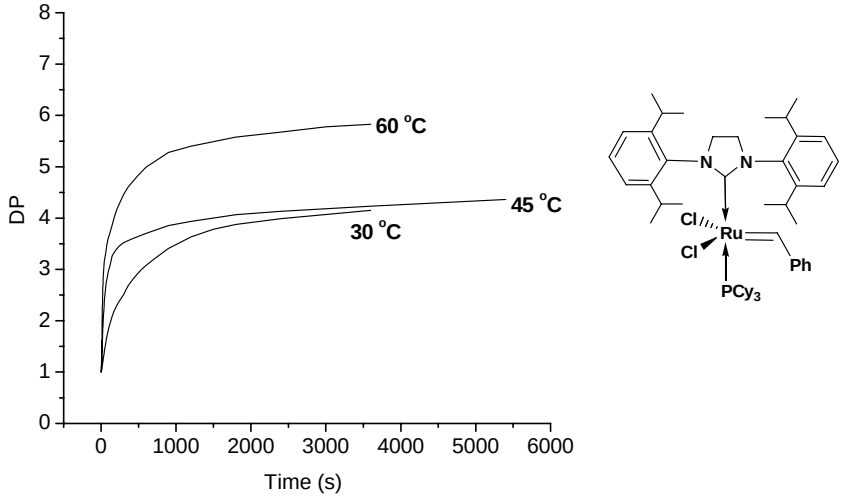

Figure 2-5. Degree of polymerization (DP) vs. time data for complex **[Ru]10** using 900:1 monomer:catalyst ratio

Although known for its particular tolerance to a variety of substrates,[95-98] complex **[Ru]9** appears to be unstable once dissolved in 1,9-decadiene, for complex **[Ru]9** affords low conversions at 30 °C and 45 °C (Figure 2-6). Consequently, no experiment was conducted at 60 °C with complex **[Ru]9**.

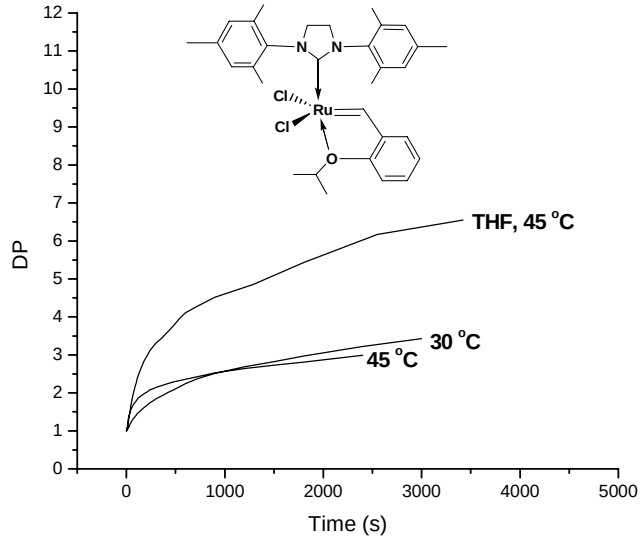

Figure 2-6. Degree of polymerization (DP) vs. time data for complex **[Ru]9** using 450:1 monomer:catalyst ratio

The low stability of complex **[Ru]9** may be attributed to its release-return mechanism, yielding an unstable 14 e^- species by the loss of isopropoxy styrene, which in turn produces the unbound ligand and/or its subsequent attachment to the chain end. We assume that the low stability of complex **[Ru]9** is due to this highly unstable 14 e^- intermediate not being restabilized by the isopropoxy ligand. This 14 e^- complex may have to be stabilized by coordination to the substrate (monomer) or solvent, and since 1,9-decadiene lacks any kind of electron donor or Lewis basic group, it is not able to serve as a stabilizing ligand. Consequently, the catalyst apparently decomposes immediately after activation. To verify this assumption, the same experiment was

conducted by adding a catalytic amount of THF to the bulk reaction mixture. As is apparent in Figure 2-6, a drop of THF improved the activity of complex **[Ru]9** when polymerizing 1,9-decadiene, which refutes the general belief that ruthenium catalysts exhibit lower metathesis activity in THF.[34]

These observations led us to synthesize complex **[Ru]11**, which in effect combines the thinking of Grubbs, Mol and Hoveyda. The complex was obtained in good yields by implementing the same synthetic procedure used to generate complex **[Ru]9**,[95] simply substituting complex **[Ru]10** as one of the starting compounds (Figure 2-7). Conveniently, **[Ru]11** can be purified in the air affording a dark green crystalline solid after flash chromatography and precipitation in hexane, where the copper-phosphine complex must be removed by filtration prior to column chromatography.

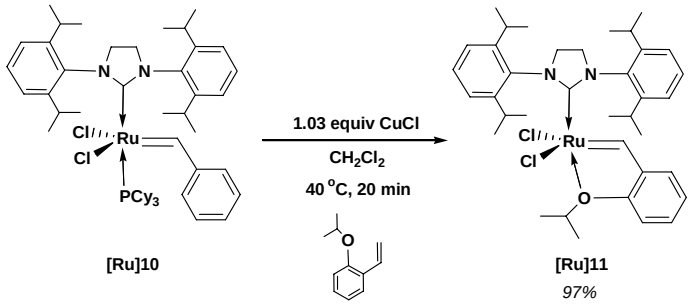

Figure 2-7. Synthesis of complex **[Ru]11**

The structure was confirmed through single-crystal X-ray analysis (Figure 2-8). Selected bond lengths and angles of both complexes **[Ru]9** and **[Ru]11** are provided in Table 2 for comparison. Complex **[Ru]11** is characterized by a distorted trigonal bipyramidal coordination about the metal center, with the alkylidene group and the chlorines in the same plan. The overall geometry and most of the bond angles and bond lengths are analogous to their related values in complex **[Ru]9**. As the bond angles show, the geometry of **[Ru]11** is a little more distorted, which was expected considering the

bulk brought about by the isopropyl groups. Noteworthy, the Ru-O bond is much shorter in complex **[Ru]11**, which indicates a stronger coordination.

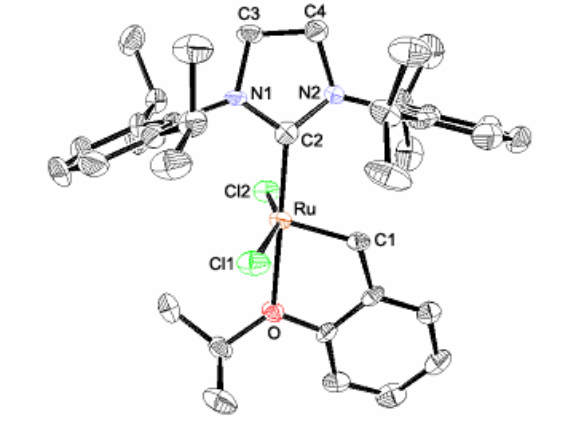

Figure 2-8. ORTEP Diagram of complex **[Ru]11**. Thermal ellipsoids are drawn at the 30% probability level

Table 2-2. Bond Lengths and Angles for Complexes **[Ru]9** and **[Ru]11**

	[Ru]9	**[Ru]11**
	Bond Length (Å)	
Ru-C(1)	1.828(5)	1.822(5)
Ru-C(2)	1.981(5)	1.978(5)
Ru-O	2.261(3)	2.247(3)
Ru-Cl(2)	2.328 (12)	2.3271(15)
Ru-Cl(1)	2.340(12)	2.3409(14)
N(1)-C(2)	1.350(6)	1.362(6)
N(2)-C(2)	1.351(6)	1.363(6)
	Bond Angles (deg)	
C(1)-Ru-C(2)	101.5(14)	102.0(2)
C(1)-Ru-O	79.3(17)	78.60(18)
C(2)-Ru-O	176.2(14)	171.94(17)
C(1)-Ru-Cl(2)	100.1(15)	99.57(15)
C(2)-Ru-Cl(2)	90.9(12)	86.24(15)
O-Ru-Cl(2)	85.3(9)	85.75(10)
C(1)-Ru-Cl(1)	100.2(15)	100.20(15)
C(2)-Ru-Cl(1)	96.6(12)	101.29(15)
O-Ru-Cl(1)	86.9(9)	86.44(9)
Cl(2)-Ru-Cl(1)	156.5(5)	156.84(6)
C(2)-N(1)-C(3)	127.2(4)	126.4(4)
C(2)-N(2)-C(4)	127.0(4)	124.6(4)

The activity of this new complex was evaluated using the same kinetic study as done previously with 1,9-decadiene. Contrary to its predecessor **[Ru]9**, complex **[Ru]11** catalyzes the ADMET oligomerization of 1,9-decadiene, as shown in Figure 2-9. The shape of the kinetic curves is the same as observed for the parent complex **[Ru]10**, and the overall activity is less a function of temperature. There is no definite trend, but 45 °C seems to be an optimal temperature. On the other hand, the initial oligomerization rate when using complex **[Ru]11** is more sensitive to temperature variations than it is for catalyst **[Ru]10**, reaching a maximum of 68×10^{-3} DP s^{-1} at 60 °C. Thus, higher temperatures are recommended to get fast initiation using this particular complex. Moreover, catalyst **[Ru]11** exhibits faster initial rates than **[Ru]9**, which is consistent with the introduction of the bulkier isopropyl groups on the imidazolylidene ligand. In fact, complex **[Ru]11** produces high molecular weight poly(octenamer) whereas complex **[Ru]9** only yields oligomers, even after 120 hours in the bulk.

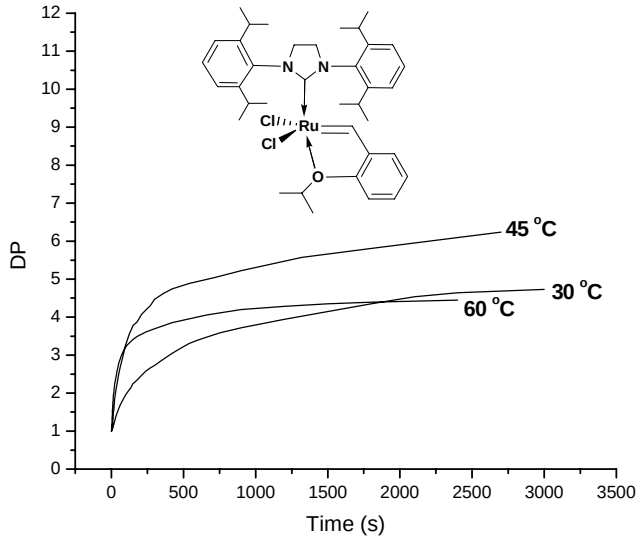

Figure 2-9. Degree of polymerization (DP) vs. time data for complex **[Ru]11** using 450:1 monomer:catalyst ratio

Interestingly, complex **[Ru]11** does not need THF to catalyze the ADMET reaction of 1,9-decadiene. To better understand the differences between catalysts **[Ru]9** and **[Ru]11** and the role of polar reaction conditions on these Hoveyda-type catalysts, kinetic experiments were completed using dipentenyl ether as the monomer instead of 1,9-decadiene. Dipentenyl ether was chosen for its inherent electron donating ability; it serves as both monomer and solvent, possibly allowing coordination to stabilize the reactive intermediate through a six-membered ring transition state (Figure 2-10).

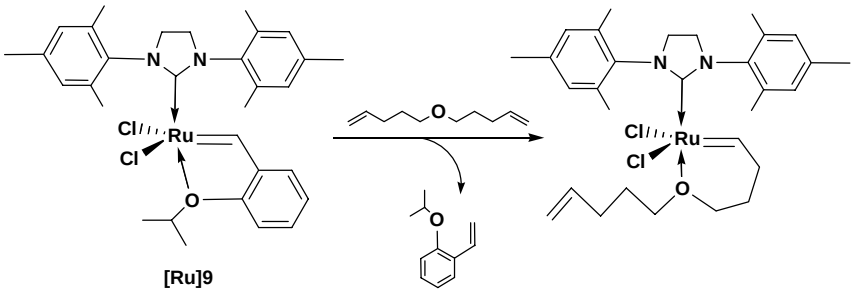

Figure 2-10. Proposed intermediate of complex **[Ru]9** during the metathesis of dipentenyl ether.

Surprisingly, the activity of complex **[Ru]9** with dipentenyl ether is actually lower than with 1,9-decadiene using the same kinetic conditions, suggesting that dipentenyl ether intramolecular complex is not sufficiently labile to allow coordination of other monomer molecules, thereby preventing further continuation of the metathesis process. Experiments conducted using complex **[Ru]11** (Figure 2-11) also show a decreased activity of about 1 DP s^{-1} where the initial rate drops from $42x10^{-3}$ DP s^{-1} (1,9-decadiene) to $15x10^{-3}$ DP s^{-1} (dipentenyl ether). The fact that a similar behavior was obtained with both complexes **[Ru]9** and **[Ru]11** suggests that these Hoveyda-type systems are sensitive to substrate polarity, and may give better results in solution with solvents of lower polarity. Another possibility could be that this particular ether is too sterically hindering to effectively stabilize the Ru center.

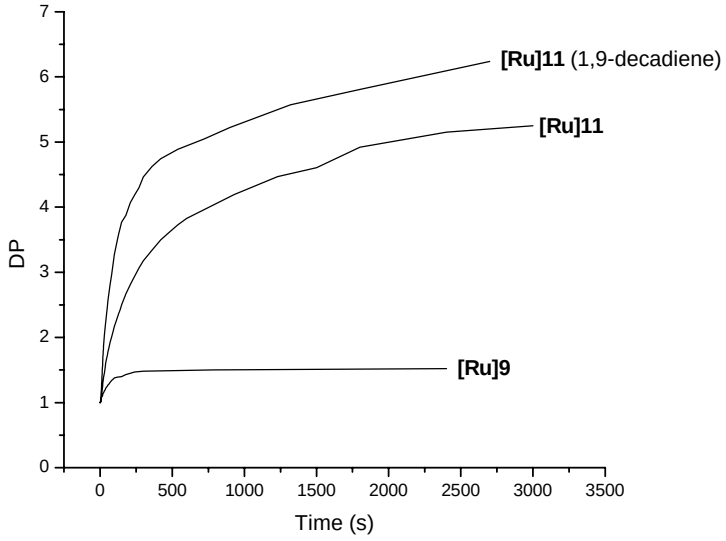

Figure 2-11. Degree of polymerization (DP) vs. time data for complexes **[Ru]9** and **[Ru]11** using dipentenyl ether as the monomer (450:1 monomer:catalyst)

Overall, **[Ru]11** is a better catalyst than **[Ru]9** for the ADMET oligomerization of either 1,9-decadiene or dipentenyl ether, although slightly less active towards the ether monomer. Considering the hypothesis of a $14e^-$ intermediate as proposed for the parent complex **[Ru]9**, the enhanced activity of **[Ru]11** can be explained in terms of olefin affinity. The isopropyl groups of the imidazolylidene should exert a stronger steric pressure on the carbene moiety and favor the formation of a metallacyclobutane with the incoming olefin. The inherent olefin affinity offers an ideal stabilization to the $14e^-$ intermediate and could account for the higher activity. In fact, the crystal structure of **[Ru]11** shows that the Ru-C bond with the N-heterocyclic carbene is slightly shorter than for complex **[Ru]9**.[95] This suggests a higher affinity of complex **[Ru]11** for π-acidic olefinic substrates. The Ru-O is also found to be shorter in complex **[Ru]11**, meaning the coordination of the oxygen to the ruthenium is stronger than in complex **[Ru]9**. Therefore, the increased stability of **[Ru]11** could be due to a higher tendency of the

isopropoxystyrene to come back and stabilize the 14e$^-$ intermediate. While the activity of complex **[Ru]11** at low conversion does not compete with the activity of complex **[Ru]10**, its long term stability, described below, renders it an attractive metathesis catalyst.

Thermal Stability of the Catalysts

The decomposition rates of complexes **[Ru]10** and **[Ru]11** were monitored by ^{1}H-NMR in d_6-benzene at 55 °C and calculated as the time for half the complex to decompose. As observed during the kinetic study, complex **[Ru]10** is not resistant to high temperatures, exhibiting a half-life of 90 min at 55 °C. On the contrary, complex **[Ru]11** remains completely intact at 55 °C for more than 3 days, showing no sign of decomposition whatsoever (Table 3). This complex is not only stable in air but also in solution even at elevated temperatures. This increased stability is desirable for RCM, CM and ADMET chemistry in solution and may also be useful for solid state ADMET polymerization.[184]

Table 2-3. Half-lives for the decomposition of complexes **[Ru]10** and **[Ru]11**

Complex	Temp.	Conc.	Half-life
[Ru]1[a]	55 °C	0.023M	8 days
[Ru]10	55 °C	0.032M	90 min
[Ru]9	55 °C	0.032M	>3 days

[a] Value taken from Grubbs *et al.* [37]

Further Comments on ADMET Polymerization

In order to expand these kinetic oligomerization measurements made using 1,9-decadiene, the utility of the complexes was investigated during full-scale polymerization of this monomer. These polymerizations were conducted using standard Schlenk techniques, with complexes **[Ru]10** and **[Ru]11** at 55 °C using both 450:1 and 900:1

monomer:catalyst ratios (Table 4). The resultant poly(octenamer)s were characterized by ^{1}H and ^{13}C-NMR and further analyzed by GPC and DSC. Molecular weights were compared to poly(octenamer)s obtained with the catalyst systems **[Ru]1**, **[Ru]4** and **[Mo]1**.

Table 2-4. Polymerizations of 1,9-decadiene at 55 °C for 120 h

Catalyst	Monomer:Catalyst ratio	M_n (g/mol)	PDI
[Ru]1	450:1	12,000	1.8
[Ru]4	450:1	78,000	1.8
[Mo]1	1200:1	15,000	1.7
[Ru]10	450:1	29,000	1.6
[Ru]10	1000:1	37,000	1.9
[Ru]11	450:1	21,000	1.6
[Ru]11	1000:1	32,000	1.6

When the polymerizations were heated at 55 °C for an extended period, poly(octenamer) was obtained with M_n of 37,000 g/mol using complex **[Ru]10** and 32,000 g/mol using complex **[Ru]11**. This is an encouraging result, as the benchmark Shrock's molybdenum catalyst **(6)** for ADMET polymerization produces a polymer half that average mass, or M_n= 15,000 g/mol poly(octenamer) under the same conditions. Both are acceptable molecular weights in step polymerization chemistry, especially for functionalized versions of polyolefins made by this route. Endgroup conversion increases from 99.1% to 99.6% in this doubling of molecular weight, clearly illustrating how clean mechanistic chemistry is essential in any step polymerization. Further, the use of complex **[Ru]10** or **[Ru]11** leads to successful polymerization with lower catalyst loadings (0.05 mol%).

Complex **[Ru]9** was not included in this polymerization study since initial experiments at 30 °C in the bulk produced only oligomeric poly(octenamer), an observation consistent with the model kinetic study. However, the situation differs when

functionalized dienes are used in a polar medium as this catalyst was successful in polymerizing amino-acid containing monomers in THF.[131]

Isomerization of the Olefin Bond

Olefin isomerization is a major side reaction of Ru-catalyzed metathesis; however, the specie(s) responsible for such transformation, whether it is a decomposition product or the metathesis catalyst itself, have not been fully identified yet.[176,185] Studying isomerization therefore occupies a significant part in the process of understanding catalyst decomposition. Besides, under ADMET conditions olefin isomerization generates irregular polymer microstructures, and since part of our group research focuses on precision in polymer synthesis, the isomerization activity of complexes **[Ru]10** and **[Ru]11** was also explored in detail. The isomerization study was done using a model compound, 1-octene as the starting reagent, and the reaction was monitored by GC analysis. Typical results are illustrated in Figure 2-12 for complex **[Ru]10**. In fact, both complexes **[Ru]10** and **[Ru]11** isomerize the olefinic bonds in the reactant as well as in the metathesis products.

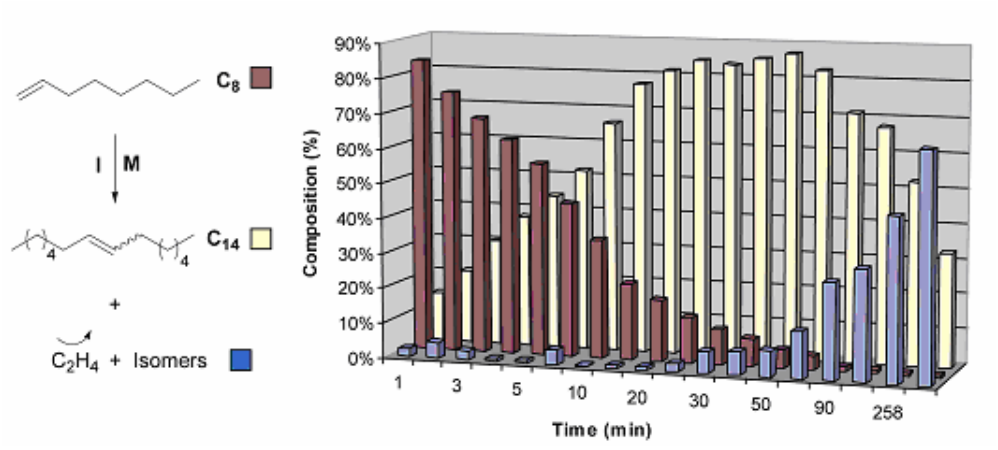

Figure 2-12. Composition of olefin mixture as a function of time for reaction of **[Ru]10** with 1-octene at 30°C

If self-metathesis were the only mechanism operating in the presence of these catalysts, then this model reaction would yield 7-tetradecene exclusively (C_{14} in the figure above). Figure 2-12 shows that not to be the case, where the concentration of isomerized products increases at the expense of the product, 7-tetradecene and the starting reagent, 1-octene. For example, exposure of 1-octene to complex **[Ru]10** at room temperature leads to 94% conversion (1 hour), where the product mixture consists of 82% 7-tetradecene and 18% isomers. By comparison, complex **[Ru]4** is less active in this model study, requiring 3 days at room temperature to generate a similar conversion (86%). Complex **[Ru]4** is slower to isomerize olefins, however, yielding a mixture containing only 3% isomers. Longer run times using complex **[Ru]10** at room temperature result in considerably higher quantities of isomer content, up to 76% of the final product mixture. The starting reagent, 1-octene, is completely consumed, and the distribution of isomerized products (as determined by GC analysis) is centered about 7-tetradecene.

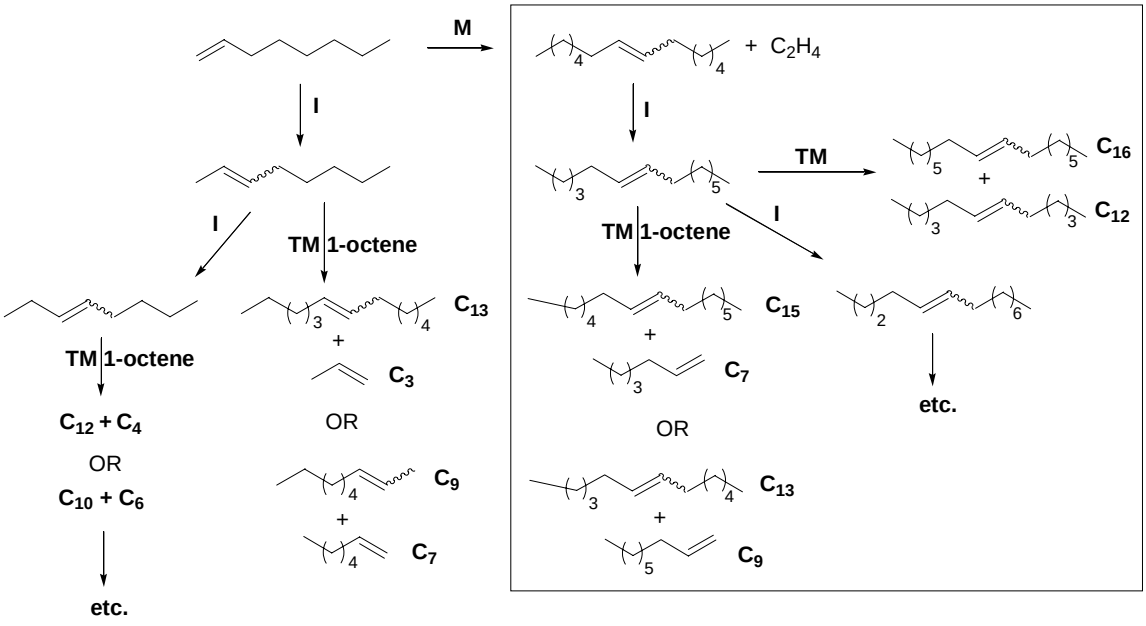

Figure 2-13. Proposed mechanism for isomerization of 1-octene

These observations are consistent with isomerization chemistry operating concurrently with metathesis, although at a slower rate than the initial condensation metathesis chemistry, which yields 7-tetradecene. In fact, three different reaction mechanisms operate concurrently throughout the conversion of 1-octene: condensation metathesis (we abbreviate this reaction as "M"), trans-metathesis (involving both internal double bonds and active metal alkylidene chain ends) (abbreviated "TM"), and isomerization chemistry (abbreviated "I") (Figure 2-13).

These three reactions compete until condensation metathesis is complete, after which only trans-metathesis (TM) and isomerization (I) continue. If the catalyst entities possess sufficiently long lives as appears to be the case for complex **[Ru]10**, then the starting reagent, 1-octene, will be completely consumed, and an equilibrium mixture of isomerized products will result. Complex **[Ru]11** approaches this situation, with conversions of 98% and a lower percentage of isomerization (23%) after 3 days. These results are consistent with the data of the kinetic study, and the product/isomer distribution indicates that isomerization occurs concurrently with metathesis. The relative rates of condensation metathesis, trans metathesis, and isomerization apparently differ depending upon the identity of the metal catalyst complex, with isomerization being significantly slower than trans-metathesis, and trans-metathesis being slower than condensation (end group) metathesis.

Since isomerization occurs at a slower rate than either metathesis reaction with complex **[Ru]10**, lower temperatures should suppress this reaction to the advantage of metathesis chemistry. This has been shown to be true in prior research,[176] and the same observation is noted here when using catalyst **[Ru]10**. In fact, the conversion of 1-octene

is quantitative at 0 °C in 3 days, with only 30% of the product mixture being isomers, as compared to 76% isomers at room temperature.

Recently, Mol *et al.*[92] demonstrated that a possible decomposition pathway of catalyst **[Ru]1** results in the formation of $(PCy_3)_2(CO)Ru(Cl)(Ph)$ which appears to be a good precatalyst for olefin isomerization. This carbonyl complex could be converted into the corresponding hydride $(PCy_3)_2(CO)Ru(Cl)(H)$ upon reaction with a terminal olefin and could promote 1-octene isomerization without any trace of metathesis product. Further, Grubbs and coworkers[72] witnessed the formation of the hydride complex $(H_2Mes)(PCy_3)(CO)Ru(Cl)(H)$ by heating complex **[Ru]4** in the presence of oxygen-containing substrates. These prior observations suggest that the ruthenium hydride equivalent of **[Ru]10** could be formed under ADMET reaction conditions and could account for the isomerization chemistry reported herein. The rapid decomposition of complex **[Ru]10** observed during our prior kinetic study is consistent with isomerization occurring early in the reaction and increasing over time, all as a result of increasing ruthenium hydride concentration. However, the possibility of isomerization catalyzed by the metathesis catalyst itself cannot be ruled out at this point.

Complex **[Ru]10** is sufficiently active to induce isomerization of the starting reagent, 1-octene to other C_8 isomers (2-, 3- and 4-octene), which happens concurrently with metathesis chemistry, and further, complex **[Ru]10** appears to induce isomerization of internal bonds at a substantially higher rate than other catalysts.

Additional evidence for the high propensity of catalysts **[Ru]10** and **[Ru]11** to isomerize internal olefins is found in the melting behavior of the materials produced when using them to polymerize 1,9-decadiene. Schrock's molybdenum catalyst

(complex **6**), which yields virtually no isomerization, produces poly(octenamer) that exhibits a melting point of 75°C,[176] close to the theoretical maximum for this polymer. On the other hand, catalysts **[Ru]10** and **[Ru]11** yield poly(octenamer) samples possessing considerably lower melting points, 40 °C and 45 °C respectively. Isomerization, in effect, creates random copolymers via migration of internal olefins along the polymer backbone or via monomer isomerization. This decrease in regioregular placement of olefinic groups in the poly(octenamer) results in a depression of the polymer peak melting point as observed for both catalyst **[Ru]10** and **[Ru]11**.

Conclusions

Complex **[Ru]10** is highly active at low temperatures for the ADMET polymerization of 1,9-decadiene; loadings as low as 0.1 mol% produced high molecular weight poly(octenamer). In addition, complex **[Ru]10** has the highest initiation rate of any phosphine ligated ruthenium complex to date. The catalyst is sensitive to thermal decomposition and therefore becomes less active as the temperature increases. The high initiation rate and activity at low temperatures make complex **[Ru]10** an interesting prospect for further metathesis considerations, notably for low boiling point reagents or thermally sensitive substrates in both organic synthesis or polymerization. On the contrary, complex **[Ru]9** does not exhibit satisfactory activity with non functionalized substrates. Although known for its robustness, complex **[Ru]9** appears to require stabilization either from a polar solvent or from a functionalized monomer in order to serve as a viable polycondensation catalyst. Complex **[Ru]11** exhibits an interesting stability and produces high molecular weight polymers. The increase of steric interactions on the 4,5 dihydroimidazolylidene carbene ligand increases the catalytic

activity, while the incorporation of Hoveyda-type ligand expands the stability of the complex.

Complexes **[Ru]10** and **[Ru]11** both catalyze olefin isomerization in high yields, however, given that both complexes are highly reactive at room temperature their isomerization/metathesis processes can be mediated by lowering the reaction temperature. In fact, complex **[Ru]10** efficiently metathesizes 1-octene at 0 °C resulting in faster metathesis rates than isomerization. This isomerization pathway could be attributed to the hydride complex, whose formation and/or catalytic activity is highly dependent on temperature conditions. Therefore, increasing the catalyst stability towards decomposition seems most important to design catalysts that will produce regular polymers via metathesis chemistry. Nonetheless, complexes **[Ru]10** and **[Ru]11** are useful catalysts for ADMET polymerization, without the temperature constraints of either catalysts **[Ru]1** or **[Ru]4**.

Experimental

General Considerations

^{1}H NMR (300 MHz) and ^{13}C NMR (75 Hz) spectra of the ADMET polymers were recorded in $CDCl_3$ on either a Mercury series or Varian VXR-300 NMR superconducting spectrometer. Chemical shifts were referenced to residual $CHCl_3$ (7.23 for ^{1}H and 77.23 for ^{13}C) with 0.03% v/v TMS as an internal reference. All organometallic spectra were recorded in d_6-benzene and the chemical shifts were referenced to residual C_6H_6 (7.16 for ^{1}H and 128.39 for ^{13}C).

Gel permeation chromatography (GPC) of the unsaturated ADMET polymers was performed using two 300 mm Polymer Laboratories gel 5μm mixed-C columns. The instrument consisted of a Rainin SD-300 pump, Hewlett-Packard 1047-A RI detector

(254 nm), TC-45 Eppendorf column heater set to 35 ^{o}C, and Waters U6K injector. The solvent used was THF at a flow rate of 1.0 mL/min. Polymer samples were dissolved in HPLC grade THF (approximately 0.1% w/v) and filtered before injection. Retention times were calibrated to polystyrene standards from Polymer Laboratories (Amherst, MA).

GC analysis was conducted on a Shimadzu GC-17A chromatograph equipped with a HP-5 (Hewlett Packard) 25 m column with FID detection. All amounts of products were calculated by a systematic ratio to the Decalin peak at 8.72 minutes, using the integrated peak areas.

Differential scanning calorimetry (DSC) was performed using a Perkin-Elmer DSC 7 at a heating rate of 10 °C/min. Thermal calibrations were made using indium and freshly distilled n-octane as references for thermal transitions. Heats of fusion were referenced against indium. The samples were scanned for multiple cycles to remove recrystallization differences between samples and the results reported are the second scan cycle. Reported values are given as T_m (melting peak).

Complex **[Ru]9** was a gift from Materia Co. and was used as received. Complex **[Ru]10** was synthesized according to the literature procedure.[101] All catalysts were stored in an argon-filled drybox prior to use in kinetic and polymerization experiments. 1,9-Decadiene (Aldrich) was distilled from Na/K alloy under reduced pressure into a Kontes flask equipped with a Teflon valve, degassed by three freeze-pump-thaw cycles, and stored in an argon-filled drybox. For the kinetic study, 1,9-decadiene was portioned into small Teflon-capped vials in the drybox and were removed and stored in a dessicator until use. All polymerizations were conducted in the bulk using the different monomer-

to-catalyst ratio displayed in the tables. 2-Isopropoxystyrene was synthesized by a standard Wittig reaction on 2-isopropoxybenzylaldehyde using (methyl)triphenylphosphine iodide and potassium *t*-butoxide (Aldrich). 2-Isopropoxybenzylaldehyde was synthesized via a Williamson-ether synthesis from salicyl-aldehyde (Aldrich) and 2-bromopropane (Aldrich). Pentenyl ether was synthesized according to the literature,[123] distilled over CaH_2 and stored in the drybox. All other starting materials were distilled over Na/K alloy before use, except chlorinated compounds which were distilled over CaH_2. After distillation, d_6-benzene was degassed by three freeze-pump-thaw cycles, and stored in an argon-filled drybox.

X-ray Experimental

Crystals suitable for X-ray structure determination were obtained from slow diffusion of pentane into a saturated solution of **[Ru]11** in CH_2Cl_2 at room temperature. Data were collected at 173 K on a Siemens SMART PLATFORM equipped with A CCD area detector and a graphite monochromator utilizing MoK_α radiation (λ = 0.71073 Å). Cell parameters were refined using up to 8192 reflections. A full sphere of data (1850 frames) was collected using the ω-scan method (0.3° frame width). The first 50 frames were remeasured at the end of data collection to monitor instrument and crystal stability (maximum correction on I was < 1 %). Absorption corrections by integration were applied based on measured indexed crystal faces.

The structure was solved by the Direct Methods in *SHELXTL6,* and refined using full-matrix least squares. The non-H atoms were treated anisotropically, whereas the hydrogen atoms were calculated in ideal positions and were riding on their respective carbon atoms. The asymmetric unit consists of two chemically equivalent but

crystallographically independent Ru complexes and a half molecule of dichloromethane (located on a center of inversion). A total of 813 parameters were refined in the final cycle of refinement using 22770 reflections with $I > 2\sigma(I)$ to yield R_1 and wR_2 of 6.48% and 8.38%, respectively. Refinement was done using F^2.

Synthesis of Complex [Ru]11

In a glovebox, complex **[Ru]10** (930 mg, 1.00 mmol) and CuCl (Aldrich) (100 mg, 1.03 mmol) were weighed into a 100 mL Schlenk flask and dissolved in 20 mL of CH_2Cl_2. 2-Isopropoxystyrene (180 mg, 0.970 mmol) was dissolved in 2 mL of CH_2Cl_2 and added to the solution of complex **[Ru]10** and CuCl at room temperature. The flask was equipped with a condenser and the solution was refluxed for 20 minutes. From this point forth, all manipulations were carried out in air with reagent-grade solvents. The reaction mixture was concentrated in vacuo to a green residue. The unpurified material was dissolved in a minimal volume of 1:1 pentane/CH_2Cl_2 and loaded onto a plug of silica gel. Insoluble copper-phosphine precipitates were removed prior to loading by passing the solution through a second Pasteur pipette containing a plug of glass wool. Elution with 1:1 pentane/CH_2Cl_2 removed a bright green band from the column. The eluant was concentrated and addition of hexanes just prior to complete removal of the solvent resulted in spontaneous precipitation of the product. Filtration and drying under high vacuum afforded 691 mg (0.970 mmol, 97%) of a pale green powder. ^{1}H NMR (C_6D_6, 300 MHz): δ (ppm)=16.4 (s, 1H, Ru=C*H*Ph), 7.53 (t, 2H, *para* C*H*, $^3J_{H,H}$= 7.2Hz), 7.43 (m, 1H, *ortho* C*H*), 7.37 (m, 4H, *meta* C*H*), 6.80 (td, 2H, *meta-para* C*H*, $^3J_{H,H}$= 7.4Hz), 6.78 (d, 1H, *ortho* CH, $^2J_{H,H}$= 8.4Hz), 4.92 (sept, 1H, (CH_3)C*H*OAr, $^3J_{H,H}$= 6.3Hz), 4.18(s, 4H, N(CH_2)$_2$N), 3.60 (sept, 1H, C*H*(CH_3)$_2$, $^3J_{H,H}$= 6.6Hz), 1.38 (d, 6H,

OCH(CH_3)$_2$, $^2J_{H,H}$ = 6.3Hz), 1.26 (d, 24H, CH(CH_3)$_2$, $^3J_{H,H}$ = 7.1Hz); ^{13}C NMR (C_6D_6, 75 MHz): δ = 296.7, 215.5, 149.6, 144.79, 130.0, 129.1, 124.8, 122.4, 122.2, 113.2, 112.1, 112.1, 75.2, 54.9, 29.3, 26.8, 23.9, 21.9.

Kinetic Study

The kinetic study was performed with the same apparatus and following the same procedure as previously described by Wagener.[144] Each catalytic run was repeated 5 times for reproducibility.

ADMET Polymerization of 1,9-decadiene

All glassware was thoroughly cleaned and oven-dried. All metathesis reactions were initiated inside the drybox using 50 mL Schlenk flasks equipped with a Teflon stirbar. The flasks were then brought out of the drybox and placed on a high vacuum line ($<10^{-3}$ mmHg) while vigorously stirring. The polymerization vessel was exposed to intermittent vacuum at room temperature until the reaction either became highly viscous or solid (stirring ceased). The flask was then placed in 55 °C oil bath at high vacuum ($<10^{-3}$ mmHg) for 120 hours. The polymerization vessel was cooled at room temperature, and finally, the unsaturated polymer was taken up into toluene and precipitated into cold acidic methanol (1 M HCl) to remove catalyst residue.

Self-Metathesis Dimerization

A clean, dry 50 mL Schlenk flask equipped with a Teflon stir bar was charged with complex **[Ru]10** or **[Ru]11** at the desired ratio in the drybox. The flask was brought out of the drybox and placed on a Schlenk line. Typically, 4.5 mmol of olefin was injected through an Ar purged syringe. The mixture was stirred vigorously at the desired temperature under Ar and open to an oil bubbler to maintain ambient pressure. For complex **[Ru]10**, samples were taken at appropriate intervals under a positive pressure of

Ar with a dry pipette and added to a chloroform solution containing traces of 2,6-di-t-butyl-4-methylphenol used as a radical inhibitor, ethyl vinyl ether used to quench the metathesis catalyst, and Decalin used as a standard internal reference.

Measurement of the Thermal Stability of Complex [Ru]10 and [Ru]11

Benzene-d_6 solutions (32 mM) of complexes **[Ru]10** and **[Ru]11** were heated to 55 °C and monitored by ^{1}H NMR spectroscopy. The half-life was calculated as the time required for half the material to decompose ($\tau_{1/2}$) through integration of the carbene peak (19.9 ppm for **[Ru]10**, 16.4 ppm for **[Ru]11**) which disappears with decomposition of the complex.

CHAPTER 3
THE UTILITY OF HOVEYDA-TYPE CATALYSTS IN ADMET CHEMISTRY: STERICS VS. ELECTRONICS

Introduction

Over the past decade, olefin metathesis has become a major synthetic method for the formation of C-C bonds,[1,2,7-10,20] especially since the discovery of the Grubbs' functional group tolerant ruthenium carbene catalyst **[Ru]1**.[37,57,80,87] Its reactivity was further enhanced by exchanging one phosphine with an *N*-heterocyclic carbene (NHC) ligand (complex **[Ru]4**[71]and **[Ru]10**[100,101]). This phosphine mimic, being a strong σ-donor but a weak π-acceptor, favors the binding of olefinic substrates to ruthenium, which results in higher turnovers.[64,70,71,74,75,101] Since then, other modified complexes have been reported (Figure 3-1), among them the Hoveyda-type catalysts bearing an isopropoxystyrene ligand (**[Ru]9**).[95] The chelating nature of the ligand provides an exceptional stability to this type of catalyst and allows its recovery after some ring-closing metathesis (RCM) and cross-metathesis (CM) reactions.[186]

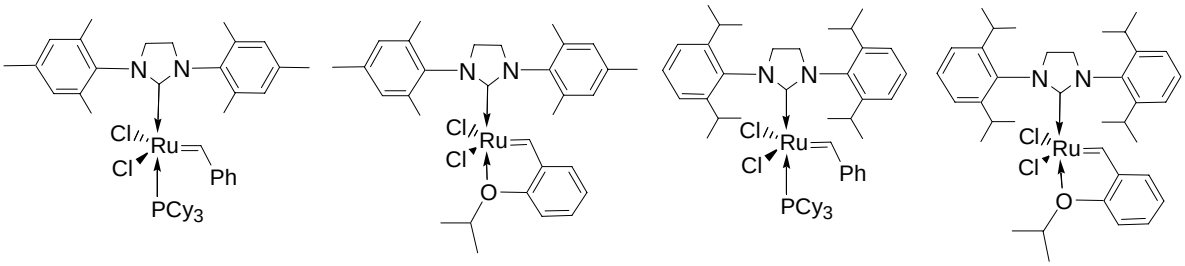

[Ru]4 **[Ru]9** **[Ru]10** **[Ru]11**

Figure 3-1. Olefin metathesis catalysts

Even though these phosphine-free alkylidenes initiate more slowly than their phosphine analogs, they have gathered much interest for both their ease of use and their

enhanced reaction rates with electron deficient olefins. In addition, the isopropoxystyrene ligand represents an ideal anchor point for modification studies involving the introduction of different steric and electronic groups[108,109,187-190] as well as ionic groups[191] and solid supports.[102-107] Fine tuning of the ligand structure can be achieved for a desired substrate, as the initiation rate and the overall activity of these catalysts have proven very sensitive to the nature of the isopropoxybenzylidene. As suggested by the dissociative mechanism, the catalytic activity can be enhanced by 1) increasing the steric hindrance around the isopropoxy group, or 2) decreasing the electron density at both the chelating oxygen atom and the benzylidene carbon.[108,109]

Our laboratory routinely uses metathesis catalysts for the synthesis of unique macromolecules via acyclic diene metathesis (ADMET) polymerization.[21,22,121-133,146-148] The extended lifetime of this class of catalyst is of particular interest, since long-living catalysts are desirable considering the reaction times required by ADMET polycondensation. Typically, the activity of a catalyst in ADMET is evaluated through comparative kinetic experiments using standard catalysts **[Ru]1** and **[Ru]4**, and 1,9-decadiene as the substrate.[155,144,192] This method has allowed to find optimal conditions of temperature and concentration for a wide range of metathesis catalysts in ADMET chemistry.[144,192] In addition, the effect of structural perturbations on catalytic activity was investigated in order to model more efficient catalyst systems. For instance, larger substituents around the NHC ligand (**[Ru]10** and **[Ru]11**) result in faster initial rates while incorporation of isopropoxybenzylidene expands the stability of the complex (**[Ru]9** and **[Ru]11**).[192]

After developing complex **[Ru]11**, whose increased activity was more suitable to ADMET polymerization,[192] the effect of electronics on the isopropoxy fragment of the catalyst was examinated. Herein, a comprehensive study is presented on a series of ruthenium catalysts bearing different isopropoxybenzilydene ligands and different NHC ligands (Figure 3-2). Their catalytic activity is measured during the ADMET oligomerization of 1,9-decadiene at different temperatures, and their initial rates are compared to standard catalysts for ADMET.

Results and Discussion

Following the introduction of faster initiators by increasing the NHC ligand bulk, the focus turned to the isopropoxy fragment of the catalyst, the idea being to enjoy the inherent stability of the Hoveyda-type catalysts while improving their catalytic activity in ADMET. Although the influence of electronics and sterics has been studied in much detail in small molecule chemistry,[108,109,187,190] the catalytic activity was only observed during monocoupling reactions such as cross-metathesis or ring-closing metathesis. The polycondensation nature of ADMET renders the catalytic profile very different, hence the use of different parameters to measure catalytic activity in this study. For example, complex **[Ru]9** has been successful in many organic reactions but only results in low conversions in the ADMET oligomerization of 1,9-decadiene.[192] Therefore, electronic modifications were applied on complex **[Ru]11**, which has proven to be an efficient ADMET catalyst. The design of catalysts **[Ru]13-[Ru]16** was based on the idea that decreasing the electron density at the chelating *i*PrO fragment would result in even higher catalytic activities, the ultimate goal being the elaboration of a Hammett plot. The same modifications were applied to complex **[Ru]9** to control the influence of sterics on the NHC ligand.

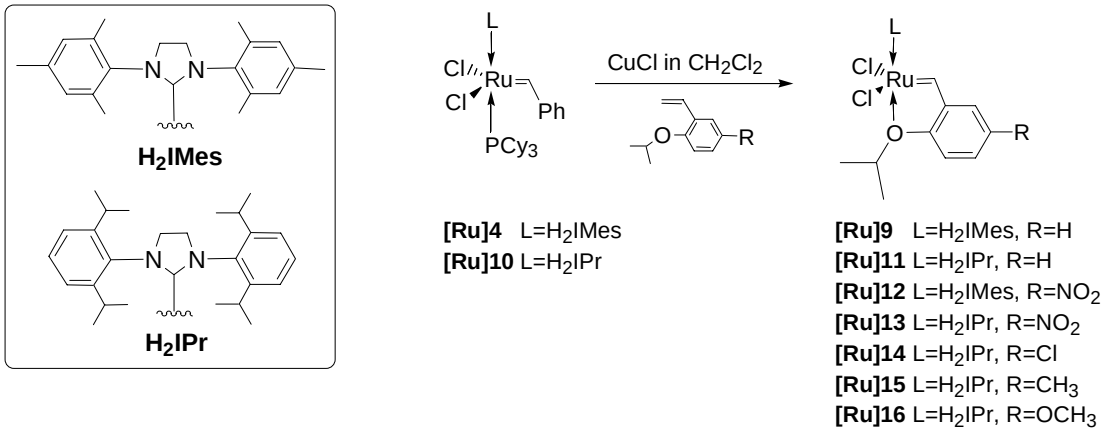

Figure 3-2. Synthesis of complexes **[Ru]9**, **[Ru]11-16**

The ligands were obtained from the corresponding substituted o-hydroxybenzaldehyde which was subjected to a Williamson substitution followed by a Wittig reaction. The synthesis of complexes **[Ru]12-16** then followed the same procedure as for complex **[Ru]9** and **[Ru]11**, affording good to excellent yields (83-95%).[95] All complexes are stable in solution and in air.

Each catalyst was subjected to a systematic reaction with 1,9-decadiene using a 450:1 monomer:catalyst ratio to reproduce typical polymerization conditions. Reaction progress was followed by quantifying ethylene as it was released, and the degree of polymerization was plotted against time.[155] The catalytic activity was evaluated in comparison with **[Ru]9** and **[Ru]11** at 30°, 45° and 60°C.

Steric effect

Table 1 shows the initial rates for catalysts **[Ru]9,11** and **[Ru]12,13** at different temperatures, calculated as the initial slope (DP vs. time) of each kinetic curve during the average dimerization (DP=2) of the monomer.[193] Rates increase with temperature for all complexes, and a straight line is obtained when the log of the initial rate is plotted against 1/T, verifying the Arrhenius law. The activation energies E_a are estimated to be 40.2

$KJ \cdot mol^{-1} \cdot s^{-1}$ and 48.9 $KJ \cdot mol^{-1} \cdot s^{-1}$ for **[Ru]11** and **[Ru]13** respectively. Introduction of the nitro group on the isopropoxybenzylidene results in an increase of the initial rate for both catalysts, for indeed, the presence of the electron withdrawing substituent *para* to the isopropoxy group should facilitate the ligand dissociation by decreasing the electron density on the coordinating oxygen, leading to the active species.[95,99,194] However, a closer examination at Table 1 indicates that the electronic effect is only minimal for catalyst **[Ru]12**, bearing the mesityl NHC ligand, conversely to what was observed in monocoupling reactions.[109,195] Indeed, catalysts **[Ru]9** and **[Ru]12** exhibit comparable initial rates regardless of the temperature (around 20 DP s^{-1} at 45°C, and 42 DP s^{-1} at 60°C). This observation emphasizes the fundamental difference between small molecule metathesis and ADMET, where the initial rate is not necessarily a direct correlation of the isopropoxystyrene dissociation rate, but also involves the stability of the 14 e^- complex. In this case, the propagating species $Ru=CH(CH_2)_6CH=CH_2$ is the same for catalysts **[Ru]9** and **[Ru]12**. The similarity of the initial rates obtained here, regardless of the dissociating ligand, seems to indicate that the propagation step is rate determining in ADMET, i.e. that dissociation is fast.

Table 3-1. Initial rates in DP s^{-1} for catalysts **[Ru]9**,**[Ru]11-13**.

Temperature	**[Ru]9**	**[Ru]12**	**[Ru]11**	**[Ru]13**
30°C	5 ± 3	10 ± 2	13 ± 2	21 ± 4
45°C	20 ± 5	22 ± 4	45 ± 4	48 ± 7
60°C	42 ± 4	42 ± 9	70 ± 10	117 ± 8

In the case of catalysts **[Ru]11** and **[Ru]13**, containing a bulkier NHC ligand, the nitro group seems to have a smaller effect on the initial rate, if any, at 30 and 45°C than at 60°C. For example, at 45°C the nitro complex **[Ru]13** only exhibits a 3 DP s^{-1} rate increase (within the experimental error) compared to parent **[Ru]11**, while a 50 DP s^{-1}

rate increase is reported at 60°C for **[Ru]13**. The difference at 30°C does not seem significant and will be further investigated by comparing other electronically modified catalysts **[Ru]14-[Ru]16**. The higher rates of complexes **[Ru]11** and **[Ru]13** versus **[Ru]9** and **[Ru]12** are due to the increase in steric bulk on the NHC ligand brought about by the isopropyl groups, which exert a stronger steric pressure on the benzylidene and therefore facilitate its dissociation.[61] As a consequence, at 60°C complex **[Ru]13** exhibits one of the fastest initiation rates (117 DP s^{-1}) ever reported for the ADMET reaction of 1,9-decadiene.

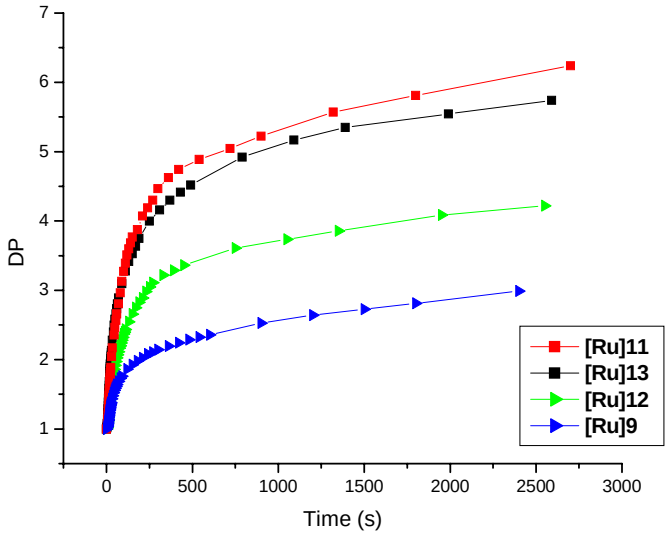

Figure 3-3. Degree of polymerization (DP) vs. time data for H_2IMes versus H_2IPr containing catalysts using 450:1 monomer:catalyst ratio at 45°C

This substituent effect is not as obvious when examining the overall activity of the catalysts **[Ru]9**,**[Ru]11-13** (Figure 3-3). The 'tailing off' of each curve is due to the reaction mixture becoming more viscous as the DP increases until reaching a solid state (around a DP of 4-5) where the rate becomes diffusion controlled. Even so, the catalysts deviate from the initial trend discussed above before reaching the solid state and after

dimerization. The catalysts bearing bulkier NHC ligands (**[Ru]11** and **[Ru]13**) seem to be unaffected by the presence of the nitro group, which is in striking contrast with analogs **[Ru]9** and **[Ru]12**. Indeed, complex **[Ru]12** shows almost a two-fold increase in its overall activity compared to the parent catalyst **[Ru]9** (at 30 minutes the DPs are 2.8 and 4.1 for **[Ru]9** and **[Ru]12**, respectively), while **[Ru]11** and **[Ru]13** show the same catalytic profile. The electronic effect on the isopropoxybenzylidene seems to be dominated by the steric hindrance of the NHC ligand. Following the model of ruthenium-phosphine complexes, if the presence of H_2IPr facilitates dissociation, then it also slows down catalyst deactivation by rebinding of free phosphine, or in this case, rebinding of the ether-tethered ligand (*i*PrO).[99] Thus, complexes **[Ru]11** and **[Ru]13** actually undergo more turnovers before being trapped by *i*PrO. The dissociation/rebinding rates ratio appears to approach an optimum with H_2IPr ligands, a ratio that is hardly disturbed by simply changing the electron density around the isopropoxystyrene. On the other hand, the rebinding of *i*PrO is rendered easier in the presence of the less hindered H_2IMes ligand. In this case, the electron density of the coordinating oxygen has a greater effect on both the dissociation and rebinding rates, which explains the higher reactivity of **[Ru]11** whose nitro-substituted ligand will be less likely to recoordinate and therefore increases the amount of active species able to react. This electronic effect is not evident during the initial rate probably because ligand rebinding only becomes substantial after several turnovers.

Electronic effect on H_2IPr ligated complexes

The series of complexes **[Ru]11-[Ru]16** should help better understand the importance of dissociation/rebinding of these ether-tethered ligands. All the synthesized complexes are efficient catalysts for the ADMET oligomerization of 1,9-decadiene

reaching DPs of 4 and 5 under 5 minutes at 45°C. As illustrated in Figure 3-4, even at DP>4 (where the viscosity becomes significant) the polymerization continues at a steady rate without any sign of extensive decomposition of the catalytic center, usually observable by a darkening of the solution, confirming the robust nature of these catalysts.

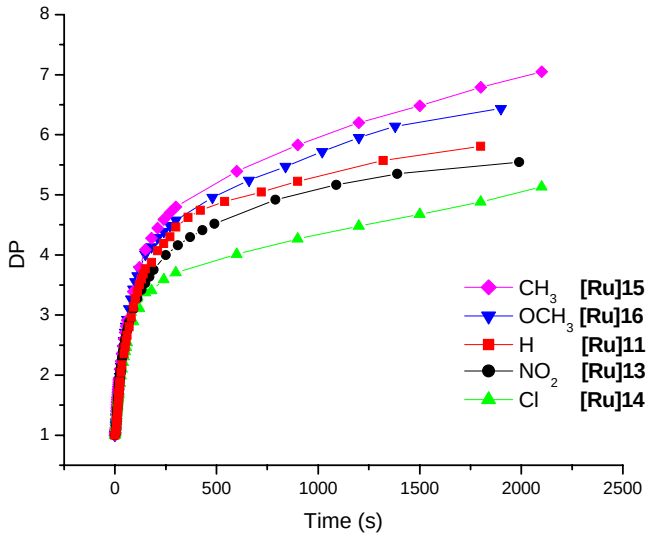

Figure 3-4. Degree of polymerization (DP) vs. time data for complexes **[Ru]11-[Ru]16** using 450:1 monomer:catalyst ratio at 45°C

Table 2 gives an overview of the initial rates for complexes **[Ru]11-[Ru]16** at 30°, 45° and 60°C. As observed earlier, initial rates at 30°C and 45°C stay the same regardless of the isopropoxybenzylidene used (around 20 DP s^{-1} at 30°C, and 45 DP s^{-1} at 45°C within experimental error) except for parent catalyst **[Ru]11**, which exhibits a slightly lower initial rate at 30°C. The difference noticed earlier (Table 1) could have been insignificant if the rates of the electronically modified catalysts **[Ru]13-[Ru]16** had not been so reproducible. The singularity of the unsubstituted catalyst **[Ru]11** proves the existence of an electronic effect, albeit not qualitative. This lack of sensitivity to the electronic nature of the substituent is again in significant contrast to what was observed

during CM and RCM reactions catalyzed by **[Ru]9** analogs; however, other reports have also referred to the unpredictability of other electronically-modified Hoveyda-type catalysts.[108,109,196] Here, the steric hindrance present on the NHC ligand seems to overshadow the electronic nature of the dissociating ligand at low temperatures, canceling the effect predicted by sigma values. This proposal finds credence in the X-ray structure of **[Ru]11**, **[Ru]13** and **[Ru]16**. The Ru-O bond length, usually indicative of the strength of the *i*PrO->Ru chelation, does not show significant variation (See the X-ray crystal structures in Appendix A). Conversely, nitro-substituted **[Ru]13** exhibits a slightly shorter Ru-O bond length (2.2462(3) Å) while methoxy-substituted **[Ru]16**'s is slightly longer (2.2486(18) Å).

Table 3-2. Initial rates in DP s^{-1} for catalysts **[Ru]11-[Ru]16**.

Temperature	**NO_2** **[Ru]13**	**Cl** **[Ru]14**	**H** **[Ru]11**	**CH_3** **[Ru]15**	**OCH_3** **[Ru]16**
σ-	**0.71**	**0.37**	**0**	**-0.06**	**0.05**
σ+	**0.79**	**0.11**	**0**	**-0.31**	**-0.78**
30°C	21 ± 4	21 ± 3	13 ± 2	22 ± 5	19 ± 4
45°C	48 ± 7	41 ± 8	45 ± 4	47 ± 2	40 ± 5
60°C	117 ± 8	118 ± 15	70 ± 10	136 ± 9	110 ± 7

Values for σ- and σ+ were taken from ref. 198

At 45°C all complexes follow about a similar catalytic profile, i.e. there is no major improvement brought about by the electronic substituents. However, there is a noticeable distinction between complexes (Figure 3-4). Electron donating groups (EDG) appear to increase the catalytic activity while e^- withdrawing groups (EWG) reduce the rate. Since the initial rates at 30°C and 45°C are the same for all catalysts, the dissociation rate of isopropoxybenzylidene cannot be the only determining factor. Theoretically, after dissociation the propagating species is the same for complexes **[Ru]11-[Ru]16**.

Therefore, the lability of isopropoxystyrene must allow its rebinding to the ruthenium center so that it influences the overall catalytic activity.

The trend observed at 45°C can be rationalized by considering the formation of the unstable $14e^-$ species, either the alkylidene or the methylidene complex. In Chapter 2, it was demonstrated that this type of catalyst was quite sensitive to substrate polarity compared to their phosphine analogs.[192] In the latter, the phosphine coordinates back to the $14e^-$ intermediate to stabilize it and forms a dormant state.[61] In Hoveyda-type complexes, this type of stabilization is lessened by the extreme lability of isopropoxy styrene. However, all substrates conventionally used to probe the metathesis activity of any catalyst contain some heteroatom that can serve as a stabilizer, along with the solvent used for the reaction. For example, during the ROMP reaction of diverse oxygen-containing monomers, Khosravi *et al.*[154] showed that Hoveyda-type catalysts were stabilized through the chelation of an oxygen contained in the monomer unit. In the case of substrates lacking any kind of electron donor or Lewis basic group, such as 1,9-decadiene, the $14e^-$ intermediate is not stabilized; therefore, the catalyst is more susceptible to decomposition, which results in slower rates. With this in mind, it is reasonable to assume that the catalysts with higher dissociation rates and/or slower rebinding rates should have a lower overall activity. According to sigma values, electron withdrawing substituents *para* to the isopropoxy group should facilitate the ligand dissociation by decreasing the electron density on the coordinating oxygen and increase its lability, while electron donating substituents should slow the dissociation step and facilitate its rebinding. Simply stated, donating groups should slow down catalyst decomposition. Consequently, complexes **6** and **7** (EDG) show a slightly higher

reactivity than complexes **4** and **5** (EWG), while neutral complex **[Ru]11** lies in between (Figure 3-2).

Temperature effect

When the temperature is raised to 60°C, the singularity of catalyst **[Ru]11** over the electronically modified **[Ru]13-[Ru]16** is accentuated. While initial rates for catalysts **[Ru]13-[Ru]16** are all around 120 DP s^{-1}, parent complex **[Ru]11** only affords a rate of 70 DP s^{-1}, broadly deriving from the predicted Arrhenius plot. Electronics now represent a determining factor on catalytic activity, which may be the result of a switch in the mechanism possibly due to a change in catalyst conformation. Similar temperature activation barriers have been witnessed with nitrogen-chelated complexes.[198]

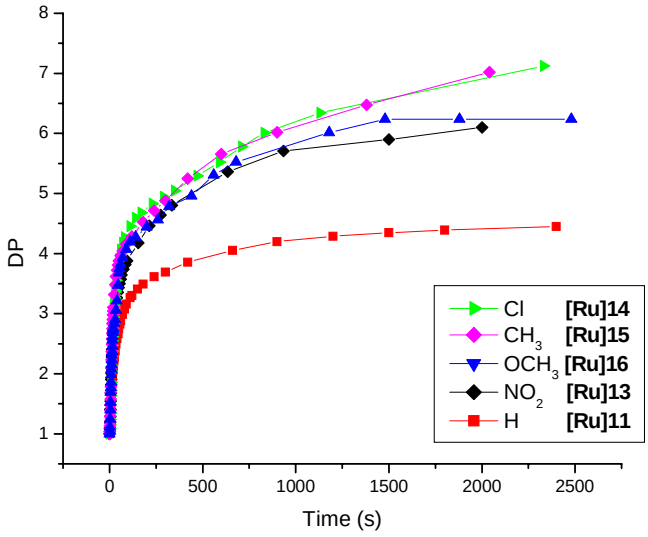

Figure 3-5. Degree of polymerization (DP) vs. time data for complexes **[Ru]11-[Ru]16** using 450:1 monomer:catalyst ratio at 60°C

The same catalytic profile persists as the reaction continues, and the overall activity is now significantly higher for the modified catalysts **[Ru]13-[Ru]16 (**Figure 3-5). This suggests that the steric effect of the H_2IPr ligand is no longer dominant, even though the

electronic factor cannot be qualified according to sigma values. This apparent lack of sensitivity towards the electronic nature of the substituents is more likely the result of several mechanistic processes operating simultaneously. While electron withdrawing groups could facilitate dissociation by weakening the iPrO->Ru chelation, electron donating groups could equally increase catalytic activity by reducing the Lewis acidity of the metal. The rate of decomposition of the methylidene intermediate, which is accelerated at elevated temperatures, is probably an important factor. Also, assuming that the H_2IPr ligand does not hinder the rebinding of the *i*PrO moiety, the $14e^-$ species can be properly stabilized, but, since the dissociation is quite fast, the catalyst quickly returns to the catalytic cycle affording higher DPs. The diminished steric effect may be due to a reorganization of the NHC ligand, possibly by ring rotation, often seen at high temperatures.

Conclusions

This report gives a different outlook on the influence of the ligand sphere's electronics/sterics on Hoveyda-type metathesis catalysts. Unlike most modification studies conducted on these complexes, the 'steric factor' is only located on the NHC ligand (isopropyl vs. methyl groups) whereas the 'electronic factor' is on the isopropoxybenzylidene. All the complexes tested are efficient catalysts for the ADMET polymerization of 1,9-decadiene. However, in the polycondensation conditions of ADMET, the steric hindrance largely dominates any electronic effect at all temperatures. Interestingly, unsubstituted complex **[Ru]11** curiously stands out at 30°C and 60°C, suggesting some participation of electronics in the catalytic potential of these Hoveyda-type complexes. The overall activity of these complexes seems to depend only on the propensity of the isopropoxystyrene ligand to rebind to the ruthenium center and stabilize

it in a similar way as their phosphine analogs, especially at low temperatures. As a result, complexes bearing EWGs result in lower DPs than complexes bearing EDGs, the more active catalyst being the better stabilized. In any case, complexes ligated to larger NHC ligands are better catalysts than any modified Hoveyda-Grubbs such as **[Ru]12**, again showing the prevalence of sterics over electronics.

At 60^{o}C, all electronically modified catalysts exhibit comparable initial rates and increased reactivities, while parent complex **[Ru]11** constitutes a significant exception. The catalytic profiles of **[Ru]13-[Ru]16** are similar and lay 2 DP over **[Ru]11**'s, implying that the different electronic groups are able to improve activity through different processes. A reorganization of the ligand sphere may occur at higher temperatures so that the steric bulk of the NHC ligand does not hinder the rebinding of isopropoxystyrene anymore. Consequently, catalysts **[Ru]13-[Ru]16** represent the fastest initiators ever tested for ADMET polymerization. Further experiments will be conducted to investigate the importance of ligand rebinding in these Hoveyda-type catalysts, which represent an interesting prospect for metathesis polycondensation.

Experimental

General

^{1}H NMR (300 MHz) and ^{13}C NMR (75 Hz) spectra of the organometallic complexes were recorded in $CDCl_3$ on either a Mercury series or Varian VXR-300 NMR superconducting spectrometer. Chemical shifts were referenced to residual $CHCl_3$ (7.27 for ^{1}H and 77.23 for ^{13}C) with 0.03% v/v TMS as an internal reference.

Complex **[Ru]9** was a gift from Materia Inc. and was used as received. Complex **[Ru]4**,[71] **[Ru]10**,[101] **[Ru]11**,[192] and **[Ru]12**[195] were synthesized according to the literature procedure. All catalysts were stored in an argon-filled drybox prior to use in kinetic and

polymerization experiments. 1,9-Decadiene (Aldrich) was distilled from Na/K alloy under reduced pressure into a Kontes flask equipped with a Teflon valve, degassed by three freeze-pump-thaw cycles, and stored in an argon-filled drybox. For the kinetic study, 1,9-decadiene was portioned into small Teflon-capped vials in the drybox and were removed and stored in a dessicator until use.

All other starting material were distilled over Na/K alloy before use except chlorinated compounds which were distilled over CaH_2. After distillation, *d*-chloroform was degassed by three freeze-pump-thaw cycles, and stored in an argon-filled drybox.

X-ray Experimental

Crystals suitable for X-ray structure determination were obtained from slow diffusion of pentane into a saturated solution of **[Ru]13** or **[Ru]16** in CH_2Cl_2 at room temperature. Data were collected at 173 K on a Siemens SMART PLATFORM equipped with A CCD area detector and a graphite monochromator utilizing MoK_α radiation (λ = 0.71073 Å). Cell parameters were refined using up to 8192 reflections. A full sphere of data (1850 frames) was collected using the ω-scan method (0.3° frame width). The first 50 frames were remeasured at the end of data collection to monitor instrument and crystal stability (maximum correction on I was < 1 %). Absorption corrections by integration were applied based on measured indexed crystal faces.

The structure was solved by the Direct Methods in *SHELXTL6,* and refined using full-matrix least squares. The non-H atoms were treated anisotropically, whereas the hydrogen atoms were calculated in ideal positions and were riding on their respective carbon atoms. Refinement was done using F^2:

- For **[Ru]13**, a total of 426 parameters were refined in the final cycle of refinement using 7198 reflections with $I > 2\sigma(I)$ to yield R_1 and wR_2 of 3.19% and 7.23%, respectively.

- For **[Ru]16**, a total of 406 parameters were refined in the final cycle of refinement using 6677 reflections with $I > 2\sigma(I)$ to yield R_1 and wR_2 of 3.85% and 11.46%, respectively. The toluene molecule were disordered and could not be modeled properly, thus program SQUEEZE, a part of the PLATON package of crystallographic software, was used to calculate the solvent disorder area and remove its contribution to the overall intensity data.

General Procedure for Ligand Synthesis

2-Isopropoxystyrene derivatives were synthesized by a standard Wittig reaction on the 2-isopropoxybenzylaldehyde parent using (methyl)triphenylphosphine iodide and potassium *t*-butoxide (Aldrich). All the 2-isopropoxybenzylaldehyde derivatives were synthesized via a Wilkinson-ether synthesis from the corresponding salicyl aldehyde (Aldrich) and 2-bromopropane (Aldrich). Spectral data for 1-isopropoxy-2-vinyl-4-methylbenzene,[108] 1-isopropoxy-2-vinyl-4-nitrobenzene,[195] and 1-Isopropoxy-2-vinyl-4-methoxybenzene[196] match the literature.

General Procedure for Carbene Exchange

In a glovebox complex **[Ru]4** (300 mg, 0.32 mmol) and CuCl (Aldrich) (32 mg, 0.32 mmol) were weighed into a 100 mL schlenk flask and dissolved in 15 mL of CH_2Cl_2. 2-Isopropoxy-5-nitrostyrene (133 mg, 0.64 mmol) was dissolved in 5 mL of CH_2Cl_2 and added to the solution of complex **[Ru]4** and CuCl at room temperature. The flask was equipped with a condenser and the solution was refluxed for 30 minutes or until

the brown solution turns to a deep green. From this point forth, all manipulations were carried out in air with reagent-grade solvents. The reaction mixture was concentrated in vacuo to a green residue. The unpurified material was dissolved in a minimal volume of 5:2 cyclohexane/ethyl acetate and loaded onto a plug of silica gel. Insoluble copper-phosphine precipitates were removed prior to loading by passing the solution through a second Pasteur pipette containing a plug of glass wool. Elution with 5:2 cyclohexane/ethyl acetate removed a bright green band from the column. The solvent was evaporated and the residue washed with *n*-pentane.

Synthesis of complex [Ru]13. (-NO_2) The general procedure was followed to afford 200 mg (0.267 mmol, 83%) of a green powder. ^{1}H NMR ($CDCl_3$, 300 MHz): δ=16.32 (s, 1H, Ru=C*H*Ph), 8.40 (d, 1H, *para* C*H*, $^2J_{H,H}$= 8.4 Hz), 7.70 (s, 1H, *ortho* C*H*), 7.58 (t, 2H, *para* C*H*, $^3J_{H,H}$= 7.2 Hz), 7.39 (d, 4H, *meta* C*H*), 6.90 (d, 1H, *meta* C*H*, $^2J_{H,H}$= 8.4 Hz), 4.98 (sept, 1H, $(CH_3)_2CHOAr$, $^3J_{H,H}$= 6.3 Hz), 4.20 (s, 4H, $N(CH_2)_2N$), 3.54 (sept, 4H, $CH(CH_3)_2$, $^3J_{H,H}$= 6.6 Hz), 1.40 (d, 6H, $OCH(CH_3)_2$, $^2J_{H,H}$= 6.3 Hz), 1.24 (d, 24H, $CH(CH_3)_2$, $^3J_{H,H}$= 7.1 Hz); ^{13}C NMR ($CDCl_3$, 75 MHz): δ = 284.4, 210.6, 156.9, 149.3, 143.9, 143.2, 136.4, 130.3, 124.7, 124.3, 117.0, 113.0, 77.9, 54.8, 29.1, 27.1, 26.8, 21.9. MS (HRMS/EI) calcd for $C_{37}H_{49}O_3N_3Cl_2Ru$ $[M]^+$ 755.2194, found 755.2161. Anal. Calcd for $C_{37}H_{49}O_3N_3Cl_2Ru$: C, 58.80; H, 6.53; N, 5.56. Found: C, 59.96; H, 7.03; N, 5.20.

Synthesis of complex [Ru]14. (-Cl) The general procedure was followed using 2-isopropoxy-5-chlorostyrene (125 mg, 0.64 mmol) to afford 202 mg (0.272 mmol, 85%) of a pale green powder. ^{1}H NMR ($CDCl_3$, 300 MHz): δ=16.28 (s, 1H, Ru=C*H*Ph), 7.55 (t, 2H, *para* C*H*, $^3J_{H,H}$= 7.2 Hz), 7.43 (s, 1H, *ortho* C*H*, $^2J_{H,H}$= 8.8 Hz), 7.38 (d, 4H, *meta*

C*H,* $^{2}J_{H,H}$ = 7.4 Hz), 6.80 (d, 1H, *para* C*H*, $^{2}J_{H,H}$ = 2.4 Hz), 6.72 (d, 1H, *meta* C*H*, $^{2}J_{H,H}$ = 8.8 Hz), 4.87 (sept, 1H, $(CH_3)_2CHOAr$, $^{3}J_{H,H}$ = 6.2 Hz), 4.19 (s, 4H, $N(CH_2)_2N$), 3.58 (sept, 1H, $CH(CH_3)_2$, $^{3}J_{H,H}$ = 6.6 Hz), 1.35 (d, 6H, $OCH(CH_3)_2$, $^{2}J_{H,H}$ = 6.3 Hz), 1.25 (d, 24H, $CH(CH_3)_2$, $^{3}J_{H,H}$ = 7.1 Hz); ^{13}C NMR ($CDCl_3$, 75 MHz): δ = 286.3, 212.3, 150.9, 149.3, 145.0, 130.0, 128.1, 127.7, 124.6, 121.4, 114.1, 75.9, 54.7, 29.0, 26.7, 23.5, 21.8. MS (HRMS/EI) calcd for $C_{37}H_{49}ON_2Cl_3Ru$ $[M+Na]^+$ 767.1846, found 767.1941. Anal. Calcd for $C_{37}H_{49}ON_2Cl_3Ru$: C, 59.63; H, 6.63; N, 3.76. Found: C, 59.52; H, 7.03; N, 3.46.

Synthesis of complex [Ru]15. (-CH_3) The general procedure was followed using 2-isopropoxy-5-methylstyrene (113 mg, 0.64 mmol) to afford 209 mg (0.288 mmol, 90%) of a pale green powder. ^{1}H NMR ($CDCl_3$, 300 MHz): δ=16.40 (s, 1H, Ru=C*H*Ph), 7.55 (t, 2H, *para* C*H*, $^{3}J_{H,H}$ = 7.6 Hz), 7.40 (d, 4H, *meta* C*H,* $^{2}J_{H,H}$ = 7.8 Hz,), 7.24 (s, 1H, *ortho* C*H*), 6.68 (d, 1H, *para* C*H*, $^{2}J_{H,H}$ = 8.3 Hz), 6.58 (s, 1H, *meta* C*H*), 4.88 (sept, 1H, $(CH_3)_2CHOAr$, $^{3}J_{H,H}$ = 6.0 Hz), 4.18 (s, 4H, $N(CH_2)_2N$), 3.62 (sept, 1H, $CH(CH_3)_2$, $^{3}J_{H,H}$ = 6.5 Hz), 2.32 (s, 3H, CH_3), 1.36 (d, 6H, $OCH(CH_3)_2$, $^{2}J_{H,H}$ = 6.2 Hz), 1.27 (d, 24H, $CH(CH_3)_2$, $^{3}J_{H,H}$ = 6.8 Hz); ^{13}C NMR ($CDCl_3$, 75 MHz): δ = 290.8, 214.4, 150.8, 149.5, 144.4, 137.1, 131.5, 129.9, 124.6, 122.6, 112.8, 74.9, 54.8, 29.0, 26.8, 23.6, 22.0, 20.2. MS (HRMS/EI) calcd for $C_{38}H_{52}O_2N_2Cl_2Ru$ $[M+Na]^+$ 747.2395, found 747.2427. Anal. Calcd for $C_{38}H_{52}O_2N_2Cl_2Ru$: C, 62.97; H, 7.23; N, 3.86. Found: C, 62.67; H, 7.31; N, 3.49.

Synthesis of complex [Ru]16. (-OCH_3) The general procedure was followed using 2-isopropoxy-5-methoxystyrene (123 mg, 0.64 mmol) to afford 229 mg (0.310 mmol, 97%) of a pale green powder. ^{1}H NMR ($CDCl_3$, 300 MHz): δ=16.33 (s, 1H, Ru=C*H*Ph),

7.53 (t, 2H, *para* C*H*, $^{3}J_{H,H}$ = 7.2 Hz), 7.37 (d, 4H, *meta* C*H*), 7.02 (dd, 1H, *meta* C*H*, $^{2}J_{H,H}$ = 8.4 Hz), 6.69 (d, 1H, *para* C*H*, $^{2}J_{H,H}$ = 7.4 Hz), 6.37 (s, 1H, *ortho* C*H*), 4.83 (sept, 1H, $(CH_3)_2CHOAr$, $^{3}J_{H,H}$ = 6.3 Hz), 4.18 (s, 4H, $N(CH_2)_2N$), 3.72 (s, 3H, OCH_3), 3.60 (sept, 1H, $CH(CH_3)_2$, $^{3}J_{H,H}$ = 6.6 Hz), 1.35 (d, 6H, $OCH(CH_3)_2$, $^{2}J_{H,H}$ = 6.2 Hz), 1.24 (d, 24H, $CH(CH_3)_2$, $^{3}J_{H,H}$ = 7.1 Hz); ^{13}C NMR ($CDCl_3$, 75 MHz): δ = 298.1, 208.9, 152.5, 149.4, 146.2, 131.9, 130.6, 129.9, 124.7, 117.7, 113.2, 111.4, 72.7, 55.8, 32.8, 29.0, 26.8, 23.6, 21.9. MS (HRMS/EI) calcd for $C_{38}H_{52}O_2N_2Cl_2Ru$ $[M+Na]^+$ 763.2344, found 763.2361. Anal. Calcd for $C_{38}H_{52}O_3N_2Cl_2Ru$: C, 61.61; H, 7.08; N, 3.78. Found: C, 61.86; H, 7.28; N, 3.63.

Kinetic Study

The kinetic study was performed with the same apparatus and following the same procedure as previously described by Wagener.[144,192]

CHAPTER 4
ISOMERIZATION BEHAVIOR UNDER METATHESIS CONDITIONS OF NHC-CONTAINING RUTHENIUM CARBENE CATALYSTS.

Introduction

In the past few years, alkene isomerization has emerged as an important side reaction of ruthenium catalyzed metathesis, disturbing the product's microstructure by apparent migration of the double bond along the alkyl chain.[160,166] Figure 4-1 illustrates the versatility of this side-reaction. First observed with **[Ru]1** during the ring-closing metathesis of allylic functionalized alkenes,[164,167,199,200] olefin isomerization rapidly appear to affect a variety of oxygen and nitrogen-containing compounds.[168,169] In some cases, double-bond isomerization even occurred *prior* to the metathesis reaction.[200] Nevertheless, **[Ru]1** remains inactive towards isomerization with unsubstituted olefins or unfunctionalized alkenes even under harsh conditions.[176] However, when the 2nd generation of catalysts were introduced, competitive isomerization became a problem with all kinds of substrates.[160,166] Fürstner *et al.*[114] reported the synthesis of a 20-membered ring in addition to the desired 21-membered lactone from the RCM of a 1,22-diene with **[Ru]3**. The ring contraction was the result of initial isomerization of one of the double-bonds followed by RCM and the release of propene. Many other examples appeared in the literature and scientists began to use isomerization to their advantage for the synthesis of 5-, 6-, 7-membered cyclic enol ethers by tandem RCM double-bond isomerization reactions.[201]

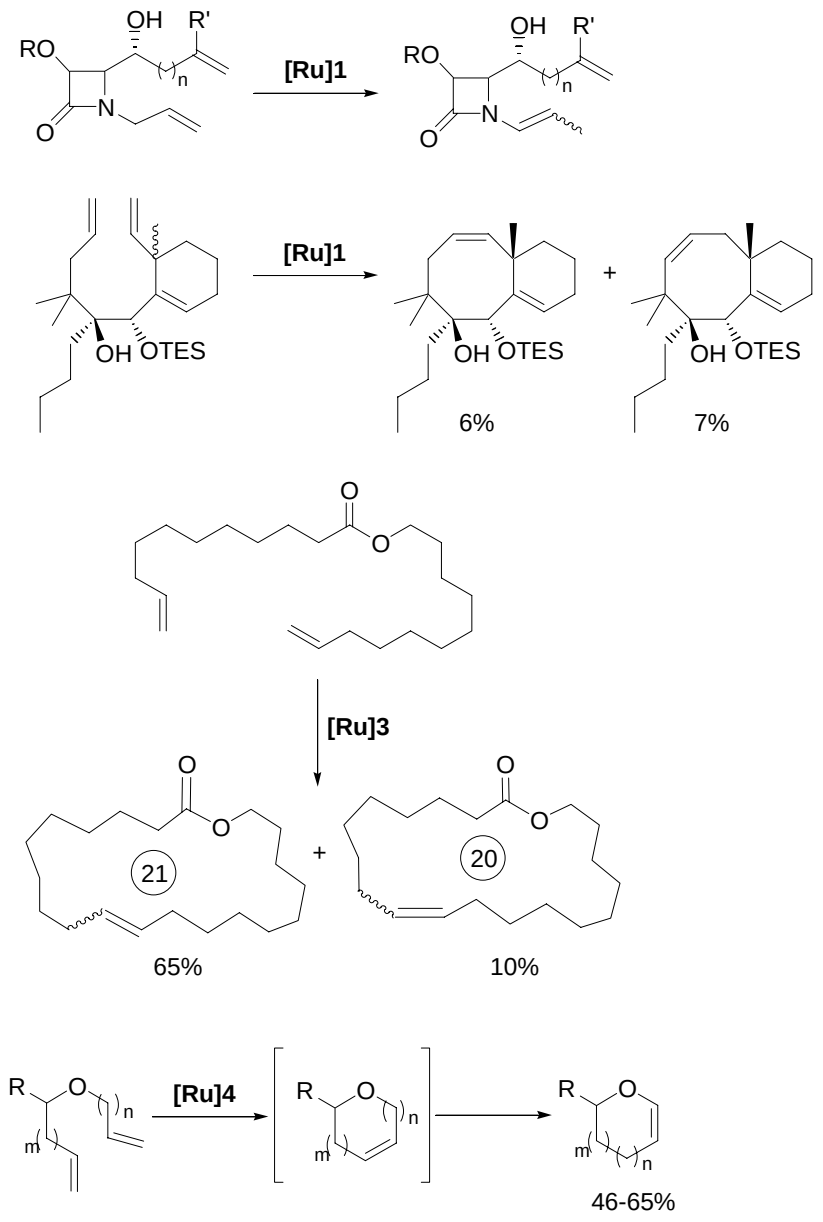

Figure 4-1. Examples of competitive isomerization reactions during olefin metathesis

The 2 established pathways for transition metal-catalyzed olefin isomerization are the π-allyl metal hydride mechanism and the metal hydride addition-elimination.[178] Despite an increasing number of studies, the ruthenium intermediate responsible for this undesirable reaction has not been identified yet, although it is often attributed to the formation of a ruthenium hydride in situ, as a decomposition product of the original carbene catalyst.

Acyclic diene metathesis has been used in our research for the modeling of precise ethylene/α-olefin copolymers.[127,128,130] Controlling isomerization is crucial as it results in irregular microstructures, whether it occurs on the monomer or on the product (Figure 4-2). Furthermore, ADMET conditions are particularly favorable to isomerization since polymerizations are typically conducted in neat diene or in concentrated solutions at high temperatures of 40-75°C, for extended periods of time to reach high molecular weight materials. Previously, we have reported the metathesis vs. isomerization activity of fast initiators using the model substrate 1-octene.[192] In an attempt to better understand the causes of isomerization, this study was extended to other modified complexes, introducing different phosphine and carbene ligands. Previous Hoveyda-type complexes **Ru]E**, **[Ru]11**, and **[Ru]13** were also included in this study.

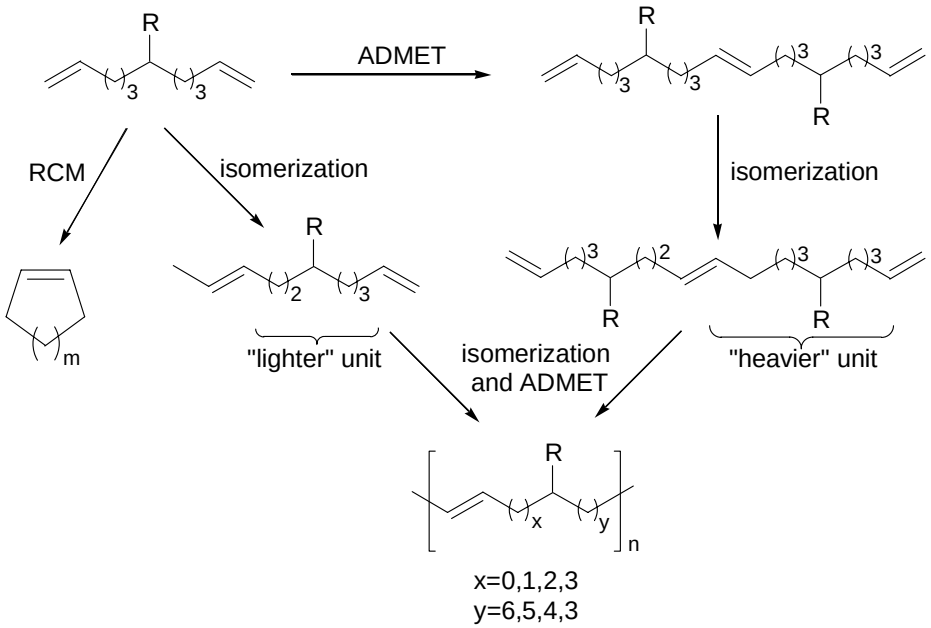

Figure 4-2. Effect of isomerization during ADMET polymerization

Results and Discussion

The fact that isomerization seemed to occur to a significant extent with fast initiators combined with previous observations showing that ruthenium vinylidene

catalysts afforded polymers with singularly high trans content,[202] prompted us to investigate a variety of slow initiators. Smaller phosphine are known to dissociate slower.[75] Tricyclopentyl phosphine (PCp_3) ruthenium dimethylvinyl carbene **[Ru]17** being readily available in the lab from previous studies, the PCp_3 equivalents of both parent complexes **[Ru]4** and **[Ru]10** represent ideal candidates to investigate the influence of both the NHC and phosphine ligands. On the other hand, dimethylvinyl carbene ruthenium complexes react slowly and incompletely with ethyl vinyl ether even when a phosphine is replaced by an NHC ligand. Despite incomplete initiation of the catalyst, vinylidene complexes are efficient catalysts for a variety of cross-metathesis applications,[203] which make them potentially suitable for ADMET chemistry.

Synthesis and Characterization

Complexes **[Ru]13-16** were synthesized from the parent catalyst **[Ru]10** by addition of the corresponding isopropoxystyrene and copper chloride as described in Chapter 3. The synthesis of complex **[Ru]18** was adapted from the literature.[203] Noteworthy, the H_2IPr analogue proved difficult to synthesize using the same conditions. The additional bulk brought about by the isopropyl groups of the NHC ligand may interact with the dimethylvinyl carbene, rendering the ligand substitution more problematic. Complexes **[Ru]21** and **[Ru]22** were obtained by phosphine exchange using the intermediate pyridine adduct **[Ru]19** and **[Ru]20**, respectively (Figure 4-3).[204] The *bis*-pyridine complexes were crystallized and reacted with 1.4 equivalents of PCp_3.

Spectroscopically, the vinylidene protons of **[Ru]18** exhibit two characteristic doublets at δ 19.14 and 7.72 ppm, while **[Ru]21** and **[Ru]22** showed a single phosphorus signal at δ 26.30 and 24.27 ppm, respectively. The upfield shift relative to PCy_3 ligated

parent complexes **[Ru]4** and **[Ru]10** indicates the presence of the less π-basic tricyclopentyl phosphine

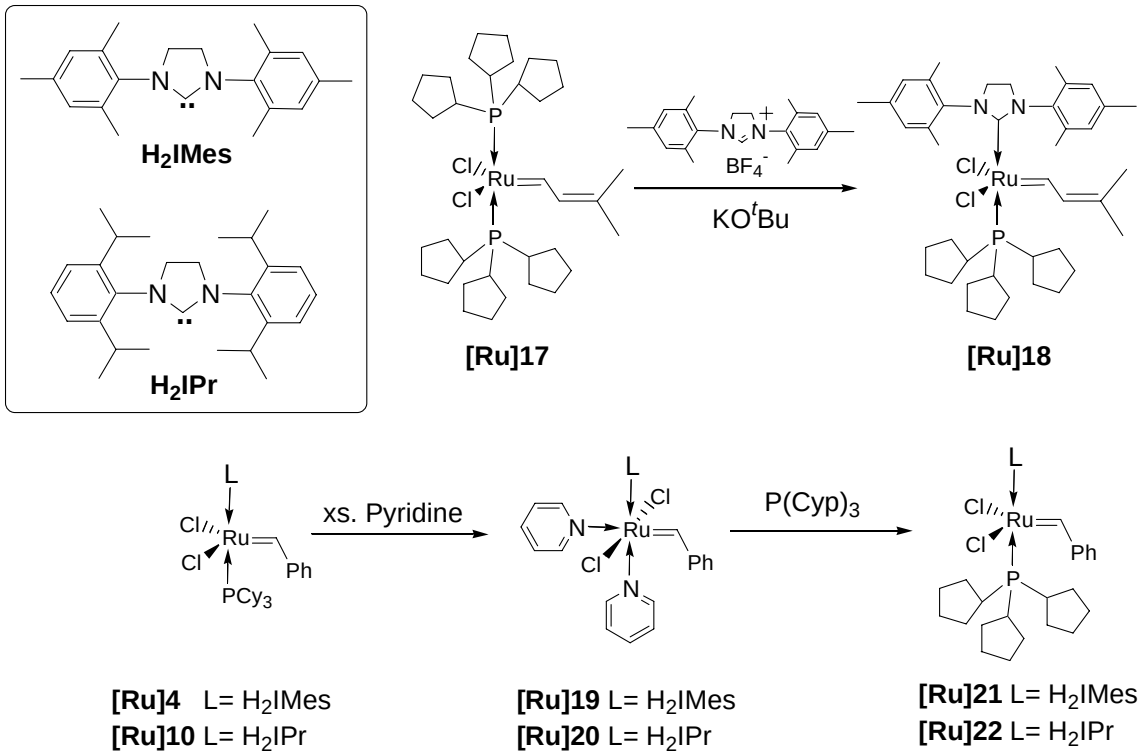

Figure 4-3. Synthesis of **[Ru]18-22**

Isomerization Behavior with 1-Octene

The extent of isomerization was tested for complexes **[Ru]E**, **[Ru]11**, **[Ru]13** and **[Ru]17-22**, using the model 1-octene, and compared to catalysts **[Ru]1**, **[Ru]4** and **[Ru]10**. The reaction conditions were typically the same as the original experiment, using 0.1 mol% catalyst in neat 1-octene at both room temperature and 55°C for 3 days.[176] The product mixture was analyzed by gas chromatography (GC), where each peak corresponds to a linear olefin of a specific carbon length. The results are expressed as the percentage of isomers in the mixture versus the percentage of metathesis product, assuming complete conversion, which is true for all catalysts except **[Ru]18** (Table 4-1). The combination of the vinylidene and the smaller phosphine, even though PCp_3 is less

π-basic than PCy_3, render this catalyst extremely slow to initiate at room temperature and the concentration of active species is probably not sufficient to drive the reaction to completion.

Table 4-1. Percentage of isomers during the metathesis of 1-octene.

Entry	Catalyst	% isomers at 25°C	% isomers at 55°C
1[a]	**[Ru]1**	0%	0%
2	**[Ru]E**	0%	12%
3[a]	**[Ru]4**	3%	76%
4[b]	**[Ru]10**	76%	-
5	**[Ru]11**	23%	50%
6	**[Ru]13**	78%	-
7	**[Ru]18**	7%	70%
8	**[Ru]21**	39%	49%
9	**[Ru]22**	84%	-

[a] Data taken from ref. 176; [b] ref. 193.

All catalysts exhibit an isomeric distribution centered around the metathesis product, indicating that isomerization occurs *subsequently* to the metathesis process (Figure 4-4). This is in stark contrast with what was observed with Grubbs' catalyst **[Ru]4** where the two reactions occurred *competitively* at 55°C. Since, **[Ru]21** is a slower metathesis catalyst,[75] it is tempting to conclude that substituting PCy_3 for PCp_3 delays the isomerization reaction but yet does not decrease its extent. The PCp_3 ligated complexes **[Ru]21**, and **[Ru]22** are actually better isomerization catalysts than **[Ru]4** at room temperature. This could be due to the slower rate of dissociation of PCp_3, combined to the lower π-basicity of the phosphine, which probably affects the rate of catalytic decomposition, in that it decreases the chances for nucleophilic attack on the methylidene complex.[89]

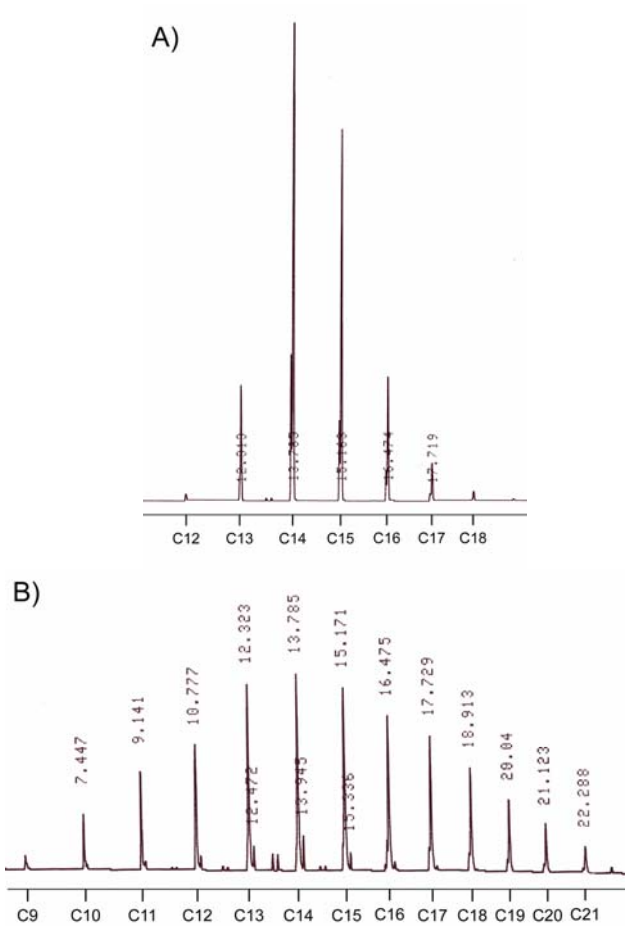

Figure 4-4. GC chromatogram of the product mixture from the self-metathesis of 1-octene: (A) with **[Ru]21** at 25°C; (B) with **[Ru]22** at 25°C. Retention scale is in minutes.

It appears that the rate of isomerization is closely related to the rate of metathesis, as the faster metathesis initiators, bearing the bulkier H_2IPr ligand, result in higher % isomerization products. For example **[Ru]13** and **[Ru]22** initiate fast and afford more than 75% isomers at room temperature (Figure 4-4A, entries 6 and 9), while **[Ru]18** and **[Ru]21** are known for their slow initiation and consequently yield 7-39% isomers in the same conditions (Figure 4-4B, entries 7 and 8). The breadth of the isomer distribution increases with the reactivity of the isomerization catalyst. However, isomerization cannot be correlated as a function of the dissociation rate. Indeed, complexes **[Ru]1** and **[Ru]E** are known for faster dissociation, still the results show little to no trace of

isomerization. On the other hand, changing the dissociating ligand or the carbene had little effect on complexes bearing NHC ligands. Accordingly, electronics on the Hoveyda-type complexes (**[Ru]11** vs. **[Ru]13**) did not significantly affect either metathesis or isomerization rates. Even though this study does not allow to conclude on the causes of isomerization it is now clear that NHC ligands play a crucial role in promoting this undesired reaction.

Since the metathesis and isomerization activity of ruthenium catalysts apparently go hand in hand, it seems logical that isomerization is promoted by the metathesis catalyst itself or by a species formed in situ during the metathesis cycle. Bourgeois *et al.*[174] proposed the π-allyl mechanism illustrated in Figure 4-5, via deprotonation of the allylic position by the carbene moiety. They postulate that the strong σ-donation of the NHC ligand increases the basicity of the carbene, therefore favoring isomerization. In addition, they proved that tricyclohexyl phosphine oxide, $O=PCy_3$, generated from oxidation of PCy_3, serves as an isomerization inhibitor.

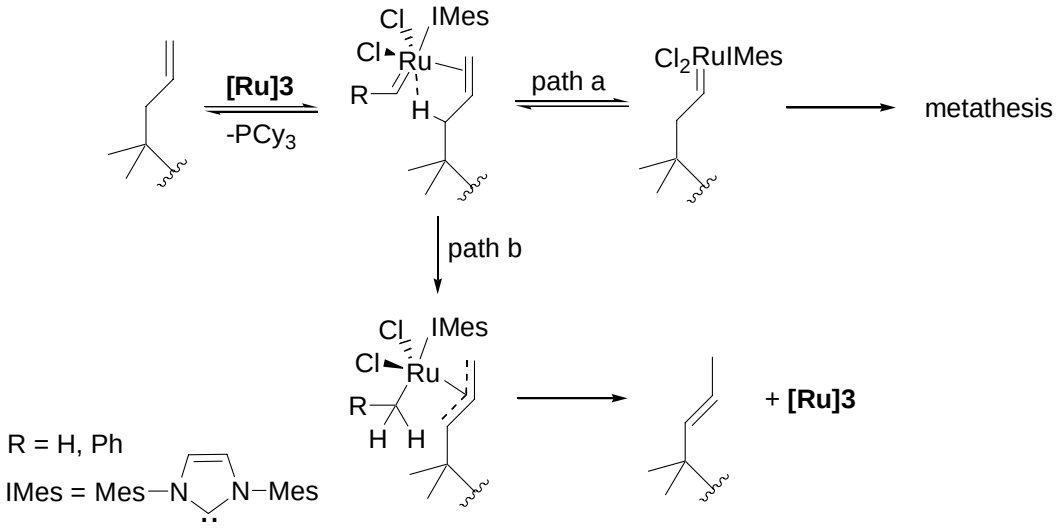

Figure 4-5. Postulated mechanism of the isomerization process.

On the other hand, ruthenium carbene catalysts are known to form hydride complexes as they decompose. Because early metathesis complex $Ru(H_2O)_6(tos)_2$ was proven to isomerize allylic functionalized substrates through a metal-hydride intermediate,[205] it is tempting to assume that one of the catalyst decomposition product might be responsible for this undesirable reaction. Therefore, understanding the isomerization process also goes along with the determination of the decomposition pathway. Several hydrido complexes have been identified as decomposition products of catalysts **[Ru]1** and/or **[Ru]4** under different conditions; however, none reproduces rigorous metathesis conditions.[72,89-94] Complexes **[Ru]6** and **[Ru]7** (Figure 4-6) have been isolated under high oxygen pressures or in alcohol solvents,[92-94] but cannot be obtained under the inert conditions typically used in this study. Even though complex **[Ru]7** has been isolated as an impurity during the synthesis of **[Ru]4**, supposedly as a consequence of the methanol wash, it is not a good isomerization catalyst. Grubbs *et al.*[89] have recently reported the hydrido complex **[Ru]5**, which directly involves the NHC ligand in the decomposition process. Finally, the C-H activation of one of the methyls of the NHC ligand is a common reaction in many ruthenium complexes,[183,206-209] even though complex **[Ru]8** is the only example so far with a ruthenium carbene and does not contain any hydride ligand.[72]

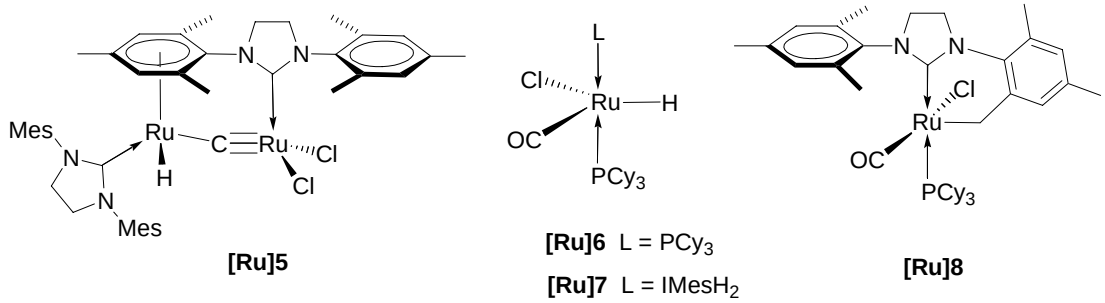

[Ru]5

[Ru]6 L = PCy_3

[Ru]7 L = $IMesH_2$

[Ru]8

Figure 4-6. Decomposition products of ruthenium carbene complexes

Therefore, before moving towards new catalyst designs, further studies will focus on the identification of the isomerization mechanism operating during ruthenium-catalyzed metathesis reactions.

ADMET Polymerization

The catalysts were also tested for their utility in ADMET chemistry by polymerizing benchmark 1,9-decadiene in the bulk (monomer:catalyst ratio 450:1), at 55^{o}C for 5 days. The primary interest was to evaluate the *cis:trans* ratio of the resulting polyoctenamer since a previous experiment indicated that vinylidene complexes may produce a polymer with a high *trans* content.[202] This is particularly attractive since high *cis* content reduces both the melting temperature and the percent crystallinity.

Molecular weights (M_n) and *cis:trans* ratios are given in Table 4-2. All polymers exhibit a *trans* content of about 80%, which is typical for ruthenium catalyzed ADMET polymers. As expected, 1st generation catalysts **[Ru]1** and **[Ru]E** are less active than NHC-containing complexes, as they produce polyoctenamer with M_n lower than 12,000 g/mol, compared to M_n of at least 18,000 g/mol using 2nd generation catalysts. Interestingly, vinylidene **[Ru]18** yields similar molecular weight material than benzylidene **[Ru]21** and **[Ru]22** even though it is known to be a slower initiator. This observation not only illustrates that vinylidene complexes are efficient ADMET catalysts, but also that faster initiators do not necessarily afford higher molecular weight polymer. Indeed, the slow initiation of the vinylidene complex allows the slow diffusion of active species in the bulk of ADMET monomer, providing a constant feed of fresh catalyst as the reaction proceeds to higher DPs. Monomers that prove hard to polymerize under standard ADMET conditions are sometimes driven to high molecular weight polymer by repeated additions of fresh catalyst to the reaction medium.[147]

Table 4-2. Results for the ADMET polymerization of 1,9-decadiene at 55 °C for 120 h

Entry	Catalyst	polyoctenamer *cis*:*trans* ratio[a]	M_n (g/mol)
1	**[Ru]1**		12,000[b]
2	**[Ru]E**	20:80	5,000[c]
3	**[Ru]4**	17:83	75,000[b]
4	**[Ru]10**	18:82	32,000[b]
5	**[Ru]11**	17:83	21,000[b]
6	**[Ru]18**	23:77	20,000[c]
7	**[Ru]21**	21:79	18,000[c]
8	**[Ru]22**	16:84	26,000[b]

[a] Determined by ^{13}C NMR. [b] Determined by GPC analysis. [c] Determined by ^{1}H NMR end-group analysis.

Phosphine substitution from PCy_3 to the smaller PCp_3 significantly depresses catalytic activity, as **[Ru]4** and **[Ru]21** afford polyoctenamers with M_n of 75,000 g/mol and 18,000 g/mol, respectively. This observation is harder to rationalize since the phosphine ligand is involved in both the rebinding step, which deactivates the catalyst, and catalyst decomposition, which is also an important consideration as ADMET is typically run for long reaction times. The smaller PCp_3 may rebind more easily, which is problematic since the methylidene complex is not likely to reenter the ADMET cycle after being trapped by free phosphine.[75] In any case none of these complexes compete with the activity of second generation Grubbs' catalyst in ADMET.

Conclusions

A series of ruthenium carbene catalysts was synthesized and tested on 1-octene to study the effect of ligand variation on olefin isomerization during metathesis reactions. Even though all complexes are efficient catalysts for the ADMET polymerization of 1,9-decadiene, they all promote structural isomerization. The isomerization extent is increased by faster metathesis initiators, and the presence of N-heterocyclic carbene ligand clearly accelerates this undesirable reaction. Otherwise, it is difficult to provide

definite conclusions on the role of other ligands on the catalyst isomerization behavior. Therefore, before pursuing the design of novel catalysts to limit olefin isomerization, it is important to identify the mechanism operating under these metathesis conditions.

Experimental

General Considerations

^{1}H NMR (300 MHz) and ^{13}C NMR (75 Hz) spectra of the ADMET polymers were recorded in $CDCl_3$ on either a Mercury series or Varian VXR-300 NMR superconducting spectrometer. Chemical shifts were referenced to residual $CHCl_3$ (7.23 for ^{1}H and 77.23 for ^{13}C) with 0.03% v/v TMS as an internal reference. All organometallic spectra were recorded in d_6-benzene and the chemical shifts were referenced to residual C_6H_6 (7.16 for ^{1}H and 128.39 for ^{13}C).

Gel permeation chromatography (GPC) was performed using a Waters Associates GPCV2000 liquid chromatography system with its internal differential refractive index detector (DRI), internal differential viscosity detector (DP), and a Wyatt Technology 3 angle light scattering detector (LS). The chromatography was performed at 45 °C using two Waters Styragel HR-5E columns (10 microns PD, 7.8 mm ID, 300 mm length) with HPLC grade tetrahydrofuran as the mobile phase at a flow rate of 1.0 mL/minute. Injections were made at 0.05-0.07 % w/v sample concentration using a 322.5 ml injection volume. In the case of universal calibration, retention times were calibrated against narrow molecular weight polystyrene standards (Polymer Laboratories; Amherst, MA). All standards were selected to produce M_p or M_w values well beyond the expected polymer's range.

GC analysis was conducted on a Shimadzu GC-17A chromatograph equipped with a HP-5 (Hewlett Packard) 25 m column with FID detection. All amounts of products

were calculated by a systematic ratio to the Decalin peak at 8.72 minutes, using the integrated peak areas.

Catalyst **[Ru]17** was a gift from Materia and complexes **[Ru]18**[203] and **[Ru]19**[204] were synthesized according to the literature. All catalysts were stored in an argon-filled drybox prior to use in kinetic and polymerization experiments. Pyridine (Aldrich) was dried over CaH_2 prior to use. Tricyclopentyl phosphine (Aldrich) was stored in the drybox and used as received. 1,9-Decadiene (Aldrich) was distilled from Na/K alloy under reduced pressure into a Kontes flask equipped with a Teflon valve, degassed by three freeze-pump-thaw cycles, and stored in an argon-filled drybox. All polymerizations were conducted in the bulk using (450:1) monomer-to-catalyst ratio. Benzene, toluene and pentane were distilled over Na/K alloy before use, and methanol was distilled over Mg/I_2. After distillation, d_6-benzene was degassed by three freeze-pump-thaw cycles, and stored in an argon-filled drybox.

Synthesis of Complexes [Ru]18-22

Synthesis of complex [Ru]21. In the drybox, a flame-dried Schlenk flask was charged with 0.102 g (0.140 mmol) of catalyst **[Ru]19** and dissolved in 3 ml of benzene. A solution of tricyclopentyl phosphine(80 mg, 0.336 mmol, 3.2 eq) in benzene was added to the Schlenk flask and the color immediately turned brown-red. The mixture was stirred at room temperature for 10 minutes under argon, and the solvent was then evaporated. The brown residue was washed with anhydrous methanol (2 x 25 mL) and pentane (50 mL). Finally, the brown-pink solid was dried under vacuum to yield 0.100 g (0.124 mmol, 88%) of complex **[Ru]21**.

^{1}H NMR (benzene-d_6, 300 MHz): δ= 19.72 (s, 1H, Ru=C*H*), 7.12-6.90 (m, 7H, *para-meta* C*H*), 6.22 (t, 2H, *ortho* C*H*), 3.43-3.15 (m, 4H, NCH_2CH_2N), 2.82 (s, 6H, mesityl CH_3), 2.40 (s, 6H, mesityl CH_3), 2.32 (m, 3H, Cyp), 2.23 (s, 3H, mesityl CH_3), 1.80 (s, 3H, mesityl CH_3), 1.49 (m, 18H, Cyp), 1.27 (m, 6H, Cyp); ^{13}C NMR (benzene-d_6, 75 MHz): δ=296.8, 221.7, 152.4, 139.9, 138.7, 138.1, 137.8, 137.5, 136.2, 131.7, 130.3, 129.7, 52.3, 51.4, 35.9, 35.6, 32.3, 29.9, 26.5, 26.4, 23.4, 21.7, 21.4, 20.9, 19.3, 14.7; ^{31}P NMR (benzene-d_6, 300 MHz): δ=26.29 ; MS (HRMS/EI) calcd for C43H59N2Cl2PRu [M]+ 806.2840, found 806.2813.

Synthesis of complex [Ru]22. The procedure was adapted from the literature.[72]

In the drybox, a flame-dried Schlenk flask equipped with a magnetic stir bar was charged with 0.130 g (0.128 mmol) of catalyst **[Ru]10** and dissolved in 4 ml of toluene. Once out of the drybox, 0.82 ml (10.1 mmol) of degassed pyridine was added to the stirring solution via cannula. The color immediately changed from brown to bright green. The mixture was stirred for another 10 minutes at room temperature, then added dropwise to 50 ml of cold pentane at –78^{o}C. A green solid precipitated and the solution was filtered out via cannula filtration. The green residue, corresponding to **[Ru]20** was washed with cold pentane and dried under vacuo. A solution of tricyclopentyl phosphine (78 mg, 0.328 mmol, 2.5 eq) in 4 ml of benzene was added to the Schlenk flask and the color immediately turned brown. The mixture was stirred at room temperature for 15 minutes under argon, then the solvent was evaporated. The brown residue was washed with anhydrous methanol (2 x 25 mL) and pentane (50 mL), and dried under vacuum to yield 0.693 g of a pink solid (0.83 mmol, 78%).

^{1}H NMR (benzene-d_6, 300 MHz): δ= 19.85 (s, 1H, Ru=C*H*), 8.32 (d, 1H, *ortho*-C*H,* $^{2}J_{H,H}$=8.4 Hz), 7.30-7.17 (multiple peaks, 5H, aryl C*H*), 7.00 (t, 2H, *para* C*H,* $^{3}J_{H,H}$=7.4 Hz), 6.72 (s, 2H, aryl C*H*), 4.22 (sept, 1H, C*H*(CH_3)$_2$), 3.89-3.67 (m, 4H, NCH_2CH_2N), 2.30 (s, 3H, C*H* in PCp_3), 1.72 (d, 6H, CH(CH_3)$_2$, $^{2}J_{H,H}$=6.5 Hz), 1.58 (d, 6H, CH(CH_3)$_2$), 1.45 (m, 16H, Cyp), 1.22 (m, 8H, Cyp), 1.18 (d, 6H, CH(CH_3)$_2$, $^{2}J_{H,H}$=6.5 Hz), 1.08 (d, 6H, CH(CH_3)$_2$, $^{2}J_{H,H}$=6.5 Hz); ^{13}C NMR (benzene-d_6, 75 MHz): δ=292.8, 222.7, 150.5, 147.6, 138.8, 136.7, 132.0,130.6, 129.5, 125.1, 124.6, 55.3, 54.7, 35.7, 35.4, 32.3, 29.9, 29.8, 28.6, 27.9, 27.2, 26.5, 26.4, 25.0, 23.4, 14.7; ^{31}P NMR (benzene-d_6, 300 MHz): δ=26.29 ; MS (HRMS/EI) calcd for $C_{49}H_{71}N_2Cl_2PRu$ $[M]^+$ 890.3780, found 890.3724.

CHAPTER 5
UNDERSTANDING STRUCTURAL ISOMERIZATION DURING RU-CATALYZED OLEFIN METATHESIS: A DEUTERIUM LABELING STUDY.

Introduction

The discovery of well-defined, functional group tolerant ruthenium carbene catalysts such as Grubbs' $(PCy_3)_2(Cl)_2Ru=CHPh$ **[Ru]1**[37,57,80,87] has considerably broadened the scope of olefin metathesis.[1,2,7-10,20,31] The versatility of this class of catalysts has contributed to their growing popularity and motivated new developments. A 'second-generation' of catalytic systems was introduced as one N-heterocyclic carbene replaced a phosphine ligand (**[Ru]3**[69,70] and **[Ru]4**[71,74,75] in Figure 5-1), further enhancing their catalytic activity and the thermal stability. Since then, many ligand modifications have been reported in order to tune in the activity and/or the stability of the catalyst according to specific reaction conditions. For example, the exchange of a phosphine for an isopropoxy-tethered benzylidene conferred an exceptional stability to the catalyst in solution, which has allowed the catalyst to be recycled after ring-closing metathesis (RCM) or cross-metathesis (CM) reactions.[56,95,186] Also, addition of more labile ligands, like pyridine derivatives, enabled fast initiation rates particularly desirable for living ring-opening metathesis polymerization (ROMP).[99,194,204]

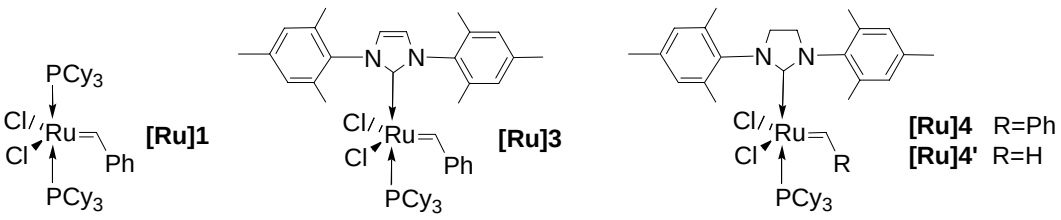

Figure 5-1. Olefin metathesis catalysts

In spite of their high reactivity in metathesis chemistry, these ruthenium catalysts were suspected to undergo non-metathesis transformations.[160-165] Among them, alkene isomerization has emerged as an important side reaction of ruthenium catalyzed metathesis, disturbing the product's microstructure by apparent migration of the double bond along the alkyl chain.[166] First observed on substrates containing allylic functionalities in combination with first generation catalysts,[167-171] double bond isomerization has since been reported with 2nd generation catalysts on a broad variety of substrates competitively and sometimes prior to olefin metathesis.[113,172-177,192] Promoted by diverse transition metals, olefin isomerization has been known to operate through two distinctive pathways: either through η^3-allyls, or through an alkyl intermediate involving a long-lived metal hydride.[178] Mechanistically, the π-allyl involves a formal *intra*molecular 1,3-H shift while the metal hydride operates through an *inter*molecular addition-elimination with an inherently competitive 1,2-H shift. Consequently, isotopic labeling experiments have often been used to probe the nature of the mechanism.[205,210-214] However, despite the increasing number of studies, the ruthenium intermediate responsible for this undesirable reaction has yet to be identified. Although it is often attributed to the formation of a ruthenium hydride *in situ*, as a decomposition product of the original carbene catalyst,[179-180] the possibility of a π-allyl mechanism cannot be ruled out.[174]

Apart from standard hydrogenolysis,[158,215,216] numerous pathways have been proposed for the transformation of ruthenium carbene into ruthenium hydride complexes. For example, carbonyl hydrides **[Ru]6** and **[Ru]7** (Figure 5-2) first isolated during the decomposition of alkoxycarbene complexes,[90,91] were identified as products of the

reaction of **[Ru]1** and **[Ru]4** with primary alcohols in the presence of a base.[72,92-94] Although the mechanism is still at a speculative stage,[90,92] both complexes are known to be efficient catalysts for isomerization, hydrogenation,[92,217-220] and hydrovinylation.[221] More recently, Grubbs *et al.*[89] isolated a dinuclear ruthenium hydride **[Ru]5** as one of the decomposition products of the methylidene intermediate **[R]4'** formed during a metathesis cycle. Other studies include the possibility of a ruthenium insertion into the C-H bond of one of the methyl groups present on the NHC ligand.[72,183] This type of activation is common for complexes containing NHC ligands and has been witnessed during the preparation of ruthenium carbene **[Ru]4**; however, not yielding a hydride complex **[Ru]8**.[72]

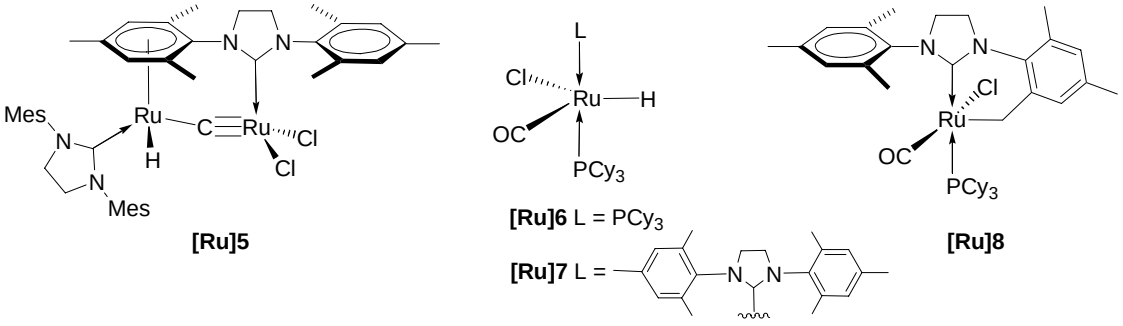

Figure 5-2. Decomposition products of ruthenium carbene complexes

Acyclic diene metathesis (ADMET) has been used for the modeling of precise ethylene/α-olefin copolymers.[127,128,130] Therefore, controlling isomerization is crucial since it results in irregular microstructures, whether it occurs on the monomer or on the product (Figure 4-2). Previously, we have reported the metathesis vs isomerization activity of ruthenium carbene catalysts using the model substrate 1-octene.[176,192] Even though metathesis consistently occurred faster, isomerization products could represent as much as 80% of the reaction mixture with catalysts containing NHC ligands. When other modified complexes were used, the isomerization activity appeared to be closely related

to the metathesis activity (Chapter 4). Because no definite conclusion could be drawn from catalyst modification, it was time to investigate the mechanism of olefin isomerization under metathesis conditions. The reaction of allyl-*1,1-d_2*-methyl ether with catalyst **[Ru]4** was monitored by ^{1}H and ^{2}H NMR spectroscopy to watch deuterium scrambling and therefore conclude on the operating isomerization mechanism. In the meantime, a deuterated version of catalyst **[Ru]4** (complex **[Ru]23** in Scheme 1) was designed to further demonstrate the role of NHC ligand in catalyst decomposition and assess the possibility of a C-H activation, which could be responsible for the formation of a metal hydride complex. Again, ^{2}H NMR was used to follow the decomposition of complex **[Ru]23** and observe its behavior in the presence of olefinic substrates; any deuterium incorporation on the olefin backbone would prove the presence of a ruthenium deuteride complex.

Results and Discussion

Mechanistic Studies

Even though both the π-allyl hydride and the metal hydride addition-elimination mechanism result in the same product, isotopic labeling studies can highlight their differences. Indeed the two pathways can be distinguished by looking at the hydrogen shift undergone during the isomerization reaction. The π-allyl mechanism, involving a metal that does not contain a hydride ligand, is typically *intra*molecular. A free olefin coordinates to the metal and undergoes an oxidative addition of the allylic proton to form a π-allyl metal hydride intermediate. The hydride fragment is then transferred to the terminal position (of an α-olefin) to yield the isomerized olefin. Hence, *a formal 1,3-H shift is observed when the π-allyl mechanism is active* (Figure 5-3).

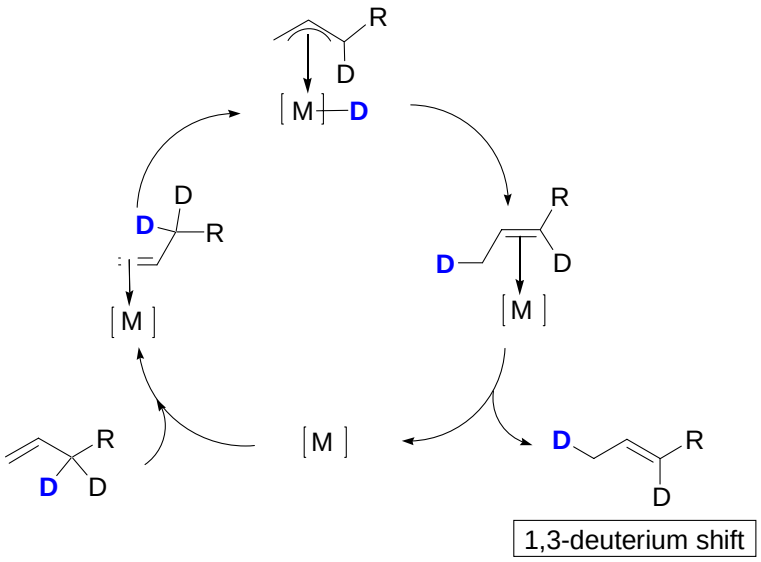

Figure 5-3. Deuterium shift with a π-allyl hydride mechanism

On the other hand, the metal hydride mechanism involves a stable metal-hydride complex already present in the reaction, and is therefore *inter*molecular, i.e. hydrogen atoms from one substrate can be transferred to the catalyst on to another substrate molecule. The olefin inserts into the metal-hydride bond to form either a primary metal alkyl (thermodynamically favored), or a secondary metal alkyl that will lead to the isomerized olefin by β–H-elimination, generating another metal-hydride. The occurrence of both Markovnikov and anti-Markovnikov additions of the metal hydride across the double bond results in a characteristic 1,2-H-shift:[213] when a primary metal alkyl undergoes a β-elimination of a different hydrogen, the resulting olefin can reinsert in the metal-hydride bond to form a secondary metal alkyl. Subsequent β-elimination of the appropriate hydrogen results in an apparent *1,2-H-shift*, as illustrated in Figure 5-4 for a deuterated olefin. A formal 1,3-H-shift can also be observed through the formation of a secondary metal-hydride.

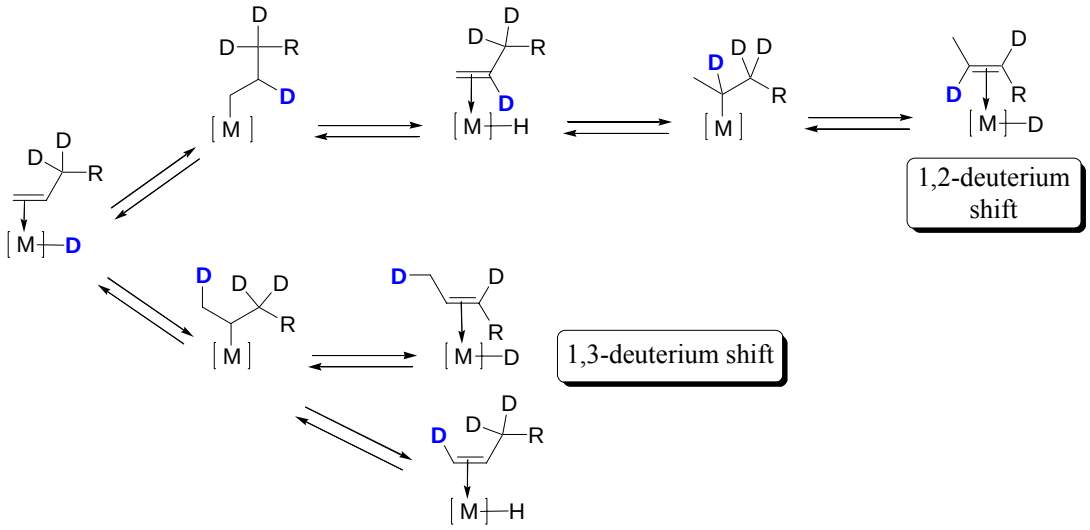

Figure 5-4. Deuterium shifts with a metal-hydride addition-elimination mechanism

Substrates such as allyl-*1,1-d*$_2$ alcohol[205,210,211] and the corresponding methyl ether[205,212,213]have often been used to probe the nature of the hydrogen shift in metal-catalyzed olefin isomerization, particularly because of the irreversibility of the reaction. Indeed, allyl-*1,1-d*$_2$ alcohol will isomerize exclusively into propionaldehyde-*1,3-d*$_2$ in the case of a π-allyl hydride mechanism, while a mixture of partially deuterated propionaldehydes with deuterium incorporation at the C-2 position will be expected in the case of the metal-hydride mechanism. Actually this method is often taken as convincing proof for the π-allyl hydride mechanism without investigating the inter/intramolecularity of the process.

In this particular case, allyl alcohol has been known to react with ruthenium carbenes and form hydride complexes.[163,164,222] Therefore only allyl methyl ether will be used, which in the end should provide the same set of observations. A 2.3 M solution of allyl-*1,1-d*$_2$-methyl ether (**4-1**) in C_6D_6 was loaded with 0.2 mol% of complex **[Ru]4** and heated at 35^{o}C for 3 days to reproduce the conditions used in previous isomerization studies.[176,192] The composition of the reaction mixture was solved using 2D NMR and

NOE experiments (See experimental section for details). The resulting sample consists of four compounds shown in Figure 5-5: *cis* and *trans*-propenyl methyl ether (**5-2*cis***** and **5-2*trans***) are the isomerization products of the starting material and represents 70% of the mixture; the remaining 30%, *cis* and *trans*-1,4-dimethoxy-but-1-ene (**5-3*cis***** and **5-3*trans***), are the result of isomerization on the metathesis product. Each of these compounds is a mixture of the four isotopomers yielding from partial deuteration in positions 2 and 3 of the alkylene ether. Interestingly, position 1 is completely deuterated while position 4 does not contain any deuterium. The relative ratios of each compound and the molar fractions of deuteration in each position are given in Figure 5-5.

Note: The sum of deuterium for each molecule of product **5-3** and **5-2** does not equal 2.00 (number of deuterium present in one molecule of allyl-*1,1-*d_2-methyl ether) because some deuterium atoms were incorporated in the ethylene released during the metathesis of allyl-*1,1,3-*d_3-methyl ether.

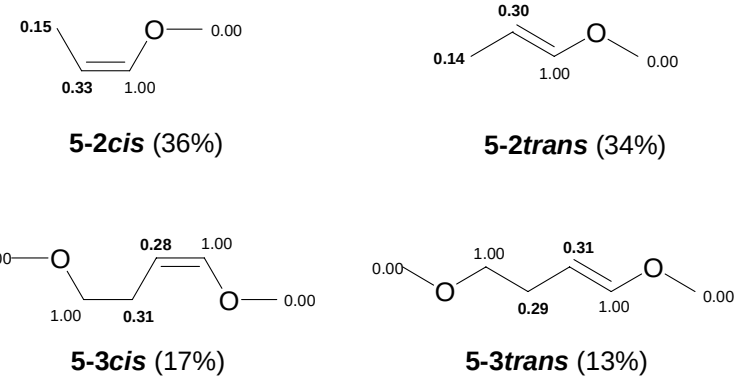

5-2*cis* (36%) **5-2*trans*** (34%)

5-3*cis* (17%) **5-3*trans*** (13%)

Figure 5-5. Products of the reaction of allyl-*1,1-*d_2-methyl ether with complex **[Ru]4**

The fact that position 4 is not deuterated at all proves that there is no deuterium exchange with the solvent, i.e. all the deuterium present on the products actually comes from the starting material, which confirms the validity of this model study. Therefore, deuterium incorporation at the C-2 position clearly indicates that *the isomerization*

mechanism operating here is a metal-hydride addition-elimination. In fact, the relative ratios of deuterium incorporation at position 2 and 3 reflect the relative rates of Markovnikov (formation of a secondary metal alkyl) versus anti-Markovnikov addition (formation of a primary metal alkyl) of the metal hydride across the olefin bond (Figure 5-5). This ratio is estimated to be about 1:2 for both **5-2cis** and **5-2trans**, which is consistent with the preferred formation of the thermodynamically favored primary metal alkyl. For example, Cramer *et al.*[223] reported that in the isomerization of 1-butene by rhodium (III) hydride, addition of D to C-2 was 15 times as fast as addition to C-3. The lower ratio obtained with our allyl ether may be a result of the directing effect of the oxygen moiety, as described previously by McGrath and Grubbs[205] during the isomerization of allylic alcohols and ethers by $Ru^{II}(H_2O)_6(tos)_2$.

In the case of **5-3*cis*** and **5-3*trans***, the relative ratios of deuterium incorporation at C-2 and C-3 are approximately 1:1, which makes sense since isomerization occurs on an internal double bond. Therefore, the metal-hydride can only add across the olefin bond of the metathesis product and forms exclusively a secondary metal alkyl.

The complete deuteration of position 1 suggests the irreversibility of the isomerization reaction. If the reaction were reversible, an isomerized olefin, methoxy-*1,3-*d_2-propene for instance, should be able to insert into a metal-hydride bond to form a secondary metal alkyl, which could subsequently undergo a β-D-elimination to produce methoxy-*3-*d_1-propene (Figure 5-6). This transfer of the methylene deuterium to the metal would automatically bring the % deuteration at C-1 under 100%, which is not the case. A similar behavior was witnessed by Krompiec *et al.*[224] with hydride complex $RuCl(H)(CO)(PPh_3)_3$. Under ADMET conditions, the reaction of allylic ether *N,N*-bis[3-

(allyloxy)-2-hydroxypropyl]aniline with **[Ru]4** also afforded complete isomerization into the vinylic ether.[175]

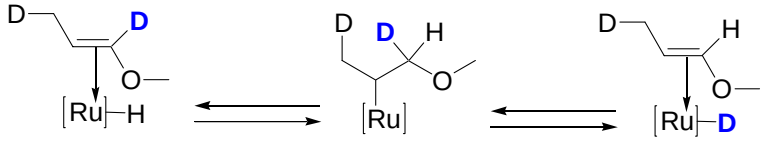

Figure 5-6. Incorporation of hydrogen at C-1 by reversible isomerization

The distribution of isomerization vs. metathesis product is a result of several factors. Although metathesis is often believed to be the faster and therefore primary reaction, the present conditions are set up in a closed system, which limits its progression. Once the system gets saturated with ethylene, it reaches equilibrium and metathesis chemistry virtually stops. Meanwhile, the isomerization reaction continues to consume starting material and produce a vinyl ether, which can then trap the metathesis catalyst into a stable, low-reactive Fisher carbene whose bis-phosphine analog is known to thermally decompose into hydride complex **[Ru]6**.[90,91] Observation of a typical color change from pink to bright yellow, indicative of alkoxy carbene decomposition, reinforces the argument for the proposed mechanism. Therefore, not only does the metathesis rate decrease overtime, but the isomerization rate also increases as the hydride concentration increases (if we consider that the source of hydride is related to catalyst decomposition). Hence only 30% of metathesis product, subsequently isomerized to **5-2*cis*** and **5-2*trans***.

Other Mechanistic Considerations

Note: The olefin isomerization mechanism operating here cannot involve a β-H shift from an allylic proton to the metal as proposed for the isomerization of allyl alcohols in the presence of **[Ru]1**.[222] Indeed, the mechanism shown in Figure 5-7

involves the stoichiometric consumption of the isomerization-metathesis catalyst and in our case would have yielded only up to 0.2 mol% of isomerized starting material. Nevertheless, this step may be responsible for the formation of the hydride species involved in the metal-hydride isomerization reaction described above, by reaction of the ruthenium carbene with vinyl ether, and subsequent decomposition of the Fisher carbene hence formed.[90,91]

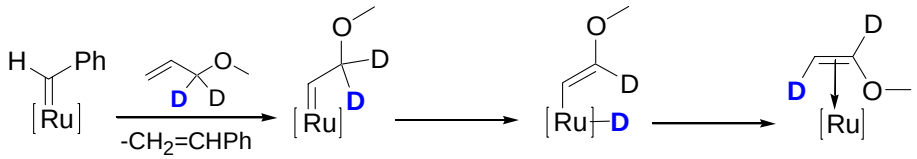

Figure 5-7. β-H abstraction-elimination mechanism proposed for allyl alcohol isomerization by **[Ru]1**

Kinetic Studies

The relative rates of isomerization versus metathesis could be measured for allyl-*1,1-d_2*-methyl ether when the system had reached metathesis equilibrium. Indeed, when the reaction was monitored by ^{1}H NMR the starting material quickly disappeared to form 1,4-dimethoxy-but-2-ene, but after 60 minutes, the rate of formation of metathesis product became slower until its concentration leveled, indicating metathesis equilibrium at only 7% conversion. (Noteworthy, traces of deuterium incorporation on the olefinic bond of the starting material were also observed, suggesting the presence of a metal hydride at this early stage of reaction.) From this point on, the steady evolution of isomerized starting material was clearly observed. Considering the rate of metathesis to be negligible and the isomerization of **5-2** to be irreversible, as proven above, the isomerization reaction then followed first-order kinetics. The rate was calculated at approximately 5.59 10^{-06} s^{-1} (Figure 5-8). The metathesis equilibrium constant could also

be estimated, at 4.04 10^{-06}, by considering the concentrations of metathesis product and starting material at equilibrium. Of course, this does not reflect the rate of the metathesis reaction, but if we consider it to be of the same order or larger than the isomerization rate, the reverse metathesis rate with ethylene should be 1 or larger, which emphasizes the importance of ethylene removal.

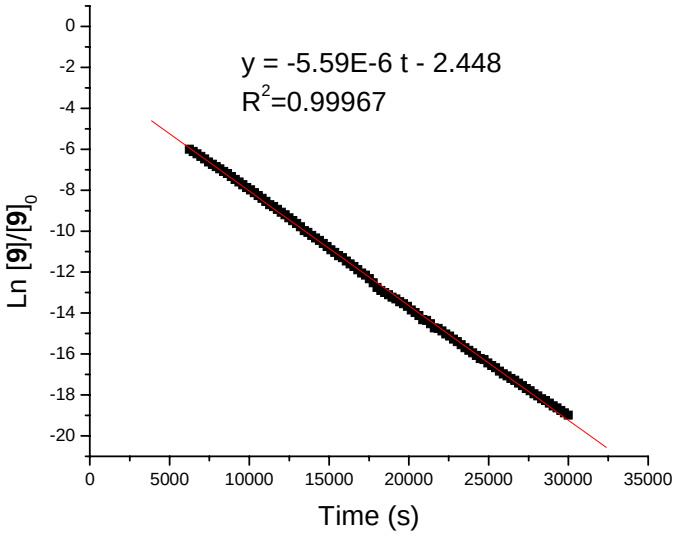

Figure 5-8. Total concentration of **4-1** versus time. Conditions: 2.3M solution of **4-1** in C_6D_6 with 0.2 mol% of **[Ru]4** at 35°C for 8 hours

Now that olefin isomerization is known to operate via a metal-hydride complex, the question remains what is the structure of this hydride species and what causes its formation? The first step would aim to understand the role of NHC ligands in the isomerization behavior of ruthenium carbene catalysts.

Design, Synthesis and Characterization

Recent reports have shown that metathesis catalysts bearing NHC ligands undergo olefin isomerization to a considerable extent compared to their phosphine analogs.[166,176,192] Ligand variation experiments on both the phosphine and carbene

ligands have further reinforced the idea that NHC ligands play a major role in the isomerization behavior of ruthenium carbene catalysts (Chapter 4). In light of the results discussed above, the eventual participation of NHC groups in the production of a metal-hydride became the focus of the following experiment. Speculations evoke a possible ruthenium insertion into the C-H bond of one of the mesityl groups. To address this issue, complex **[Ru]23** (Figure 5-9) was designed with fully deuterated *ortho* methyl groups on the NHC aryl rings. The structure similarity should guarantee comparable reactivities to parent **[Ru]4** while the deuterium atoms should allow its traceability through isotopic labeling experiments. Any sign of ruthenium insertion should be easily detected by NMR spectroscopy.

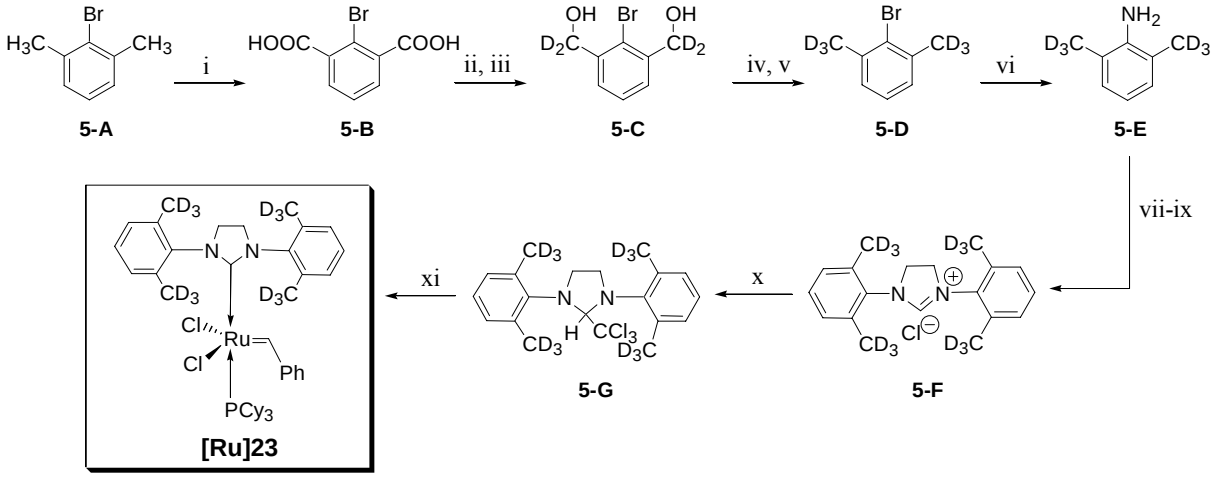

Figure 5-9. Synthesis of Complex **[Ru]23**[a]

[a] Reagents and conditions: (i) $KMnO_4$, 50% *t*BuOH in water, reflux, 16h; 99%. (ii) K_2CO_3, CH_3I, cat. $CsCO_3$, DMF, reflux 12h; 81%. (iii) LAD, THF, 0°C, 20 min; 85%. (iv) CBr_4, PPh_3, CH_2Cl_2; 70%. (v) LAD, THF, room temperature; 90%. (vi) (a) Mg, ether, reflux, 2h; (b) TMSDA, room temperature, 3h; 55%. (vii) glyoxal, *n*-PrOH, water, room temperature to 60°C, 6h; 80%. (viii) $NaBH_4$, 1:2 MeOH:THF, room temperature, 16h, 1M HCl; 85%. (ix) $CH(OEt)_3$, reflux, 4h; 60%. (x) NaH, $CHCl_3$, room temperature 2h; 82%. (xi) **[Ru]1**, toluene, 60°C, 90 min; 75%.

Starting material bromo-*m*-xylene (**5-A**) was sequentially oxidized and reduced to afford deuterated xylene **5-D**. Direct reduction of the diacid **5-B** by lithium aluminum

deuteride only yielded unidentified decomposition products. The reaction was rendered successful by switching to the corresponding diester, but still necessitated controlled conditions to reach reasonable yields. The alcohol groups of **5-C** were substituted to bromine groups to allow further reduction into the fully deuterated bromoxylene **5-D**. Deuterated 2,6-dimethyl aniline was obtained by substitution of the bromine group through a Grignard reaction with trimethylsilylmethyl azide (TMSDA). The corresponding ligand salt **5-F** was then easily prepared according to the regular procedure. However, the chloroform adduct **5-G** was used for the synthesis of final complex **[Ru]23** to ensure a better yield and avoid salt contamination.[72]

Both ^{1}H and ^{31}P NMR spectra of complex **[Ru]23** are very similar to catalyst **[Ru]4** showing the same exact carbene shift at 19.63 ppm and the same phosphine at 29.5 ppm.[71] No hydride trace was detected at this point. The ^{2}H NMR shows 2 singlets at 2.35 and 2.75 ppm, suggesting the asymmetry of the 2 aryl groups provoked by a distortion of the imidazolylidene ring. The crystal structure exhibits a typical square-pyramidal geometry with the carbene moiety in the apical position (Figure 5-10). However, almost the entire molecule is affected with an inherent disorder related to the existence of two mirror images within the asymmetric unit. Representative bond lengths and angles of complexes **[Ru]4** and **[Ru]23** are reported in Table 1 for comparison.[194] Apart from the chlorine atoms, whose bond length to ruthenium vary of about 0.1 Å, both solid-state structures appear to be very similar. The deviation of the chlorines is just a result of the global molecular disorder. In fact, the Ru-Cl bond length averages at 2.3929 Å from the 2 disordered structures. This augmented freedom of the NHC ring could be due to the missing *para*-methyl group on the aryl substituents compared to

complex **[Ru]4**, but does not disturb the overall characteristics. The superposition of complex **[Ru]4** and one of the mirror image of **[Ru]23** shows little variation between the two crystal structures and clearly illustrates their similarity. Since complexes **[Ru]4** and **[Ru]23** are so related characteristically, it is reasonable to expect a comparable catalytic behavior.

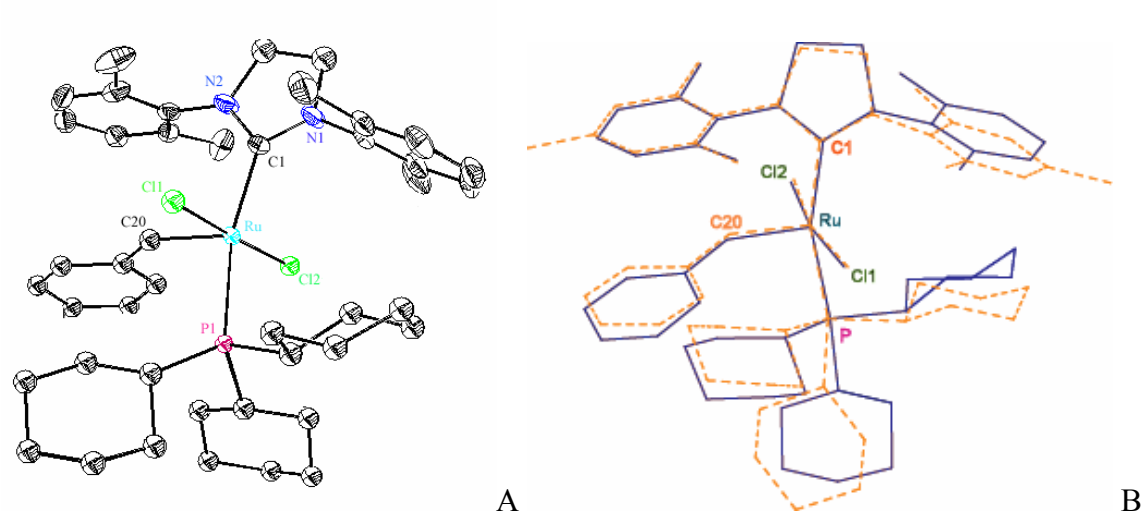

A B

Figure 5-10. X-Ray structure of complex **[Ru]23**. A) ORTEP Diagram of complex **[Ru]23**. B) Superposition of the crystal structures of complex **[Ru]4** (orange) and **[Ru]23** (blue)

Table 5-1. Selected bond lengths (Å) and angles (deg) for complexes **[Ru]4** and **[Ru]23**

Bond lengths	Complex **[Ru]4**	Complex **[Ru]23**
Ru-C(1)	2.085(2)	2.076(3)
Ru-C(20)	1.835(2)	1.844(3)
Ru-Cl(1)	2.3988(5)	2.3644(9)
Ru-Cl(2)	2.3912(5)	2.4302(10)
Ru-P	2.4245(5)	2.4298(8)
Bond angles	**Complex [Ru]4**	**Complex [Ru]23**
C(20)-Ru-C(1)	100.24(8)	98.37(11)
C(1)-Ru-Cl(1)	94.55(5)	88.90(8)
C(1)-Ru-Cl(2)	83.26(5)	89.65(8)
C(20)-Ru-Cl(1)	89.14(7)	105.17(9)
C(20)-Ru-Cl(2)	103.15(7)	87.50(9)
Cl(1)-Ru-Cl(2)	167.71(2)	167.32(4)
C(1)-Ru-P	163.73(6)	163.29(7)
C(20)-Ru-P	95.89(6)	97.33(9)

Thermal Stability

When complex **[Ru]23** was left at 70°C in an airtight solution of benzene-d_6, no sign of ruthenium deuteride was detected by ^{2}H NMR, even after 21 days, where the decomposition process was already at an advanced stage. In fact, observation of the ^{31}P NMR spectrum indicates that only 4% of the original complex remained. Other typical peaks have emerged at 10.4 ppm, 34.6 ppm, 47.0 ppm and 47.4 ppm, along with what appears to constitute 70% of the phosphorus products centering around 72 ppm. The first signal can be attributed to free PCy_3. The peak at 34.6 ppm seems consistent with the phosphonium salt $[PCy_3CH_2Ph]^+[Cl]^-$, observed by Grubbs[89] as a by-product of methylidene **[Ru]4'** decomposition. Interestingly, the peaks at 47.0 ppm and 47.4 ppm, representing 15% of the phosphorus products, correspond to carbonyl hydride complex **[Ru]6** and **[Ru]7**, respectively, usually formed by reaction of **[Ru]4** with primary alcohols.[93] Contamination during the methanol wash following the synthesis cannot possibly account for the 15% of hydride produced here, especially since ^{1}H NMR only confirmed the presence of **[Ru]6** and **[Ru]7** (characteristic triplet at -24.25 ppm and a doublet at -24.95 ppm) as traces. Therefore, some unknown phosphorus compound must appear around the same shifts as the carbonyl compounds. A third unidentified hydride is visible on the ^{1}H NMR as a doublet at δ -7.43 ppm (^{2}J=50 Hz) that had also been observed by reaction of **[Ru]4** with primary alcohols.

Even though the ^{2}H NMR does not indicate the presence of a ruthenium deuteride, a number of deuterated species have formed. Most signals overlap between 1 and 3 ppm collapsing into a broad base, which accounts for the deuterated methyls of the NHC ligand whether it is free or coordinated to a ruthenium atom (i.e. complexes **[Ru]7** and

[Ru]23). The ^{13}C NMR did not reflect the presence of any carbonyl compounds nor carbide. Since no compound could be isolated, the isomerization behavior of this decomposition mixture was tested on 1-octene using typical reaction conditions.[192] After 24h at 55°C, a 2.3M solution of catalyst **[Ru]4** in neat 1-octene affords 76% isomers. In this case, the catalytic mixture was dried under vacuo once fully decomposed (no more carbene signal on the ^{1}H NMR), and 0.5 g of 1-octene was added. The reaction was allowed to stand at 55°C for 24h, and the isomers content was determined by ^{1}H NMR by integration of the internal olefin peak at δ 5.40 ppm. No decomposition product of complex **[Ru]23** was able to isomerize olefins at the rate observed with the original metathesis catalyst (5% of isomers vs. 76% obtained with catalyst **[Ru]4** in similar conditions).[176]

Because the methylidene is a key intermediate in most metathesis reactions, its decomposition was also checked in situ by reacting **[Ru]23** with excess ethylene in benzene at 60°C and stirring it for 3 days. When the reaction was sampled for ^{1}H NMR, these conditions led to the complete transformation of benzylidene **[Ru]23** into the methylidene, which decomposed rapidly as indicated by the disappearance of the methylidene signal at 18.40 ppm. But again, no sign of ruthenium deuteride was detectable by ^{2}H NMR, and the same peaks, observed during the decomposition of the benzylidene, appeared between 1 and 3 ppm. Interestingly, a singlet at δ 7.14 ppm indicated the presence of partially deuterated benzene, the deuterium content largely exceeding the amount naturally found in benzene. This suggests the existence of an exchange process since the only original source of deuterium in this case was the methylidene of complex **[Ru]23**. A similar exchange to solvent was observed with

ruthenium dihydride (IMes)Ru(H)$_2$(H$_2$)$_2$PCy$_3$,[225] and other dihydrides have shown to undergo exchange processes.[206,207] The species responsible for this H/D exchange may also be a ruthenium dihydride, which may not be detectable because of NMR detection/concentration limits.

The catalytic mixture once fully decomposed was again tested for isomerization activity using 1-octene in the same conditions as previously. Even though the isomerization extent was increased to 25% isomers, the decomposition products of complex **[Ru]23**'s methylidene did not match the isomerization behavior observed with catalyst **[Ru]4** in metathesis conditions, which suggests that the isomerization process involves more than simply decomposition products. Other intermediates of the metathesis cycle must play a role in the formation of the hydride responsible for this side-reaction. For example, Forman *et al.*[226] have described the decomposition of a metallacyclobutane through β-H-abstraction to form a ruthenium hydride, and explain the appearance of different alkenes from the metathesis of ethylene with **[Ru]1'**. Hence, hydride formation in the presence of olefinic substrates was further investigated to reflect true metathesis conditions.

Catalytic Behavior Under Metathesis Conditions

If there was formation of a ruthenium deuteride by metal insertion in one of the methyl bonds, inevitably there would be deuterium incorporation on the olefin, which should be easily detectable by NMR. To avoid any solvent contamination and allow the detection of both catalyst and substrate on the NMR scale, the experiments were run neat, the only deuterium source being complex **[Ru]23**. First, 1-octene was used as the substrate since previous isomerization studies were based on this model.[176,192] A 0.5

mol% solution of complex **[Ru]23** in 1-octene was monitored by ^{1}H and ^{2}H NMR at 35^{o}C for 4 hours. These reaction conditions will ensure significant amounts of both metathesis and isomerization.[176,192] The ^{1}H and ^{2}H spectra were systematically superimposed to match chemical shifts, since no internal standard was available. Because of the chemical simplicity of the substrate, the distinction between isomers and metathesis products is virtually impossible by standard ^{1}H NMR. Still, in the present conditions metathesis is known to occur much faster than the isomerization process.

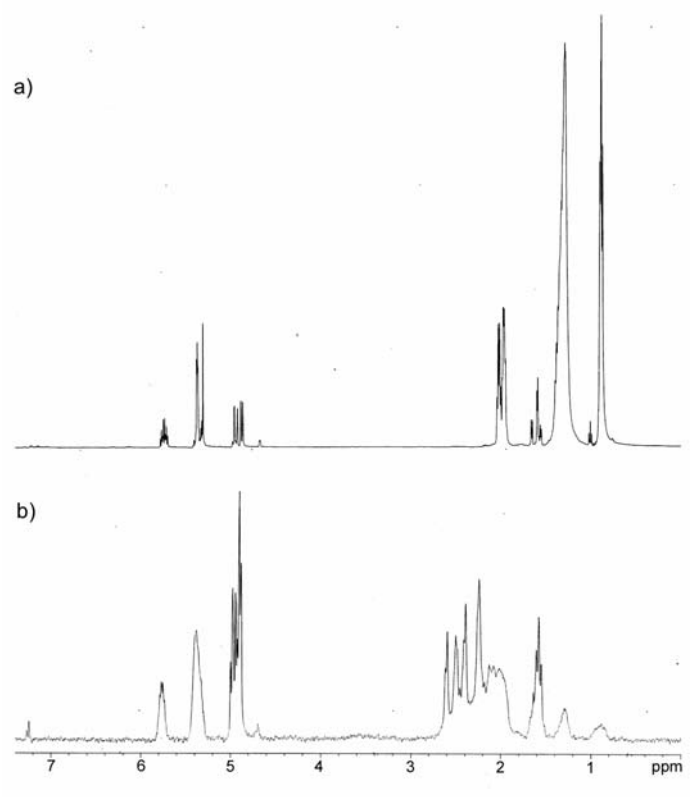

Figure 5-11. NMR spectrum of neat 1-octene with 0.5 mol% of complex **[Ru]23**, after 4h at 35^{o}C and 20h at 55^{o}C: a) ^{1}H NMR; b) ^{2}H NMR

Shortly after the experiment was started, an internal olefin signal appeared on the proton spectrum marking the beginning of the metathesis process, while the deuterium spectrum only showed the two singlets from the catalyst deuterated methyl groups. However, after 4 hours, several other peaks became visible on the deuterium spectrum,

confirming incorporation of deuterium at various positions of the olefin backbone. For easier reading, Figure 5-11 shows the ^{1}H and ^{2}H NMR spectra taken *after 24 hours* of reaction. A multiplet corresponding to the terminal olefin suggests the formation of $CHD{=}CH(CH_2)_5CH_3$. Two other vinyl signals at δ 5.75 and 5.38 ppm, though smaller, evidence deuterium incorporation at the C-2 position of 1-octene and on an internal double-bond probably from an isomer of either 1-octene or 7-tetradecene. These observations are consistent with the presence of a metal deuteride, which is further supported by the emergence of peaks in the allylic region (around δ 2.0 ppm) followed by peaks in the alkane region (at δ 1.30 and 0.90 ppm), supposing that the isomerization reaction progresses along the olefin backbone to produce *1,d_1*-2-, -3-, -4-octene and *8,d_1*-3-, -2-, -1-octene, for example (Figure 5-12). The formation of the metal alkyl may be fast relative to the decomplexation of the olefin, so the same molecule of substrate can undergo several transformations before being released.[214] Despite the large excess of 1-octene, it is also possible that some of the deuterated products come from isomerization of the metathesis product, although this cannot be quantified. Noteworthy, the alkyl deuteron signals are usually broader and flatter than their vinyl analogs because of multiple couplings. For example, the methyl signal expected for *1,d_1*-2-octene at δ 1.60 ppm only becomes visible by ^{2}H NMR after longer reaction times. Nevertheless, deuterium atoms appear to preferentially incorporate at the C-1 position, suggesting a predominant Markovnikov addition of the metal deuteride across the double bond. When the temperature was raised to 55°C, the concentration of these deuterated terminal olefins seemed to increase even faster. According to fundamental entropy thermodynamics, decomplexation of the olefin must occur to a greater extent at higher temperatures,

therefore generating more olefins at a lower degree of isomerization. Indeed, after 20 hours at 55°C, the signal for the allylic methyl of *1,d*$_1$-2-octene at 1.60 ppm has increased significantly and is now larger than other allylic or alkyl signals (Figure 5-11).

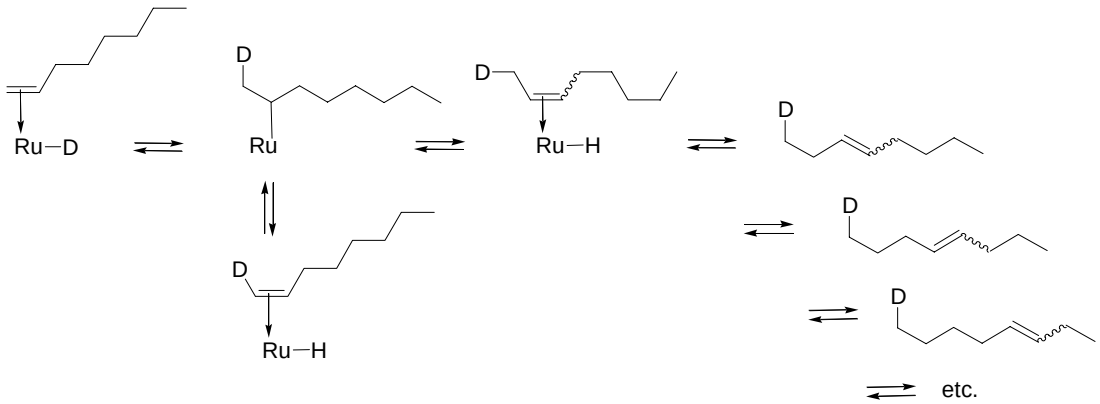

Figure 5-12. Formation of 1-octene isomers catalyzed by a ruthenium deuteride complex

Aside from the signals of the deuterated methyl groups of the metathesis catalyst, 2 broad singlets arise at δ 2.25 and 2.50 ppm. This indicates a transformation of the original complex, whether it represents a dissociating NHC ligand or a different organometallic species. Yet, none of the complexes identified so far from catalyst decomposition could match our observations. Even though the multiple peaks between δ 2 and 3 ppm recall hydride complex **[Ru]5** formed by thermal decomposition of the methylidene **[Ru]4'**, it does not account for the formation of the metal deuteride evidenced in this experiment.[89] Likewise, the characteristic signal from the Ru-C*D*$_2$Ar moiety is not observed, which would have probed the presence of complex **[Ru]8**'s equivalent. Of course, this does not exclude the possibility of a different C-D activation. In fact, hydride complex **[Ru]24** shown in Figure 5-13, formed by insertion of ruthenium into the C-H bond of a mesityl group in the presence of alkenes, exhibits a broad 'triplet' at 2.76 ppm from the protons of the Ru-C*H*$_2$Ar moiety. Other examples of C-H

activation from ruthenium carbenes could partially match these signals; however these assignments must remain speculations as long as the components of the mixture are not isolated.

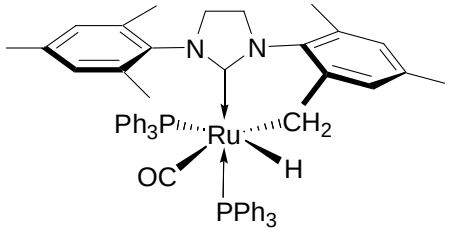

Figure 5-13. Complex **[Ru]24**

As a matter of fact, no ruthenium deuteride species was detected even after longer reaction times. The complex responsible for the isomerization process probably reacts faster than the NMR time scale allows for detection or its concentration is simply too low. But, if there were indeed formation of a ruthenium deuteride complex in sufficient amounts, then for each deuterium atom incorporated onto a substrate molecule, the corresponding ruthenium hydride species would be produced, according to the metal-hydride addition-elimination mechanism. So this hydride complex should be visible by ^{1}H NMR as the isomerization process, producing the D/H exchange, goes on. As predicted, a doublet appeared at δ –20.36 ppm with $^{2}J_{HP}$=17.8 Hz, characteristic of a hydride situated *trans* to an empty coordination site and *cis* to a phosphine. The same signal had been observed during the decomposition of the methylidene, and interestingly, only the methylidene remains at this point, implying that all the catalyst has either been activated by the olefin or decomposed. However, the information collected thus far does not allow to conclude whether this hydride complex is in fact the one responsible for olefin isomerization under metathesis conditions or if it is simply a product of the methylidene decomposition.

The same experiment was performed with allyl methyl ether, which was used to evaluate the isomerization mechanism. Dealing with an irreversible isomerization reaction should facilitate products identification, which is limited to NMR spectroscopy. Again, 0.5 mol% of catalyst was used to provide sufficient deuterium content for NMR detection.

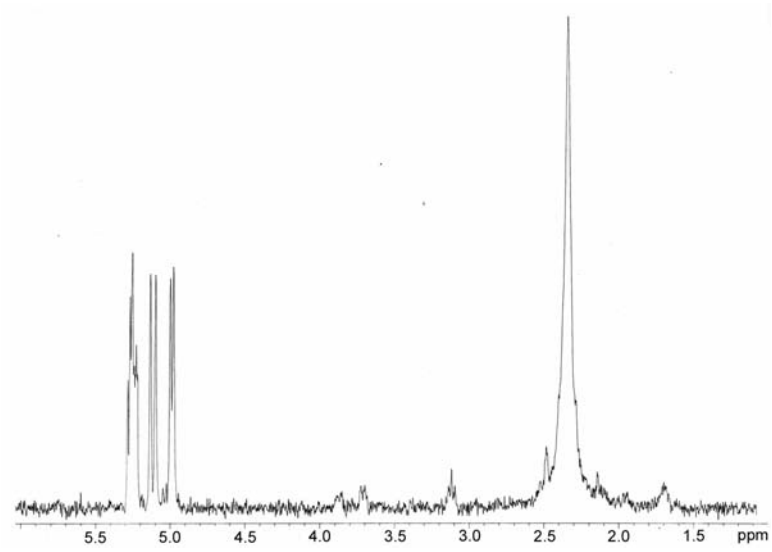

Figure 5-14. ^{2}H NMR spectrum of neat allyl methyl ether with 0.5 mol% of complex **[Ru]23**, after 4h at 35^{o}C

After 4 hours at 35^{o}C, about 30% of metathesis product had formed, with no isomerization product detectable on the ^{1}H NMR, the high concentration of ether favoring the bimolecular metathesis process over the monomolecular isomerization reaction. The ^{2}H NMR spectrum shows deuterium incorporation mostly at the terminal carbon of the olefin, as allyl-*3*-d_1-methyl ether, the signal matching perfectly the pattern of the ^{1}H spectrum (Figure 5-14). *Note:* Due to the large excess of allyl methyl ether, it is assumed that the molecules are only monodeuterated at early reaction times, since they are not likely to react again with another ruthenium deuteride. Deuterated ethylene is also present in significant amounts, more likely by metathesis of allyl-*3*-d_1-methyl ether.

Again, this is consistent with the presence of a metal deuteride complex. Smaller resonances at 1.68 ppm indicate the formation of isomerized product, as *3-d_1*-1-methoxy-propene, suggesting that the secondary metal-alkyl preferentially eliminates the proton at the C-3 position rather than at the C-1 position. This could be due to precoordination of the oxygen atom to the metal center of the alkyl complex, hence forcing the C-1 hydrogens away from the Ru-C_α-C_β plan for *β*-H-elimination (Figure 5-15). Surprisingly, a triplet at 3.13 ppm and a doublet at 3.72 ppm suggest the presence of deuteron at the C-4 and C-1 position of the starting material (less than 0.3%), respectively. A classical metal-hydride mechanism cannot explain deuteration at these positions, nor can a π-allyl mechanism. Hence, an alternate mechanism must be proceeding competitively; however, to a much lower extent. The exchange process observed during the decomposition of complex **[Ru]23**'s methylidene may also be operating here. If this is the case, the introduction of a non-isomerizable olefin, such as 3,3-dimethylbutene, should result in the deuteration of every position, and more particularly on the methyl groups.

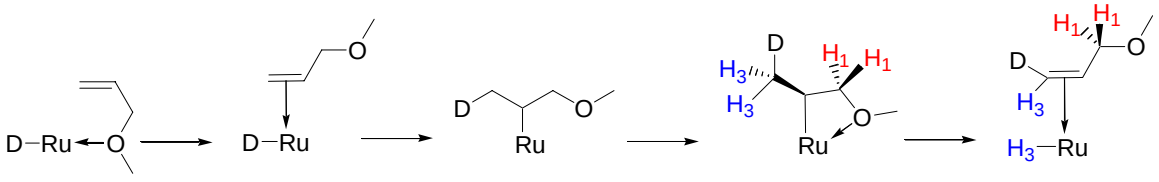

Figure 5-15. Orientation by oxygen precoordination into β-H-elimination at the C-3 position

Noteworthy, the two original singlets from the catalyst methyl groups merge into a broad singlet around 2.35 ppm, unlike what was observed when 1-octene was used as the substrate. The catalyst may adopt a more symmetrical coordination in the presence of the polar allyl ether solvent.

To look into this potential exchange process, the experiment was repeated with 3,3-dimethylbutene for its inherent inability to isomerize. If there was indeed formation of a "classical" ruthenium deuteride, deuterium incorporation would occur *exclusively* at the C-1 and C-2 position. In addition, the metathesis reaction of olefins containing allylic methyls is known to proceed at a slow rate, if at all. In fact, the cross-metathesis of 3,3-dimethylbutene with **[Ru]1** only resulted in an accumulation of the methylidene complex by non-productive metathesis.[80] Accordingly, after 4 hours at 35°C, metathesis conversions merely reached 10%.

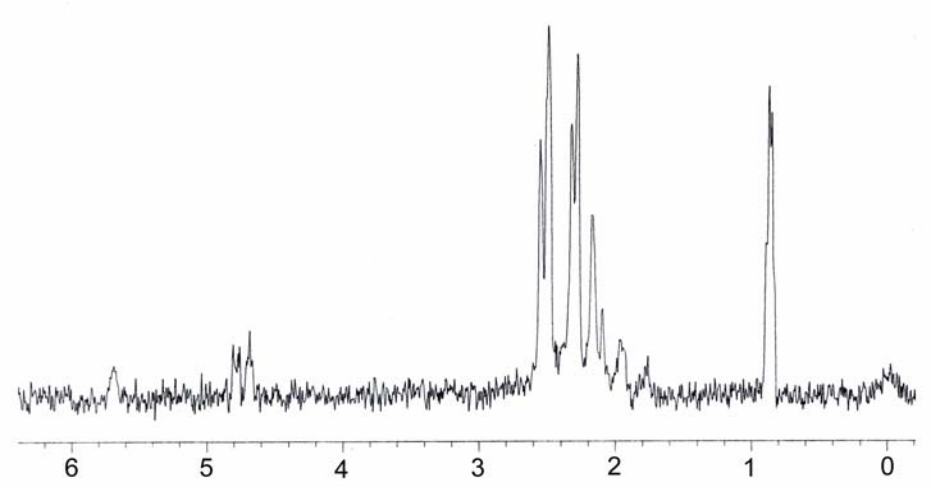

Figure 5-16. ^{2}H NMR spectrum of neat 3,3-dimethylbutene with 0.5 mol% of complex **[Ru]23**, after 4h at 35°C

Figure 5-16 illustrates the corresponding ^{2}H NMR. Even though there are signs of deuteration on the double bond (signals at δ 5.70 and 4.70 ppm), most displaced deuteron are on the methyl groups as indicated by the major peak at 0.86 ppm. This is clearly the result of an exchange process, although not necessarily direct, between the methyl groups of the NHC ligand and the substrate. It is likely that the deuterium atoms are transferred to the metal center from the NHC methyl groups, and then onto the substrate. Again, this type of transfer could very well be the result of ruthenium insertion into the methyl C-D

bond, the cyclometallation of a substituent on a nitrogen-ligated carbene on ruthenium being a fairly common reaction, albeit not well understood.[72,183,206-209] Interestingly, ruthenium dihydride (IMes)$Ru(H)_2(H_2)_2PCy_3$ promotes a similar exchange from the mesityl methyl groups to a variety of aromatic compounds, although preferentially exchanging with sp^2 rather than sp^3 C-H bonds.[225] Even though the event of the formation of a dihydride complex from a ruthenium carbene in the absence of dihydrogen may seem unlikely,[158,215,216] the reactivity of the phosphine free methylidene offers many possibilities. For instance, Stradiotto *et al.*[227] reported a reversible α-H elimination allowing the interconversion of Ru=C and Ru-alkyl species. The electrophilicity of the methylidene carbon also renders it highly sensitive to nucleophilic attack.[228] In fact, Grubbs *et al.*[89] propose that the first step towards formation of bimetallic complex **[Ru]5** involves a nucleophilic attack by free phosphine to form a ruthenium alkyl complex. Certainly, the hypothesis of a ruthenium dihydride is not ruled out by the spectroscopy analysis of **[Ru]4'** decomposition. One of the observed hydride signals may very well be one of a dihydride.

The rate of the exchange process apparently depends on the substrate. Indeed, deuterium incorporation is greater on the methyls of 3,3-dimethylbutene than on allyl methyl ether. The extensive production of the methylidene complex inherent to the metathesis of olefins containing allylic methyls, accelerates the rate of catalyst decomposition, which is probably in direct correlation with the formation of the species promoting the exchange process.

Conclusions

A deuterium labeling study was undertaken to determine the mechanism of olefin isomerization during the metathesis reactions catalyzed by 2nd generation Grubbs' catalyst. The reaction of allyl-*1,1-d*$_2$-methyl ether with **[Ru]4** at 35°C was followed by ^{1}H and ^{2}H NMR spectroscopy. The evidence of deuterium incorporation at the C-2 position allowed to conclude that a metal-hydride addition-elimination mechanism was operating under these conditions. In closed-system, the metathesis rate was calculated at approximately 5.59 10^{-06} s^{-1} while the equilibrium constant was about 4.04 10^{-06}.

The next step was attempted to identify the eventual role of the NHC ligand in the formation of the hydride species responsible for the isomerization reaction. Complex **[Ru]23**, an analogue of **[Ru]4**, was synthesized with deuterated *o*-methyl groups on the aromatic rings of the NHC ligand. Its decomposition afforded several metal hydride species; however, no deuteride complex was detected by ^{2}H NMR spectroscopy. The methylidene analogue **[Ru]23'** was also subjected to thermal decomposition, but again did not afford any detectable ruthenium deuteride complex. The isomerization activity of the catalytic decomposition mixtures were tested with benchmark 1-octene, but did not match the isomerization rates observed with **[Ru]4** under similar metathesis conditions. This suggests that other metathesis intermediates, such as the metallacyclobutane, must be involved in the isomerization process. When complex **[Ru]23** was tested with 1-octene, a variety of deuterated olefins were produced, indicating the presence of a deuteride complex, albeit not isolable spectroscopically. Finally, reaction of **[Ru]23** with allyl methyl ether and 3,3-dimethylbutene actually revealed the existence of a competitive exchange process between the NHC ligand and the substrate. The exchange might be promoted by a ruthenium dihydride intermediate whose formation is closely

related to the methylidene decomposition. Further studies must be conducted to isolate and characterize these hydride complexes. Meanwhile, hydride traps should be used during metathesis reactions catalyzed by ruthenium carbenes in order to prevent competitive isomerization.

Experimental

General

Routine ^{1}H NMR (300 MHz) and ^{13}C NMR (75 Hz) measurements were recorded on either a Mercury series or Varian VXR-300 NMR superconducting spectrometer. Chemical shifts are reported in ppm relative to tetramethylsilane (TMS) or residual proton from the solvent. All organometallic spectra were recorded in d_6-benzene, previously dried over Na/K alloy and degassed by three freeze-pump-thaw cycles.

All materials were purchased from Aldrich and used as received, except for the THF and ether that were previously dried over a catalyst bed. Complex **[Ru]4**,[71] allyl-*1,1-*d_2-methyl ether,[205] and trimethylsilylmethyl azide (TMSMA)[229] were synthesized according to the literature. Allyl-*1,1-*d_2-methyl ether was distilled, degassed by three freeze-pump-thaw cycles and stored in a glovebox.

Deuterium Labeling Study with Allyl-*1,1-*d_2-methyl ether

In the drybox, 4 mg (0.005 mmol) of complex **[Ru]4** was dissolved with 0.8 mL of C_6D_6 or toluene-*d8* in a J. Young® Valve NMR Tube, which was then layered with 185 mg (2.5 mmol) of allyl-*1,1-*d_2-methyl ether. The tube was shaken right before being loaded in the NMR instrument.

NMR spectra were recorded on a Varian Inova spectrometer equipped with a 5 mm indirect detection probe, operating at 500 MHz for ^{1}H and at 125 MHz for ^{13}C. The temperature was 35°C. Chemical shifts are reported in ppm relative to TMS. The

residual methyl signal of the solvent was used as reference (2.09 ppm for ^{1}H and 20.4 ppm for ^{13}C).

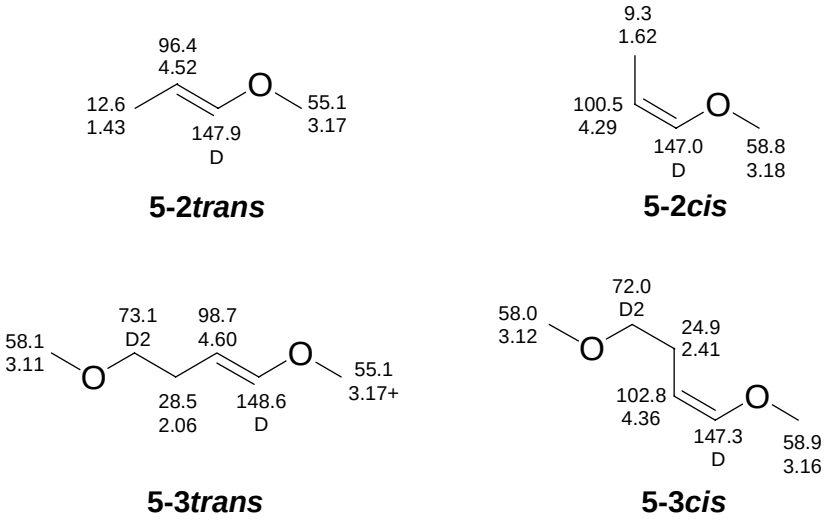

Figure 5-17. ^{1}H and ^{13}C chemical shifts assignment in compounds **5-2*cis***, **5-2*trans***, **5-3*cis*** and **5-3*trans***

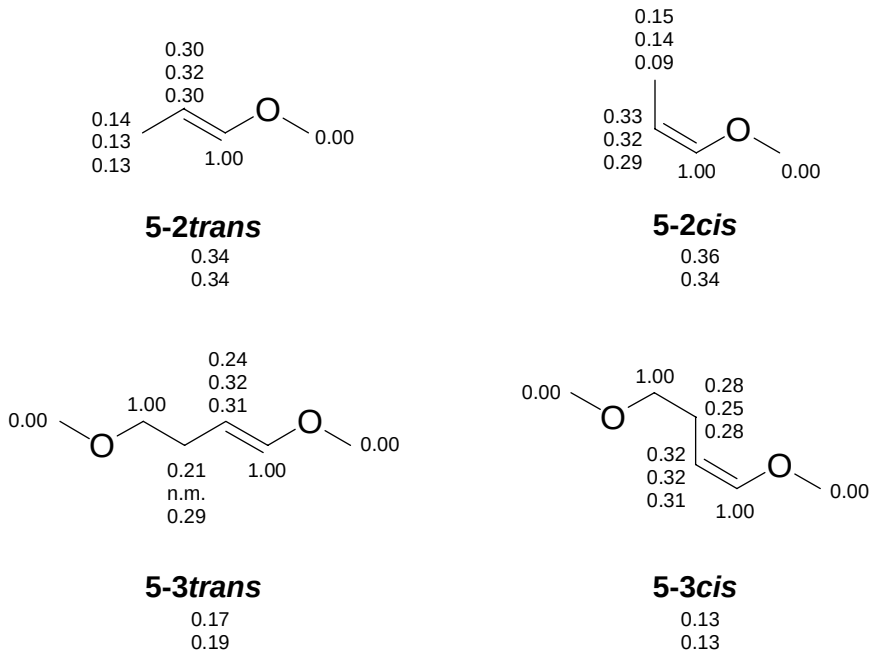

Figure 5-18. Molar fractions of compounds **5-2*cis***, **5-2*trans***, **5-3*cis*** and **5-3*trans*** in the product (under the compound number) and molar fraction of deuteration at each position.[a]

(a) The number on top was based on the proton spectrum, and the second number on the deuterium spectrum. The number on the bottom for the molar fraction of deuteration was

based on the integral of the proton signal at that position and the composition determined in the deuterium spectrum, and it is the most reliable.

The sample is a mixture of four compounds, **5-2*cis***, **5-2*trans***, **5-3*cis*** and **5-3*trans*** shown in Figure 5-17. Each of these compounds is a mixture of the four isotopomers resulting from partial deuteration in positions 2 and 3 of the alkylene ether. Positions 1 and 4 are completely deuterated. The relative ratios of the four compounds, and the molar fractions of deuteration in each position are given in Figure 5-20.

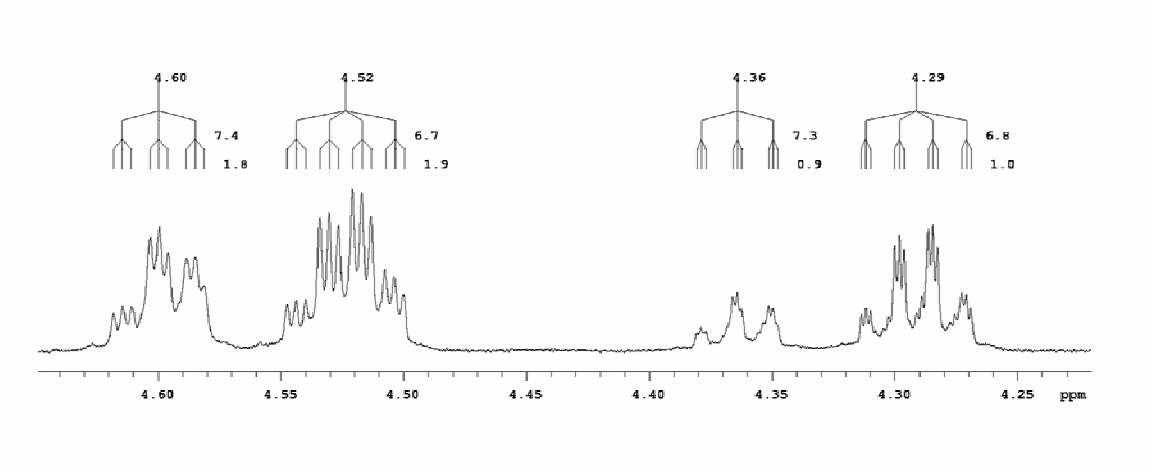

Figure 5-19. Expansion of the proton spectrum, the CH_2 region

The proton spectrum displays in the region 4.70-4.20 ppm the signals of a mixture of four compounds (Figure 5-19), quartets for compounds **5-2*cis*** and **5-2*trans*** and triplets for compounds **5-3*cis*** and **5-3*trans***. All these signals display an extra coupling with deuterium, triplet in a 1:1:1 ratio.

These signals present in the gHMBC spectrum (Figure 5-20) a one-bond coupling to a carbon in the range 96-102 ppm and two long-range couplings, one with a carbon at 9-28 ppm and one with a carbon at 147-149 ppm. This later carbon displays a triplet in *f1*, consistent to a one-bond coupling with deuterium, and also a long-range coupling to protons at 3.16-3.18 ppm, protons which are on carbons at 55-60 ppm. The protons on the

carbons at 9-28 ppm are in the range 1.43-2.41 ppm and couple with both the carbons at 96-102 and with the carbons at 147-149. These proton-carbon couplings, together with the characteristic chemical shifts, identify the methyl-1-propenyl ether fragment in all four compounds. In compounds **5-3*cis*** and **5-3*trans***, the aliphatic protons at 2.06 and 2.41 couple with carbons at 73.1 and 72.0, respectively. Both these carbons carry no protons and couple with the protons of a methoxy group. The NOESY spectrum reveals nOe's between the alkene proton and the methoxy protons of the methyl-vinyl ether fragment in compounds **5-2*trans*** and **5-3*trans*** only, therefore in these compounds the double bond is E. In these compounds the proton-deuterium coupling across the double bond is *ca*. 1.8 Hz, while in the Z compounds **5-2*cis*** and **5-3*cis***, it is *ca*. 0.9 Hz.

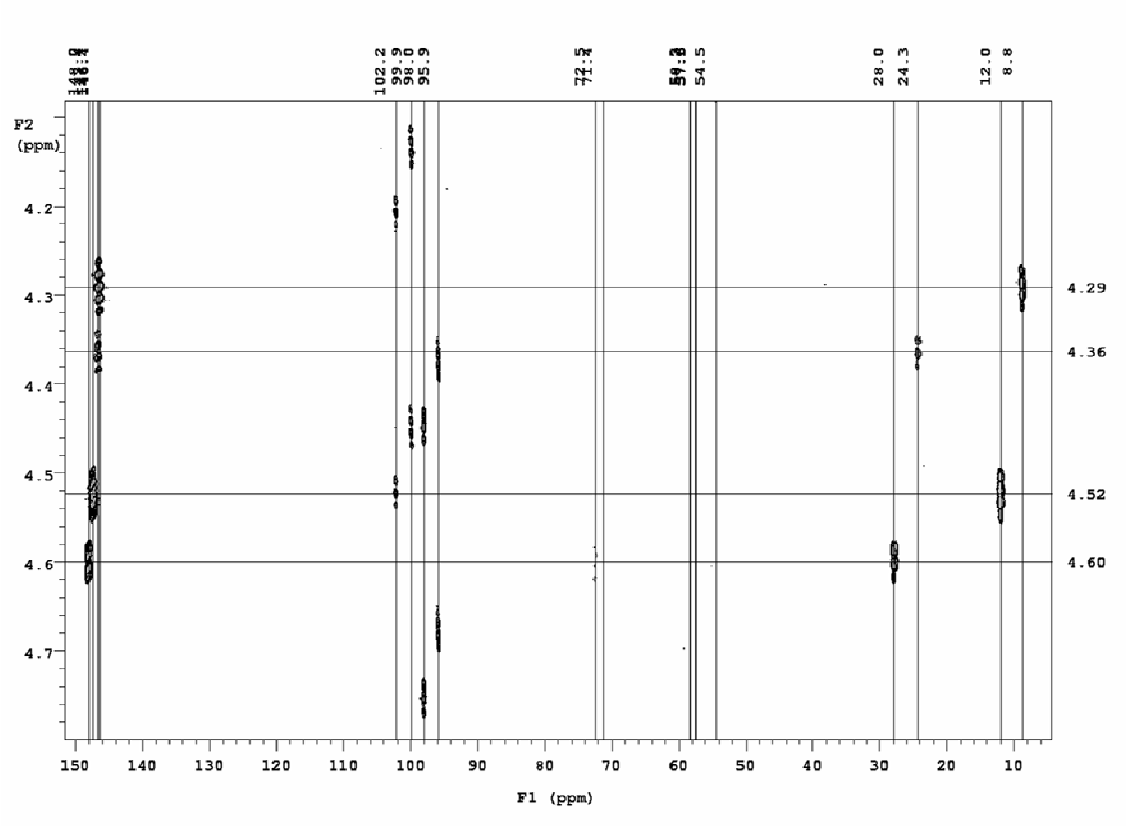

Figure 5-20. Expansion of the gHMBC spectrum

The carbon spectrum (Figure 5-21) confirms the lack of deuterium on the methoxy groups and the complete deuteration in position 1 of the alkene fragment, for all of four compounds. In compounds **5-3*cis*** and **5-3*trans***, the signals at 73.1 and 72.0 could barely be seen, as broad multiplets, confirming that these carbons carry only deuterium. With two positions with partial deuteration, compounds **5-2*cis***, **5-2*trans***, **5-3*cis*** and **5-3*trans*** are each present as four isotopomers. This is why the carbons in position 3 of the alkene fragments display a pattern of eight lines – the one at higher field is the H3,H2 isotopomer, followed by the one of the H3,D2 isotopomer. The next six lines are less intense and belong to the triplets of the D3,H2 and D3,D2 isotopomers. The carbon chemical shifts in Figure 5-17 are those of the H2,H3 isotopomer.

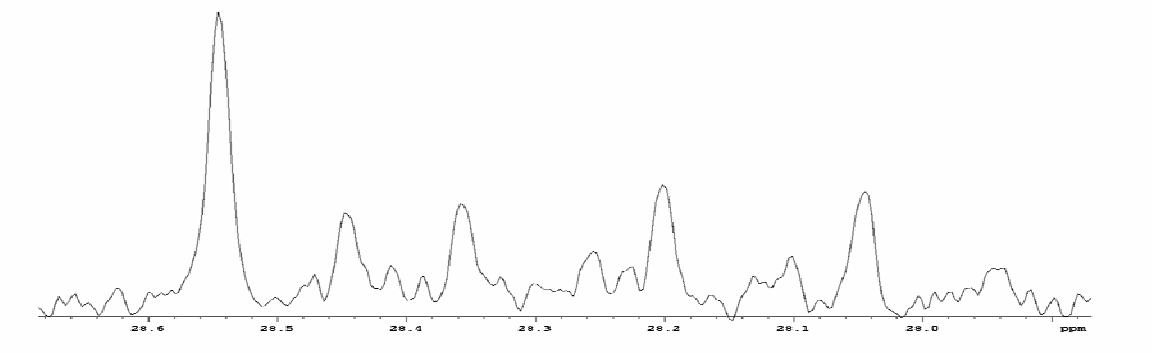

Figure 5-21. Expansion of the carbon spectrum, C3 region

The molar fraction of the four compounds in the mixture and the fraction of deuterium substitution at each position were determined by integration of the signals in both the proton and the deuterium spectra. They are given in Figure 5-18, as the first and the second sets of values, respectively. The spectra were taken at 70°C, when the separation of the signals of interest was optimal. In the proton spectrum, the signals of the methoxy groups were used, since there is no deuteration of these groups. Four signals could be integrated separately, 3.22-3.20 (**5-2*cis***), 3.20-3.18 (**5-2*trans*** + **5-3*cis*** + **5-**

3trans), 3.14-3.12 (**5-3*cis***) and 3.12-3.11 (**5-3*trans***). The separation of the last two signals is marginal, and for this reason the values for the relative ratio of the four compounds determined in the proton spectrum are considered to be less precise than the ones determined in the deuterium spectrum. Four signals in the deuterium spectrum were used, 6.30-6.12 (position 1 in **5-2*trans*** + **5-3*trans***), 5.78-5.62 (position 1 in **5-2*cis*** + **5-3*cis***), 3.30-3.20 (position 3 in **5-3*cis***), and 3.20-3.09 (position 3 in **5-3*trans***).

The fraction of deuteration at positions 2 and 3 was determined in both the proton and the deuterium spectra. The separation of the signals was poorer in the deuterium spectrum, in which also the signal of position 3 in **5-3*trans*** was overlapping the methyl signal of toluene. We consider that the best approach is to determine the relative ratios of compounds in the deuterium spectrum and then to use these ratios and the integrals from the proton spectrum to calculate the fraction of deuteration at each position. Values determined this way are presented on the third row in Figure 5-17.

X-ray Experimental

Crystals suitable for X-ray structure determination were obtained from slow diffusion of pentane into a saturated solution of **[Ru]23** in benzene at room temperature. Data were collected at 173 K on a Siemens SMART PLATFORM equipped with A CCD area detector and a graphite monochromator utilizing MoK_α radiation ($\lambda = 0.71073$ Å). Cell parameters were refined using up to 8192 reflections. A full sphere of data (1850 frames) was collected using the ω-scan method (0.3° frame width). The first 50 frames were re-measured at the end of data collection to monitor instrument and crystal stability (maximum correction on I was < 1 %). Absorption corrections by integration were applied based on measured indexed crystal faces.

The structure was solved by the Direct Methods in *SHELXTL6,* and refined using full-matrix least squares. The non-H atoms were treated anisotropically, whereas the hydrogen atoms were calculated in ideal positions and were riding on their respective carbon atoms. The structure has two disorders, a minor one where the C2-C3 moiety is refined in two parts with their site occupation factors dependently refined. The second disorder is a major one involving the triphenylphosphine group and the C20 ligand according to a pseudo-mirror symmetry passing through Ru, C1 and bisecting the C2-C3 bond. A total of 539 parameters were refined in the final cycle of refinement using 13498 reflections with $I > 2\sigma(I)$ to yield R_1 and wR_2 of 3.77% and 8.40%, respectively. Refinement was done using F^2.

Synthesis of Complex [Ru]23

Synthesis of 2-bromo-isophthalic acid (5-B). In a round-bottom flask equipped with a condenser, 25.0g of bromoxylene (0.135 mol) was dissolved in 200 mL of 1:1 ^{t}BuOH:water. Two equivalents of $KMnO_4$ (42.7g, 0.270 mol) were added portionwise, and the solution was refluxed for 4 hours. Upon cooling, 2 more equivalents of KMnO4 were added, and the solution was refluxed overnight. The mixture was filtered through a celite bed while still hot, and the filtrate was concentrated to 1/3. Concentrated H_2SO_4 was added slowly until a white precipitate formed. Filtration and drying under vacuum afforded 32.7g (0.133 mol, 99%) of a white powder. (mp>250^{o}C). ^{1}H NMR (CD_3OD, 300 MHz): δ=7.73 (d, 2H, *meta* C*H*, $^2J_{H,H}$= 7.6 Hz), 7.48 (t, 1H, *para* C*H*, $^3J_{H,H}$= 7.8 Hz), 5.32 (s, 2H, COO*H*); ^{13}C NMR (CD_3OD, 75 MHz): δ = 169.9, 137.7, 138.5, 128.4, 118.3; LRMS/EI $C_8H_5BrO_4$ = 245, found 245.

Synthesis of 2-bromo-dimethyl isophtalate. 2-Bromo-isophthalic acid **5-B** (32.7g, 0.133 mol) was dissolved in DMF. Two equivalents (37.0g, 0.270 mol) of K_2CO_3 and 38.0g (0.27 mol, 2.0 eq) of methyl iodide were added to the solution as well as a catalytic amount of $CeCO_3$. The reaction was stirred overnight at room temperature and quenched with acidic water until all the base dissolved. The aqueous solution was extracted with diethyl ether. Afterwards the organic layer was washed with water, dried over $MgSO_4$ and concentrated into a yellow oil (30.0g, 0.110 mol, 81%). ^{1}H NMR ($CDCl_3$, 300 MHz): δ= 7.68 (d, 2H, *meta* C*H*, $^2J_{H,H}$= 7.4 Hz), 7.40 (t, 1H, *para* C*H*, $^3J_{H,H}$ = 7.8 Hz), 3.94 (s, 3H, COOCH_3); ^{13}C NMR ($CDCl_3$, 75 MHz): δ= 166.6, 135.2, 132.1, 127.1, 118.7, 52.6; MS (LRMS/EI): $C_{10}H_9BrO_4$= 273, found 273.

Synthesis of 2-bromo-1,3-benzenedimethyl-*d*$_4$ alcohol (5-C). In a flame-dried round bottom flask immersed in an ice bath, 9.23g (0.219, 2.0 eq.) of lithium aluminum deuteride were suspended in 200 ml of dry THF. 2-Bromo-dimethyl isophtalate (30.0g, 0.110 mol) diluted in 20 ml of dry THF was added dropwise at 0^{o}C. After the addition was complete, the slurry was stirred for 20 minutes. The reaction was quenched and worked up following the standard procedure,[230] to yield 20.6g (0.093 mol, 85%) of a white powder (mp=152-154^{o}C). ^{1}H NMR (Pyridine-*d*$_5$, 300 MHz): δ= 7.95 (d, 2H, *meta* C*H*, $^2J_{H,H}$= 7.2 Hz), 7.50 (t, 1H, *para* C*H*, $^3J_{H,H}$= 7.5 Hz), 5.14 (s, 2H, O*H*); ^{13}C NMR (Pyridine-*d*$_5$, 75 MHz): δ= 140.9, 126.3, 125.6, 112.1, 62.2 (q, C*D*$_2$OH); MS (LRMS/EI): $C_8H_5D_4BrO_2$= 221, found 221.

Synthesis of 2-bromo-α,α'-dibromo-*m*-xylene-*d*$_4$. 2-Bromo-1,3-benzenedimethyl-*d*$_4$ alcohol **5-C** (20.6g, 0.093 mol) was suspended in a solution of CBr_4 (71.2g, 0.214 mol, 2.3 eq) in CH_2Cl_2. Triphenylphosphine (57.4g, 0.219 mol, 2.35 eq.) was added

portionwise at room temperature to avoid overheating. After the addition was complete, the clear solution was precipitated in diethyl ether and filtered. As the solvent was evaporated, any remaining triphenylphosphine was further filtered. The crude product was purified via column chromatography using 5:1 hexanes: ethyl acetate to yield 22.5g (0.065 mol, 70%) of a white powder. (mp= 85-88°C). ^{1}H NMR ($CDCl_3$, 300 MHz): δ= 7.41 (d, 2H, *meta* C*H*, $^{2}J_{H,H}$= 7.3 Hz), 7.28 (t, 1H, *para* C*H*, $^{3}J_{H,H}$= 7.2 Hz); ^{13}C NMR ($CDCl_3$, 75 MHz): δ= 138.4, 128.4, 127.9, 126.9, 33.9 (q, CD_2Br, $^{5}J_{C,D}$= 18.9 Hz); MS (LRMS/EI): $C_8H_3D_4Br_3$= 347, found 347.

Synthesis of 2-bromo-*m*-xylene-d_6 (5-D). In a flame-dried flask, 2-bromo-α,α'-dibromo-*m*-xylene-d_4 (22.5g, 0.065 mol) in THF was added dropwise to a slurry of lithium aluminum deuteride (2.73, 0.065 mol) in dry THF at room temperature. Then, the reaction was quenched and worked up following the standard procedure,[230] to yield 11.2g (0.058 mol, 90%) of a colorless liquid. ^{1}H NMR ($CDCl_3$, 300 MHz): δ= 7.05 (m, 3 Hz); ^{13}C NMR ($CDCl_3$, 75 MHz): δ= 138.4, 128.3, 127.8, 126.7, 23.2 (q, CD_2Br, $^{5}J_{C,D}$= 18.8 Hz); MS (LRMS/EI): $C_8H_3D_6Br$= 191, found 191.

Synthesis of 2,6-dimethyl-d_6 aniline (5-E). In a flame-dried three-neck round botton flask equipped with a condenser, 11.2g (0.058 mol) of 2-bromo-*m*-xylene-d_6 (**5-D**) was added dropwise to a mixture of 1.71g (0.070 mol, 1.2 eq.) of magnesium in 50 ml of anhydrous ether or a minimum amount. The solution refluxed upon addition and was subsequently maintained at reflux for 2 hours. After cooling down to room temperature, a 1.2M solution of TMSMA in ether was dripped into the reaction mixture, which was then stirred at room temperature for an additional 3 hours. Water was added to quench the reaction and the etheral phase was extracted, washed with brine and dried over $MgSO_4$.

The crude product was purified through column chromatography in CH_2Cl_2 to afford 4.09g (0.032 mol, 55%) of an orange-yellow liquid. ^{1}H NMR ($CDCl_3$, 300 MHz): δ= 7.45 (d, 2H, *meta* C*H*, $^2J_{H,H}$= 7.8 Hz), 7.19 (t, 1H, *para* C*H*, $^3J_{H,H}$= 7.5 Hz), 4.46 (s, 2H, N*H*$_2$); ^{13}C NMR ($CDCl_3$, 75 MHz): δ=142.8, 128.4, 121.7, 118.2, 17.4 (q, C*D*$_3$, $^5J_{C,D}$= 18.8 Hz) ; MS (LRMS/EI): $C_8H_5D_6N$= 127, found 127.

Synthesis of glyoxal-bis-(2,6-dimethyl-*d*$_6$ phenyl)imine. The procedure was modified from the literature.[67] Under argon, a mixture of 2.12g (0.014 mol) of a 40% aqueous solution of glyoxal, 2.3 ml of n-propanol and 5.8 ml of water was combined with 4.09g (0.032 mol, 2.2 eq) of 2,6-dimethyl-*d*$_6$ aniline **(5-E)** in 20 ml of n-propanol. The solution was stirred at room temperature for 4 hours and then at 60^{o}C for 2 hours. Upon addition of 30 ml of water, a yellow solid precipitated. The mixture was chilled in ice to allow further precipitation and 3.09g (0.011 mol, 80%) was collected by filtration (mp=145-146^{o}C). ^{1}H NMR ($CDCl_3$, 300 MHz): δ= 8.13 (s, 2H, C*H*=N), 7.12 (d, 4H, *meta* C*H*, $^2J_{H,H}$= 7.4 Hz), 6.98 (t, 2H, *para* C*H*, $^3J_{H,H}$= 7.7 Hz); ^{13}C NMR ($CDCl_3$, 75 MHz): δ=163.7, 150.1, 128.5, 126.5, 125.0, 17.4 (q, C*D*$_3$, $^5J_{C,D}$= 18.9 Hz); (HRMS/EI) calcd for $C_{18}H_8D_{12}N_2$ $[M+Na]^+$ 299.2272, found 299.2282.

Synthesis of N,N'-bis-(2,6-dimethyl-*d*$_6$ phenylamino)ethane dihydrochloride. A suspension of 3.09g (0.011 mol) of the glyoxal-bis-(2,6-dimethyl-*d*$_6$ phenyl)imine in 45 ml of 2:1 THF:methanol was treated with 1.70 g (0.044 mol, 4.0 eq) of sodium borohydride at room temperature. The mixture was stirred for 16 hours at room temperature and refluxed for one hour. Upon cooling, 45 ml of iced-water were added followed by 45 ml of 3M hydrochloric acid. A white solid precipitated, filtered and washed with diethyl ether and acetone. Yield : 3.35 g (9.9 mmol, 85%); mp>250^{o}C. ^{1}H

NMR (DMSO-d_6, 300 MHz): δ= 7.12 (s, 6H, *para-meta* C*H*), 3.60 (s, 4H, NCH_2); ^{13}C NMR (DMSO-d_6, 75 MHz): δ=135.5, 131.7, 129.9, 127.9, 17.8 (q, CD_3, $^5J_{C,D}$ = 18.8 Hz) ; MS (LRMS/EI): $C_{18}H_{14}D_6N_2Cl_2$=352, found 352.

Synthesis of 1,3-bis-(2,6-dimethyl-d_6 phenyl)imidazolinium chloride (5-F). A mixture of 3.35 g (9.9 mmol) of N,N'-bis-(2,6-dimethyl-d_6 phenylamino)ethane dihydrochloride, 40 ml of triethyl orthoformate, and two drops of 96% formic acid was heated in a distillation apparatus until the distillation of ethanol ceased. Once the temperature raised towards 130°C, the heating was stopped and the reaction was cooled to room temperature. At this point, a white solid precipitated which was isolated by vacuum filtration. Recrystallization from 2:1 CH_3CN:ethanol afforded 1.67 g (5.7 mmol, 58%) of white crystals. ^{1}H NMR (CD_3CN, 300 MHz): δ= 9.38 (s, 1H, NC*H*N), 7.32 (t, 2H, *para* C*H*, $^3J_{H,H}$ = 7.7 Hz), 7.24 (d, 4H, *meta* C*H*, $^2J_{H,H}$ = 7.4 Hz), 4.44 (s, 4H, NCH_2); ^{13}C NMR (CD_3CN, 75 MHz): δ=161.3, 137.0, 131.3, 130.1, 118.4, 52.1, 17.4 (q, CD_3, $^5J_{C,D}$ = 19.0 Hz) ; MS (HRMS/EI) calcd for $C_{19}H_{11}D_6N_2Cl$ $[M]^+$ 291.2609, found 291.2621.

Synthesis of 1,3-bis-(2,6-dimethyl-d_6 phenyl)-2-(trichloromethyl)imidazolidine (5-G). To a solution of chlorine salt **5-F** (1.67 g, 5.7 mmol) in dry chloroform was added 0.230 g (5.7 mmol) of a 60% dispersion of sodium hydride. The reaction was stirred at room temperature for 2 hours and subsequently filtered. The filtrate was evaporated into a yellowish solid, which was flushed through a silica plug with 9:1 hexane:ethyl acetate. The ligand was further purified by recrystallization in boiling hexane, affording 3.28 g (4.7 mmol, 82%) of a white solid (mp=118-120°C). ^{1}H NMR ($CDCl_3$, 300 MHz): δ= 7.03 (m, 6H, *para-meta* C*H*), 5.66 (s, 1H, C*H*CCl_3), 3.98 (m, 2H, NCH_2), 3.37 (m, 2H,

NCH_2); ^{13}C NMR ($CDCl_3$, 75 MHz): δ= 144.1, 138.4, 134.2, 129.5, 129.3, 125.6, 107.9, 86.1, 51.8, 19.0 (q, CD_3, $^5J_{C,D}$ = 19.0 Hz) ; MS (HRMS/EI) calcd for $C_{19}H_{10}D_{12}N_2$ $[M+H]^+$ 291.2609, found 291.2622.

Synthesis of complex [Ru]23. The procedure was adapted from the literature.[72] In the drybox, a flame-dried Schlenk flask was charged with 0.879 g (1.07 mmol) of catalyst **[Ru]1** and 1.640 g (2.35 mmol, 2.2 eq) of ligand **5-G**. The mixture was dissolved in 25 ml of toluene and stirred at 60°C for 90 minutes under argon. The solvent was then evaporated, and the brown residue was washed with methanol (2 x 25 mL) and pentane (50 mL). Finally, the pink solid was dried under vacuum to yield 0.693 g (0.83 mmol, 78%) of complex **[Ru]23**. ^{1}H NMR (toluene-d_8, 300 MHz): δ= 19.57 (s, 1H, Ru=CH), 7.17 (t, 2H, *para* CH, $^3J_{H,H}$ = 7.2 Hz), 7.13-6.94 (m, 9H, *para-meta* CH), 6.54 (t, 1H, $^3J_{H,H}$ = 7.3 Hz), 3.43-3.15 (m, 4H, NCH_2CH_2N), 2.41 (q, 3H), 1.55 (m, 15H), 1.08 (m, 15H); ^{13}C NMR (toluene-d_8, 75 MHz): δ=147.8, 129.5, 128.9, 128.6, 127.9, 125.8, 125.1, 32.4, 32.2, 30.3, 28.6, 28.5, 27.0, 20.8 (q, CD_3, $^5J_{C,D}$ = 19.7 Hz); ^{31}P NMR (toluene-d_8, 300 MHz): δ=29.69 ; MS (HRMS/EI) calcd for $C_{44}H_{48}D_{12}N_2Cl_2PRu$ $[M]^+$ 831.3656, found 831.3648. Anal. Calcd for $C_{44}H_{48}D_{12}N_2Cl_2PRu$: C, 64.38; H, 7.49; N, 3.41. Found: C, 64.80; H, 7.39; N, 3.31.

Thermal Decomposition of Complex [Ru]23

In the drybox, 32 mg (0.038 mmol) of complex **[Ru]23** was dissolved with 0.8 mL of C_6D_6 in a glass ampoule, which was then equipped with a swedgelock connected to a Teflon Schlenk valve. The system was taken out of the glovebox, and the ampoule was sealed under argon. The ampoule was left in a 70°C bath for 21 days and shaken

regularly. It was then taken back into the drybox and transferred into a J. Young® Valve NMR Tube.

Thermal Decomposition of Methylidene Complex [Ru]23'

In the drybox, a Schlenk tube was charged with 200 mg (0.038 mmol) of complex **[Ru]23** dissolved in 10 mL of degassed benzene. The tube was taken out of the glovebox, connected to argon and immersed in a 60°C oil bath. Ethylene gas was bubbled rapidly through the solution for 30 minutes, resulting in a color change from pink to dark brown. The mixture was sampled to confirm full conversion of the benzylidene by ^{1}H NMR.

The mixture was then left stirring at 60°C for 3 days, after which the solvent was evaporated under vacuo. The flask was taken back into the drybox and transferred into a J. Young® Valve NMR Tube.

Isomerization Experiment

Once no more carbene signal was visible by ^{1}H NMR spectroscopy (δ 19.63 and 18.40 ppm for **[Ru]23** and **[Ru]23'**, respectively), the catalytic mixture was considered fully decomposed. The J. Young® Valve NMR Tube was fitted onto a vacuum hook-up and the solvent was evaporated. The tube was then taken into the drybox, and 0.5 g of 1-octene were added to the decomposed mixture. The tube was allowed to stand at 55°C for 24h, and the isomers content was determined by ^{1}H NMR by integration of the internal olefin peak at δ 5.40 ppm.

CHAPTER 6
UNDERSTANDING THE EFFECT OF ALLYLIC METHYLS IN OLEFIN CROSS-METATHESIS

Reproduced in part with permission from: Courchay, F. C.; Baughman, T.W.; Wagener, K. B. *Journal of Organometallic Chemistry* **2005** accepted.

Introduction

Olefin metathesis has been applied to a variety of organic synthetic challenges by allowing the simple formation of carbon-carbon double bonds in a single step where other routes would sometimes require several tedious steps.[1,2] The development of well-defined metathesis carbene catalysts, such as Schrock's molybdenum catalyst **[Mo]1**,[27,28,231] and the more recent Grubbs' ruthenium catalysts **[Ru]1**[37,57,80,87] and **[Ru]4**,[69] has considerably widened the scope of olefin metathesis in both organic and polymer chemistry (Figure 6-1).[7-11,19-20,31] This success has inspired many catalyst modifications to introduce heterogeneous catalysts,[41-45,102-107] water-soluble catalysts,[38-40,105,232,233] recyclable catalysts,[56,95,186] slower and faster initiators,[75,99,194] so as to accommodate any particular set of conditions.

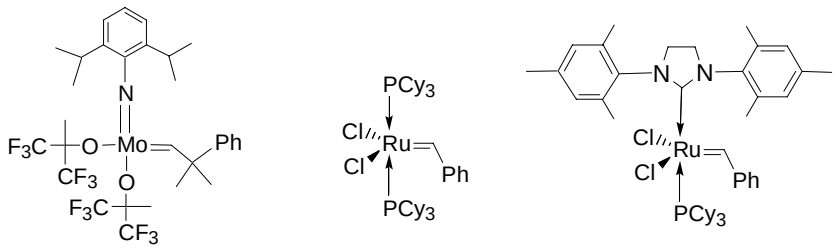

[Mo]1 **[Ru]1** **[Ru]4**

Figure 6-1. Olefin metathesis catalysts

Despite the broad range of applications of these catalysts, challenges remain that must be addressed. On one hand, Schrock's highly active carbene complexes are oxophilic which renders them sensitive to air and moisture, and thus inappropriate when used with certain functionalities such as aldehydes and alcohols.[12] On the other hand, ruthenium complexes, which possess a much higher functional group tolerance, are less active towards electron-poor or sterically demanding olefins.[12,29] Although the 2nd generation catalyst **[Ru]4** displays activities comparable to early transition metal complexes,[14,69,77] it also promotes double bond isomerization at elevated temperatures, competetively with metathesis, which can be problematic for the synthesis of precise polymer microstructures.[166,176,177,192]

Part of our group research effort has recently focused on building a family of α-olefin/ethylene copolymers to better understand the structure-properties relationship of widely commercialized polyethylene materials.[21,22] Using acyclic diene metathesis (ADMET), ethylene-propylene copolymers [EP(n+1)] with exact ethylene run length of n= 4, 6, 8, 14, 18 and 20 carbons were synthesized, the methyl branch content being determined during the monomer design.[127,128,132] Although much progress has been made, the EP3 diene monomer (**6-9** in Figure 6-2) refused to polymerize since allylic methyl groups seem to pose problem.

Consequently, the influence of allylic methyls in condensation metathesis chemistry was investigated using standard catalysts **[Mo]1**, **[Ru]1**, and **[Ru]4**, in both cross-metathesis (CM) and ADMET conditions. Herein, is the report of an NMR spectroscopy study highlighting mechanistic features of both molybdenum and ruthenium

metathesis catalysis in this reaction, and the importance of steric arrangement in the metallacyclobutane intermediate.

Results

ADMET Monomer **6-9**, the target monomer possessing allylic groups, was synthesized starting with 3-methyl-4-pentenoic acid which was reduced and tosylated to yield diester **6-4** by addition to diethyl malonate (Figure 6-2). Saponification and decarboxylation produced acid **6-6**, which then was reduced and tosylated. Substitution with LAH afforded monomer **6-9** in 29% overall yield.

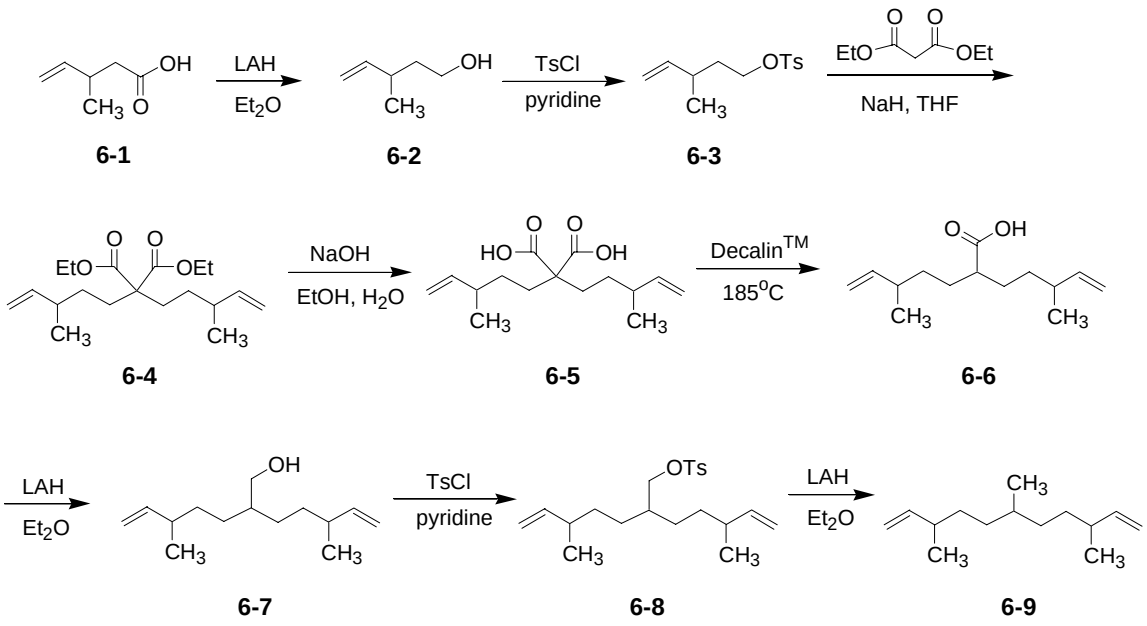

Figure 6-2. Synthesis of monomer **6-9**

Efforts to polymerize **6-9**, 3,6,9-trimethylundeca-1,10-diene, to create unsaturated polyethylene containing methyl branches on every third carbon led to little if any conversion (Figure 6-3). Color changes during the reaction suggested catalyst decomposition very early in the reaction; olefin conversion was calculated at 4% for catalyst **[Mo]1** and 8% for catalyst **[Ru]1** at best. These results warranted a detailed NMR study with catalysts **[Mo]1**, **[Ru]1**, and **[Ru]4**, probing for key intermediates

during the catalytic cycle. To facilitate interpretation and broaden the scope of our study, the polymerization of **6-9** was examined more carefully along with the cross metathesis reaction of 3-methyl-1-pentene, research which had been previously reported by Grubbs with catalyst **[Ru]1**.[80]

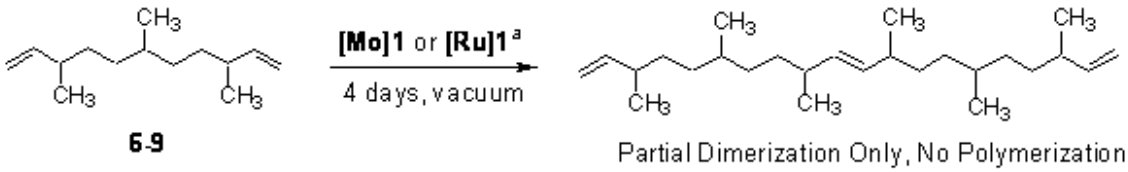

Figure 6-3. ADMET reaction of **6-9**

Schrock's Molybdenum Catalyst

The experiments described below demonstrate that the dominant reaction pathway when using catalyst **[Mo]1** leads to an accumulation of the nonproductive metallacyclobutane intermedate, rather than full metathesis conversion. The experiments were set up using conditions that would allow monitoring dynamic catalytic behavior by NMR spectroscopy. For example, when examining the cross reaction of 3-methyl-1-pentene (the "control" reaction for ADMET chemistry of monomer **6-9**), a typical experiment consisted of loading an NMR tube with a 0.2 M solution of olefin in C_6D_6 and 30 mol% of complex **[Mo]1** (Typical catalyst loading for CM reactions are in the order of 0.1 to 1 mol% for **[Mo]1**, 2 to 10 mol% for **[Ru]1**, and 1 to 5 mol% for **[Ru]4**).

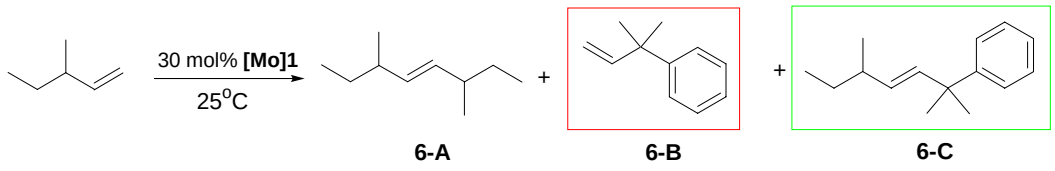

Figure 6-4. Cross metathesis of 3-methyl-1-pentene catalyzed by **[Mo]1**

After 30 minutes at room temperature, the proton NMR spectrum indicates the presence of the expected metathesis product 3,6-dimethyl-oct-4-ene (**6-A**), and products of the catalyst initiation (1,1-dimethyl-allyl)-benzene (**6-B**), and (1,1,4-trimethyl-hex-2-enyl)-benzene (**6-C**) (Figure 6-4). However, product **6-A** only formed in 46% yield, which is insufficient for ADMET chemistry, again illlustrating the difficulty associated with the homodimerization of this class of olefins. Products **6-B** and **6-C,** formed by reaction of one molecule of substrate with the original molybdenum catalyst (and therefore present in catalytic quantities), normally are not observed. They are visible here because of the use of high catalyst concentrations.

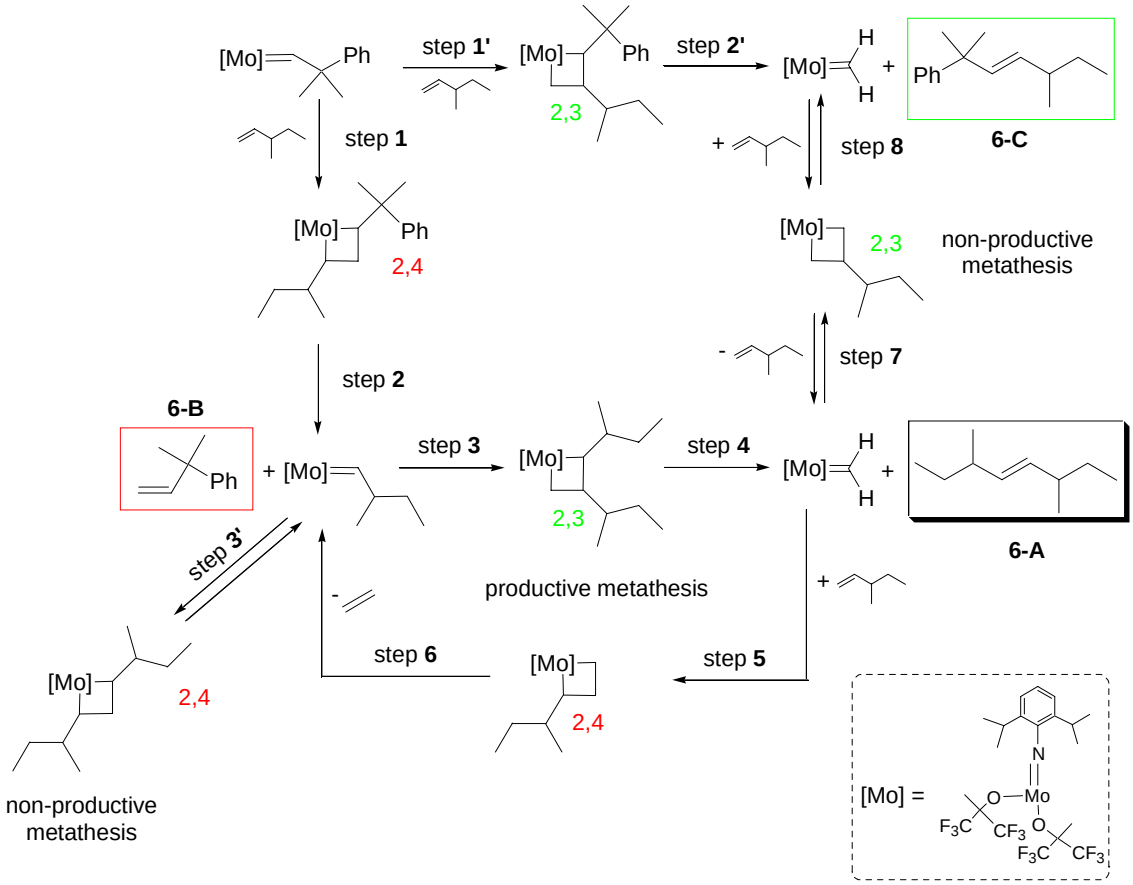

Figure 6-5. Catalytic cycle for the metathesis of 3-methyl-1-pentene with a molybdenum carbene catalyst

Figure 6-5 depicts the catalytic cycle involved in each products presented in Figure 6-4. For clarity, note that single arrows are drawn instead of equilibrium arrows, but according to the metathesis mechanism it is implied that each step actually exists as an equilibrium. Further, it should be noted that steps 3', 7 and 8 do not represent equilibrium conditions, but rather the non-productive metathesis cycle.

As the reaction starts, the first feature observed is the major production of $CH_2=C(CH_3)_2Ph$ (**6-B**) compared to the alternate product **6-C**, which indicates that formation of the 2,4-metallacyclobutane is largely favored when 3-methyl-1-pentene coordinates to the original Schrock's alkylidene (Step 1 in Figure 6-5). The two doublets at δ 13.18 and 13.23 ppm ($^2J_{H,H}$= 5.6 Hz) confirm the presence of the new alkylidene $Mo=CHCH(CH_3)Et$, each signal corresponding to one enantiomer of the racemic mixture (Figure 6-6a).[231] Two metallacyclobutanes can form from this intermediate, the 2,3-addition leading to productive metathesis (step 3), and the 2,4-addition leading to non-productive metathesis (step 3'). After 10 minutes, two broad singlets appear in equal ratios at –0.17 and –1.06 ppm, characteristic of the two β protons of a trigonal-bipyramidal metallacyclobutane ring, therefore implying the formation of the 2,4-metallacyclobutane, further confirmed by the two α protons singlets at 5.10 and 4.84 ppm.[231] The 2,3-metallacycle would have given rise to a single signal in the upper field region. The fact that it is undetectable by NMR may be simply a result of its instability, forcing the metallacycle intermediate to decompose quickly into the methylidene and the metathesis product (step 4), as proven by the internal olefin resonance at 5.32 ppm. Because the methylidene complex is highly unstable, its signals cannot be assign unambiguously. Moreover, the few methylidene complexes that were ever observeable

by NMR were adducts stabilized by a protic solvent such as dme or THF, which is not possible here.[28,234] The most common decomposition routes for high oxidation state ("d0") alkylidene complexes in the presence of olefins are rearrangement of metallacyclobutanes complexes by β-hydride mechanism and bimolecular coupling, methylidenes being the most susceptible to bimolecular decomposition.[234] However, the broad singlet at δ 12.36 ppm, assigned to the N*H* proton of an amido alkylidyne complex, indicates yet another substantial decomposition pathway. This kind of proton transfer reaction from carbon to nitrogen was observed by Schrock *et al.*[235] during the preparation of $Mo(NAr_{Cl})(CHCMe_2Ph)$[Biphen].

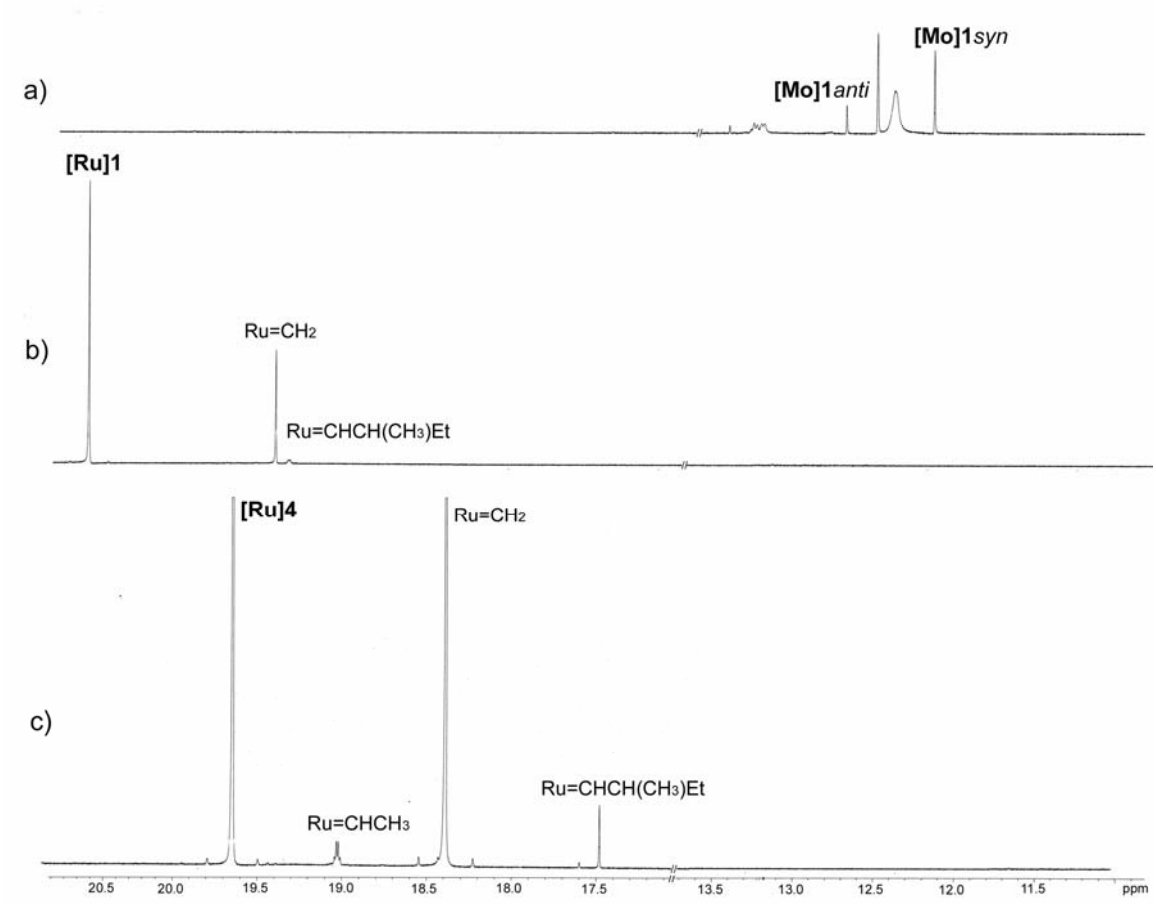

Figure 6-6. ^{1}H NMR alkylidene region for the reaction of 3-methyl-1-pentene. (a) With catalyst **[Mo]1**; (b) with **[Ru]1**; (c) with **[Ru]4**.

In any case, the metathesis reaction only reaches 46% conversion after 30 minutes, while the 2,4-metallacyclobutane already constitutes 50% of the catalyst mixture, which highlights the significant extent of non-productive metathesis. The product distribution is similar when 3-methyl-1-pentene is substituted with monomer **6-9**, although ADMET conversions are slightly lower probably because of the substrate's longer carbon chain.

Grubbs' Ruthenium Catalysts

The NMR experiments with 3-methyl-1-pentene (CM conditions) and monomer **6-9** (ADMET conditions) were repeated using ruthenium catalysts **[Ru]1** and **[Ru]4**. Unlike what is observed in the case of early transition metals, the ruthenium metallacyclobutane is highly unstable, and it is still debated whether it is an intermediate or a transition state in the metathesis catalytic cycle.[61,81,82] As had been done before, an NMR tube was loaded with a 0.2 M solution of 3-methyl-1-pentene in C_6D_6 and 30 mol% of complex **[Ru]1**.

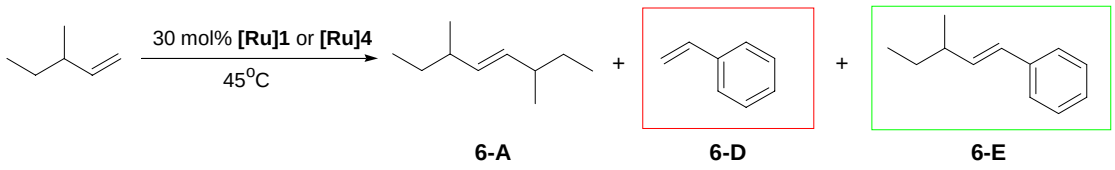

Figure 6-7. CM of 3-methyl-1-pentene catalyzed by **[Ru]1** or **[Ru]4**

After 30 minutes at 45°C, the proton NMR spectrum indicates the presence of the metathesis product 3,6-dimethyl-oct-4-ene (**6-A**) in low yields and products of the catalyst initiation: styrene (**6-D**), and (3-methyl-pent-1-enyl)-benzene (**6-E**) that are formed by reaction of one molecule of substrate with the ruthenium benzylidene (Figure 6-7). Product **6-A** is formed in 5% and 30% yields with catalyst **[Ru]1** and **[Ru]4**, respectively, again too low to be useful in ADMET step-growth polymerization. As before, products **6-D** and **6-E** are only visible because of the high catalyst concentrations.

Figure 6-8 depicts the catalytic cycle involved in each product formation. Downfield in the NMR spectrum, there is a steady disappearance of ruthenium benzylidene while the methylidene resonance at δ 19.40 ppm appears almost at a comparable rate. At the end of the experiment, three times more $Ru=CH_2$ (15%) is present than the expected $Ru=CHCH(CH_3)Et$ (5% of the catalyst mixture), evidenced by a doublet at δ 19.28 ppm (Figure 6-6b).

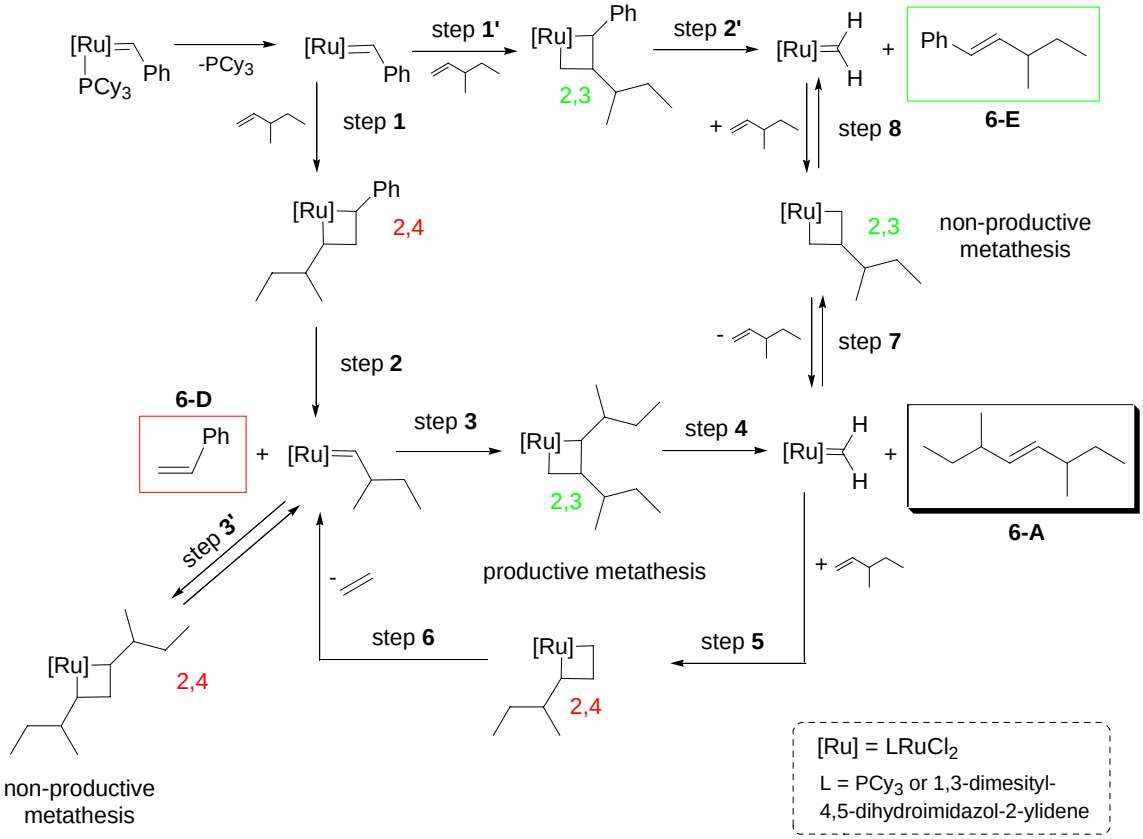

Figure 6-8. Catalytic cycle for the metathesis of 3-methyl-1-pentene with ruthenium carbene catalyst **[Ru]1** or **[Ru]4**

As observed with the molybdenum catalyst, styrene is produced in much larger quantities than product **6-E**, which indicates the preferred formation of the 2,4-metallacyclobutane from the ruthenium benzylidene (step 1 and 1' in Figure 6-8). Theoretically, the amount of styrene released corresponds to the amount of catalyst

activated for productive metathesis, Ru=CHCH(CH_3)Et. Since this alkylidene is not detected by NMR, it must react quickly with a substrate molecule through the intermediate of a 2,3-metallacyclobutane to afford the metathesis product **6-A** and the methylidene (step 3 and 4). This analysis is further supported by the fact that the amount of **6-A** equals the amount of styrene generated. At this point, the methylidene continues to increase in concentration, while the metathesis reaction seems to cease, indicating that upon coordination of a new olefin molecule, the 2,3-metallacyclobutane is formed preferentially to regenerate the methylidene through step 7. Step 1' and 2' could also generate the methylidene, but this would involve a build-up of product **6-E**, which we do not observe. Further, the saturation of the reaction vessel with ethylene cannot be held entirely responsible for the methylidene build-up either, since little ethylene is present in solution compared to the excess of starting material.

In any case, after 30 minutes, only 5% of starting material has reacted even though more than 20% of the benzylidene precatalyst has been consumed, mostly forming the highly unstable ruthenium methylidene. Apparently, decomposition of the catalyst system occurs at a faster rate than the metathesis reaction.

Hence, complex **[Ru]1** can not be regarded as a suitable catalyst for the homodimerization of 3-methyl-1-pentene, and probably not for any other olefin containing allylic methyls.[80] Indeed, when the reaction was repeated with the corresponding ADMET diene, similar patterns were observed; in fact, conversions were even lower. Metathesis products **6-A** and **6-E** were undetectable, and half less styrene was produced compared to the CM experiment, implying that less metallacyclobutane had formed. After 30 minutes, the methylidene constitutes 13% of the catalyst mixture

and seems to be the only species besides the original benzylidene. These data indicate that with the ADMET monomer the rate of formation of any metallacyclobutane is slower, more likely because of the larger olefin.

Catalyst **[Ru]4** was subjected to scrutiny under the same conditions. At room temperature, approximately the same amounts of styrene and **6-E** are detected at room temperature, while at 45°C styrene seems to be in slight excess. Phosphine dissociation is so slow at low temperatures that an equilibrium between the 2,3 and 2,4-metallacyclobutane is created. When the dissociation event becomes faster, a greater amount of active catalyst is generated and the rate difference between formation of the 2,3- or 2,4-metallacyclobutane becomes evident because of the higher catalyst concentration.

After 30 minutes the methylidene represents about 30% of the catalyst mixture whereas $Ru{=}CHCH(CH_3)Et$ is only present in 1%, appearing as a doublet at δ 17.48 ppm (Figure 6-6c). A quadruplet at 19.0 ppm also indicates the presence of $Ru{=}CHCH_3$ formed from the metathesis of isomerized starting material. Indeed ruthenium catalysts, particularly those containing N-heterocyclic carbene ligands (NHC), can isomerize olefins by migration of the double bond along the backbone.[176,177,192] The appearance of a multiplet at δ 5.19 ppm confirms the presence of 3-methyl-2-pentene by structural isomerization of the starting material. Traces of 2-methyl-1-butene also become visible at δ 4.67 ppm, formed by reaction of 3-methyl-2-pentene with the ruthenium methylidene. Nevertheless, the expected metathesis product **6-A**, 3,6-dimethyl-oct-4-ene, constitutes only 30% of the olefinic mixture, while 50% of starting material still remains. This level of conversion obviates any ADMET chemistry. The reaction does proceed, albeit only at

slow rates. Noteworthy, 34% of the original precatalyst **[Ru]4** has already been consumed at this point, which is equivalent to a 10 mol% catalyst loadings, already surpassing the typical catalytic quantities.

Since Ru=CHCH(CH_3)Et is not detected in significant amounts, we can still assume that the 2,3-metallacyclobutane is preferred during step 3. However, the amount of metathesis product formed far exceeds the amount of styrene detected, which implies that productive metathesis does occur, unlike what was observed with catalyst **[Ru]1**. This observation is consistent with the higher reactivity of NHC-containing complexes towards olefinic substrates, attributed to the stabilizing effect of the NHC ligand on the metallacyclobutane.[81] The ligand sphere may also allow a better arrangement of the alkyl bulk during the formation of the 2,4-metallacyclobutane.

As seen with 1st generation complex **[Ru]1**, the reaction profile of catalyst **[Ru]4** with the ADMET monomer **6-9** is identical to the CM reaction, but affords much lower conversions. Under the same conditions as CM chemistry, 70% of starting material remains even though more catalyst has been activated (46%). The amount of methylidene formed is also higher than during the CM reaction, which suggests that non-productive metathesis occurs to a larger extent through the preferred formation of a 2,3-metallacyclobutane. This favored conformation is likely a direct result of the additional sterics brought about by the larger diene monomer. In addition, four hydride complexes have formed during the course of the reaction indicating the start of the catalytic decomposition process, accelerated by the accumulation of the unstable methylidene complex.

Discussion.

Although the conditions used in this study do not reflect exact polymerization conditions (where the metathesis equilibrium is driven by removal of ethylene) these experiments reflect a general catalytic behavior, since they demonstrate a steric conflict rather than a rate problem.

In the case of the Schrock's molybdenum catalyst, 3-methyl-1-pentene (or its diene analog, monomer **6-9**) seem to consistently coordinate to the metal in order to minimize steric interactions between the alkyl branches, hence forming the 2,4-metallacyclobutane, which, during step 3' (Figure 6-5), only leads to non-productive metathesis. Moreover, this somewhat stable intermediate traps the catalyst in an inactive form. Even though productive metathesis occurs to some extent, it is insufficient to promote ADMET polymerization, a step-growth process that requires high conversions (>99%) in order to reach high molecular weigh polymer.

A different mechanism operates with ruthenium catalysts to prevent the metathesis of allylic methyl-containing substrates. The ruthenium methylidene accumulates when catalyst **[Ru]1** is used with either 3-methyl-1-pentene or the corresponding ADMET momomer, through the consecutive steps 1 to 4 in Figure 6-8. The original benzylidene first forms a 2,4-metallacyclobutane upon olefin coordination to create a new alkylidene complex (steps 1 and 2 in Figure 6-8), which then forms the 2,3-metallacyclobutane by reacting with another olefin (steps 3 and 4). However, since the alkylidene is the most reactive intermediate, it is impossible to assert the amount of non-productive metathesis occurring through step 3'. From this point on, the methylidene complex only reacts with incoming olefins to promote non-productive metathesis and regenerate itself (step 7), even though formation of the methylidene is not kinetically favored.[80]

It has been suggested that the steric effects orient the bulk away from the crowded ruthenium metal center, while the electronic effects favor alkyl substitutents adjacent to the metal.[80] Consequently, when the olefin reacts with the benzylidene complex, the benzene ring adjacent to ruthenium may be sufficiently electron-withdrawing to place the alkyl group next to the metal center, minimizing in the same time the steric repulsions between the alkyl branch and the phenyl group (step 1). On the other hand, when the methylidene complex is involved, no electronic effect directs the coordination of the olefin, which positions its steric bulk *away* from the metal center to form the 2,3-ruthenacyclobutane (step 7). The fact that the same reaction with linear olefins affords the inverse conformation[80] reveals the directing effect of allylic methyls, more likely by steric interactions with the ligand sphere of the complex.

These conclusions also apply to catalyst **[Ru]4**, although the steric directing effects seem to be diminished in the presence of the NHC ligand. This could be due to a different arrangement of the ligand sphere reducing steric interactions, or to the propensity of the NHC ligand to stabilize the ruthenacyclobutane. Despite better yields, the conditions required by ADMET polycondensation could not be achieved. In addition, a significant amount of olefin isomerization interferes with the metathesis process and therefore renders this 2nd generation of catalysts unsuitable for the modeling of precise molecules.

Conclusion

ADMET polymerization of dienes possessing allylic methyl groups is not possible, principally due to interaction of this methyl group with the metathesis catalyst. A series of NMR spectroscopy experiments conducted with both the diene monomer (**6-9**) and model compound 3-methyl-1-pentene, the corresponding mono-olefin, demonstrated that

the reaction limitations depend on catalyst selection. With Schrock's molybdenum catalyst **[Mo]1**, the reaction led to an accumulation of metallacyclobutane, trapping the catalyst into an inactive form. With Grubbs' ruthenium catalysts **[Ru]1** and **[Ru]4**, the substrate coordinates to the metal center only to yield non-productive metathesis, which results in a build-up of the methylidene complex, more prompt to decomposition. Although the NHC-containing complex **[Ru]4** affords better yields than its phosphine analog, this experiment also illustrate the competitive nature of double-bond isomerization during olefin metathesis. These results are dictated by the steric arrangement of the substrate within the catalyst ligand sphere during the metallacyclobutane formation, the alkyl branch being adjacent to the metal center for the molybdenum **[Mo]1**, and opposite to it in the case of ruthenium catalysts **[Ru]1** and **[Ru]4**.

Experimental

General

^{1}H NMR (300 MHz) and ^{13}C NMR (75 Hz) spectra were recorded on either a Mercury series or Varian VXR-300 NMR superconducting spectrometer for small molecule structure determination. Chemical shifts were referenced to residual C_6H_6 (7.15 for ^{1}H and 128.39 for ^{13}C) or $CHCl_3$ (7.27 for ^{1}H and 77.23 for ^{13}C), and the NMR solvents were distilled, degassed by three freeze-pump-thaw cycles, and stored in an argon-filled drybox prior to use. Thin layer chromatography (TLC) was performed on EMD silica gel coated (250 μm thickness) glass plates cut to custom sizes. Developed TLC plates were stained with iodine absorbed on silica to produce a visible signature. Reaction conversions and relative purity of crude products were monitored by TLC chromatography and NMR. High-resolution mass spectral (HRMS) data were obtained

on a Finnegan 4500 gas chromatograph/mass spectrometer using either the chemical ionization (CI) or electrospray ionization (ESI) mode.

Materials and Methods

All materials were purchased from Aldrich chemical and used as received unless otherwise specified. Complex **[Mo]1**,[231,27,28] and **[Ru]4**[69] were synthesized according to literature procedure. Complex **[Ru]1** was a gift from Materia Inc., and was used as received. Catalysts were stored in an argon-filled drybox prior to use.

Bulk Polymerization Experiment

Monomer **6-9** (1.5 g, 77 mmol) was vacuum transferred from potassium mirror into a schlenk flask and taken into an argon-filled glove box. The catalyst (monomer:catalyst ratio is 1500:1 for **[Mo]1**, 450:1 for **[Ru]1**) was added to the monomer in a 50 ml round-bottom flask equipped with a magnetic stirbar, and allowed to react approximately 15 minutes before sealing the reactor with a schlenk adaptor and connecting to high vacuum line. Vacuum was applied intermittently for the first 2 hours, then polymerization was heated at 40^{o}C and put under full vacuum (10^{-3} Torr) for 4 days. NMR samples were taken in *d*-chloroform directly from the reactor with no purification. Conversions were calculated by the ratio of integral values of the internal olefin (δ 5.20 ppm, m, 2H) to the terminal olefin (δ 4.95 ppm, m, 2H).

NMR Catalyst Experiments

NMR spectra were recorded on a Varian Inova spectrometer equipped with a 5 mm indirect detection probe, operating at 500 MHz for ^{1}H and at 125 MHz for ^{13}C. The solvent was *d6*-benzene and the temperature was 25°C for catalyst **[Mo]1** and 45^{o}C for catalysts **[Ru]1** and **[Ru]4**. Chemical shifts were referenced to residual C_6H_6 (7.15 for ^{1}H and 128.39 for ^{13}C). In the drybox, 0.036 mmol of catalyst was introduced in an NMR

tube equipped with a Teflon valve. Approximately 0.8 ml of C_6D_6 was added to the tube so as not to dissolve the catalyst extensively, and 0.119 mmol of substrate (3-methyl-1-pentene or monomer **6-9**) was carefully layered on top of the mixture. The NMR tube was sealed and shaken right before being introduced in the spectrometer. Proton spectra were recorded every 5 minutes, and quantitation was obtained by integration of the appropriate peaks against the solvent peak, which served as internal standard.

Synthesis of EP3 Monomer (6-2 to 6-9)

3-Methyl-4-pentene-1-ol (6-2). Under an argon atmosphere a solution of 3-methyl-4-pentenoic acid (30.0 g, 263 mmol) in diethyl ether (100 mL) was added dropwise to a suspension of LAH (12.0 g, 342 mmol) in diethyl ether (350 mL) over 45 minutes at 0^{o}C. When the addition was complete, the slurry was stirred cold for 15 minutes, then the reaction was warmed to room temperature for 2 hours. The reaction was then cooled to 0^{o}C and quenched by addition of water (200 mL) and concentrated HCl (~30 mL) until the aqueous layer was pH=3. The organic layer was collected, combined with a second ether wash (200 mL), and dried with brine and $MgSO_4$. Filtration, followed by distillation of the filtrate yielded a 21.5 g of colorless oil. 81.6 % yield. bp = 149^{o}C, 760 mmHg. ^{1}H NMR matched reported spectral data.[236] ^{13}C NMR (300 MHz, $CDCl_3$): δ (ppm) 20.61, 35.10, 39.48, 61.41, 113.32, 144.45.

3-Ethenyl-1-butanol tosylate (6-3). To a stirred solution of **6-2** (21.45 g, 214 mmol) in pyridine (100 mL) at 0^{o}C was added tosyl chloride (53.06 g, 278 mmol). The suspension was stirred cold for 10 minutes, then the viscous slurry was warmed to room temperature for 2 hours. Addition of water (200 mL) and diethyl ether (200 mL) produced a biphasic mixture. The organic phase was isolated and combined with a

second diethyl ether wash. Washing twice with 1N HCl (200mL), followed by drying over $MgSO_4$, and column chromatography (15% diethyl ether in hexane) afforded 53.6 g of colorless oil. 98.3% yield. ^{1}H NMR (300 MHz, $CDCl_3$): δ (ppm) 0.96 (d, 3H), 1.64 (m, 2H), 2.24 (m, 1H), 2.46 (s, 3H), 4.04 (m, 2H), 4.90 (m, 2H), 5.55 (m, 1H), 7.35 (d, 2H), 7.79 (d, 2H). ^{13}C NMR (300 MHz, $CDCl_3$): δ (ppm) 20.27, 21.84, 34.34, 35.40, 69.01, 114.31, 128.10, 130.00, 133.40, 142.70, 144.86.

Diethyl 2,2-bis(3-methyl-4-pentenyl) malonate (6-4). A solution of diethyl malonate (15.7 g, 98 mmol) in THF (100 mL) was added to a stirred solution of **6-3** (53.6 g, 210 mmol) and sodium hydride (5.6 g, 233 mmol) in THF (100mL) over 30 minutes at 0^{o}C. The mixture was stirred cold for 1 hour, then warmed to room temperature for 18 hours. The reaction was quenched by addition of water (250 mL), extracted with diethyl ether (300 mL), and dried with brine. Column chromatography (10% diethyl ether in hexane) afforded 18.9 g of colorless oil. 59.5% yield. ^{1}H NMR (300 MHz, $CDCl_3$): δ (ppm) 0.95 (d, 6H), 1.14 (q, 4H), 1.24 (t, 6H), 1.85 (m, 4H), 2.08 (m, 2H), 4.17 (q, 4H), 4.96 (m, 4H), 5.64 (m, 2H). ^{13}C NMR (300 MHz, $CDCl_3$): δ (ppm) 14.33, 20.35, 29.96, 30.87, 38.10, 57.51, 61.16, 113.35, 144.11, 172.06. Elemental analysis calcd. for $C_{19}H_{32}O_4$: 70.33 C, 9.94 H; found: 69.93 C, 9.54 H.

2,2-Bis(3-methyl-4-pentenyl)malonic acid (6-5). Potassium hydroxide (26.3 g, 470 mmol) was added to a solution of **6-4** (18.9g, 58 mmol) in ethanol (100 mL) and water (20 mL) which was then brought to reflux for 3 hours. The reaction was cooled, quenched with water (150 mL) and conc. HCl (until pH=3), and washed twice with diethyl ether (200 mL). The ether phase was dried with brine and concentrated to 15.0 g of a white solid with no further purification necessary. 95.7% yield. ^{1}H NMR (300

MHz, $CDCl_3$): δ (ppm) 1.01 (d, 6H), 1.25 (m, 4H), 1.83 (m, 4H), 2.11 (m, 2H), 4.98 (m, 4H), 5.65 (m, 2H), 11.18 (br, 2H). ^{13}C NMR (300 MHz, $CDCl_3$): δ (ppm) 20.40, 31.18, 32.09, 38.14, 57.85, 113.73, 143.75, 177.96. CI/HRMS: $[M+H]^+$ cacld for $C_{15}H_{25}O_4$: 269.1753, found: 269.1749; Elemental analysis calcd. for $C_{15}H_{25}O_4$: 67.14 C, 9.01 H; found: 66.98 C, 8.89 H.

5-Methyl-2-(3-methyl-4-pentenyl)-6-heptenoic acid (6-6). Decalin™ (15 mL, 1:1 wt%) was added to **7** (14.5 g, 54 mmol) and heated to 185°C in a 250mL round bottom flask equipped with an air cooled condenser under nitrogen. Production of CO_2 was monitored with a mineral oil bubbler, and the reaction was stirred vigorously until gas evolution ceased after about 30 minutes. Upon cooling, Decalin™ was removed via rotary evaporation affording crude acid. Column chromatography (20% ethyl acetate in hexane) afforded 11.4 g colorless oil. 94.0% yield. ^1H NMR (300 MHz, $CDCl_3$): δ (ppm) 1.01 (d, 6H), 1.33 (m, 4H), 1.50 (m, 2H), 1.61 (m, 2H), 2.12 (m, 2H), 2.31 (m, 1H), 4.96 (m, 4H), 5.67 (m, 2H). ^{13}C NMR (300 MHz, $CDCl_3$): δ (ppm) 20.34, 20.51, 29.96, 30.06, 34.25, 34.36, 37.96, 38.08, 45.70, 45.86, 46.05, 113.13, 113.17, 144.38, 144.45, 183.01. CI/HRMS: $[M+H]^+$ cacld for $C_{14}H_{25}O_2$: 225.1855, found: 225.1845; Elemental analysis calcd. for $C_{14}H_{25}O_2$: 74.95 C, 10.78 H; found: 74.89 C, 10.68 H.

5-Methyl-2-(3-methyl-4-pentenyl) hept-6-en-1-ol (6-7). Same procedure as for **6-2** using **6-6** as starting material. 8.6g of colorless oil was isolated with no further purification needed. 84% yield. ^1H NMR (300 MHz, $CDCl_3$): δ (ppm) 1.00 (d, 6H), 1.20-1.41 (br, 9H), 1.66 (br, 1H), 2.09 (m, 2H), 3.53 (d, 2H), 4.95 (m, 4H), 5.69 (m, 2H). ^{13}C NMR (300 MHz, $CDCl_3$): δ (ppm) 20.44, 20.47, 28.55, 28.58, 28.65, 33.97, 38.35, 40.94, 40.99, 65.74, 65.78, 112.78, 144.92, 144.94. CI/HRMS: $[M+H]^+$ cacld for $C_{14}H_{27}O$:

211.2062, found: 211.2062; Elemental analysis calcd. for $C_{14}H_{26}O$: 79.94 C, 12.46 H; found: 79.71 C, 12.31 H.

5-Methyl-2-(3-methyl-4-pentenyl)-6-heptenyl tosylate (6-8). Same procedure for **6-3** with **6-7** as starting material, 103% crude yield after concentration. No further purification performed. ^{1}H NMR (300 MHz, $CDCl_3$): δ (ppm) 0.93 (d, 6H), 1.15 (m, 4H), 1.22 (m, 4H), 1.56 (br, 1H), 1.99 (m, 2H), 2.45 (s, 3H), 3.90 (d, 2H), 4.91 (m, 4H), 5.60 (m, 2H), 7.34 (d, 2H), 7.78 (d, 2H). ^{13}C NMR (300 MHz, $CDCl_3$): δ (ppm) 20.31, 20.39, 21.79, 28.29, 28.36, 28.40, 33.38, 33.41, 33.49, 37.97, 38.08, 38.10, 72.81, 112.94, 112.97, 128.11, 129.97, 133.25, 144.81, 144.43, 144.46. CI/HRMS: $[M+H]^+$ cacld for $C_{21}H_{33}O_3S$: 365.2150, found: 365.2143; Elemental analysis calcd. for $C_{21}H_{33}O_3S$: 69.19 C, 8.85 H; found: 68.93 C, 8.58 H.

3,6,9-Trimethylundeca-1,10-diene (6-9). Same procedure as for **6-7** with **6-8** as starting material. Isolated 2.5 g of a colorless oil after column chromatography (hexane). 81.1% yield. ^{1}H NMR (300 MHz, C_6D_6): δ (ppm) 0.87 (d, 3H), 0.98 (d, 6H), 1.12 (m, 2H), 1.30 (7H), 2.03 (m, 2H), 4.97 (m, 4H), 5.68 (2H). ^{13}C NMR (300 MHz, C_6D_6): δ (ppm) 19.85, 19.92, 19.98, 20.40, 20.64, 33.34, 33.42, 33.54, 34.48, 34.89, 34.92, 34.99, 35.01, 38.54, 112.65, 112.75, 144.96, 145.07. CI/HRMS: $[M+H]^+$ cacld for $C_{14}H_{26}O$: 194.2035, found: 194.2037; Elemental analysis calcd. for $C_{14}H_{26}O$: 86.52 C, 13.48 H; found: 86.32 C, 13.51 H.

APPENDIX A
CRYSTALLOGRAPHIC DATA

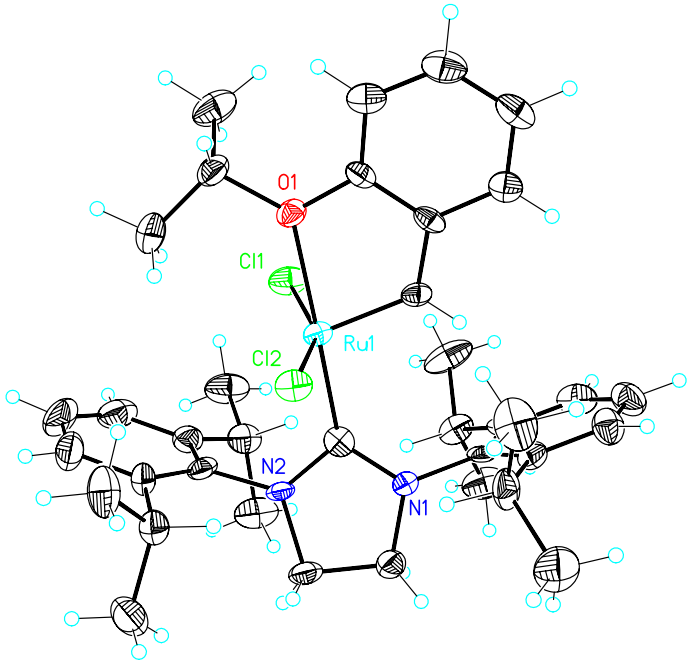

Figure A-1. Crystal structure of **[Ru]11**, $(H_2IPr)(Cl)_2Ru{=}CH(2\text{-}i\text{PrO})C_6H_4$

Table A-1. Crystal data and structure refinement for **[Ru]11**.

Empirical formula	C74.5 H101 Cl5 N4 O2 Ru2	
Formula weight	1463.98	
Temperature	193(2) K	
Wavelength	0.71073 Å	
Crystal system	Triclinic	
Space group	P-1	
Unit cell dimensions	a = 8.5827(6) Å	α= 70.824(2)°.
	b = 19.9621(13) Å	β= 83.083(2)°.
	c = 22.5391(15) Å	γ = 80.542(2)°.
Volume	3588.6(4) $Å^3$	
Z	2	
Density (calculated)	1.355 Mg/m^3	
Absorption coefficient	0.654 mm^{-1}	
F(000)	1530	
Crystal size	0.34 x 0.11 x 0.06 mm^3	
Theta range for data collection	1.66 to 27.50°.	
Index ranges	$-10\leq h\leq 11$, $-19\leq k\leq 25$, $-20\leq l\leq 29$	
Reflections collected	22770	
Independent reflections	15797 [R(int) = 0.0772]	
Completeness to theta = 27.50°	95.8 %	
Absorption correction	Integration	
Max. and min. transmission	0.9623 and 0.8615	
Refinement method	Full-matrix least-squares on F^2	
Data / restraints / parameters	15797 / 0 / 813	
Goodness-of-fit on F^2	0.896	
Final R indices [I>2sigma(I)]	R1 = 0.0648, wR2 = 0.0838 [7310]	
R indices (all data)	R1 = 0.1709, wR2 = 0.1099	
Largest diff. peak and hole	0.747 and -0.734 $e.Å^{-3}$	

$R1 = \sum(||F_o| - |F_c||) / \sum|F_o|$

$wR2 = [\sum[w(F_o^2 - F_c^2)^2] / \sum[wF_o^{22}]]^{1/2}$

$S = [\sum[w(F_o^2 - F_c^2)^2] / (n-p)]^{1/2}$

$w= 1/[\sigma^2(F_o^2)+(0.0370*p)^2+0.31*p]$, $p = [\max(F_o^2,0)+ 2* F_c^2]/3$

Table A-2. Atomic coordinates (x 10^4) and equivalent isotropic displacement parameters ($Å^2$x 10^3) for **[Ru]11**.
U(eq) is defined as one third of the trace of the orthogonalized U^{ij} tensor.

	x	y	z	U(eq)
Ru1	3379(1)	2495(1)	2676(1)	22(1)
Cl1	1150(2)	1891(1)	2990(1)	35(1)
Cl2	5205(2)	3213(1)	2727(1)	30(1)
O1	1667(4)	3509(2)	2423(2)	25(1)
N1	6260(5)	1429(2)	2522(2)	22(1)
N2	5541(5)	1396(2)	3497(2)	23(1)
C1	3408(6)	2708(3)	1824(2)	22(1)
C2	2600(6)	3380(3)	1455(2)	22(1)
C3	2695(6)	3637(3)	799(3)	28(1)
C4	1911(7)	4288(3)	480(3)	36(2)
C5	1011(7)	4704(3)	821(3)	37(2)
C6	872(6)	4473(3)	1469(3)	30(2)
C7	1670(6)	3817(3)	1784(3)	24(1)
C8	585(7)	3841(3)	2843(3)	31(2)
C9	1133(7)	3482(3)	3491(3)	43(2)
C10	-1105(7)	3731(3)	2784(3)	48(2)
C11	5113(7)	1689(3)	2892(3)	23(1)
C12	7473(6)	904(3)	2894(2)	30(2)
C13	7206(6)	1035(3)	3522(3)	30(2)
C14	4560(6)	1477(3)	4044(3)	26(1)
C15	4889(7)	1943(3)	4346(3)	29(2)
C16	3843(9)	2031(3)	4846(3)	46(2)
C17	2546(8)	1655(4)	5035(3)	53(2)
C18	2313(7)	1168(3)	4762(3)	46(2)
C19	3314(7)	1052(3)	4265(3)	31(2)
C20	3102(7)	482(3)	3989(3)	35(2)
C21	1430(7)	235(3)	4140(3)	49(2)
C22	4346(7)	-178(3)	4198(3)	49(2)
C23	6391(7)	2306(3)	4186(3)	33(2)
C24	7678(7)	1844(3)	4620(3)	47(2)
C25	6090(8)	3064(3)	4235(3)	49(2)
C26	6171(6)	1485(3)	1879(3)	21(1)
C27	7011(6)	1979(3)	1410(3)	25(1)
C28	6913(7)	2010(3)	793(3)	34(2)
C29	6040(8)	1584(3)	643(3)	39(2)
C30	5222(7)	1106(3)	1108(3)	40(2)
C31	5286(6)	1038(3)	1741(3)	30(2)
C32	4438(6)	482(3)	2246(3)	32(2)
C33	2675(7)	561(3)	2153(3)	55(2)
C34	5233(7)	-267(3)	2279(3)	48(2)

Table A-2. continued

	x	y	z	U(eq)
C35	7995(7)	2464(3)	1564(3)	35(2)
C36	7468(8)	3253(3)	1233(3)	50(2)
C37	9754(7)	2255(3)	1393(3)	58(2)
Ru2	11116(1)	-3492(1)	2438(1)	22(1)
Cl3	9247(2)	-4276(1)	2630(1)	30(1)
Cl4	13167(2)	-3009(1)	2680(1)	36(1)
O2	12923(4)	-4449(2)	2427(2)	25(1)
N3	8535(5)	-2705(2)	3010(2)	22(1)
N4	8373(5)	-2311(2)	1991(2)	23(1)
C38	11547(6)	-3321(3)	1597(3)	25(1)
C39	12586(6)	-3850(3)	1370(3)	24(1)
C40	12919(7)	-3789(3)	734(3)	35(2)
C41	13976(7)	-4301(3)	549(3)	36(2)
C42	14681(7)	-4883(3)	1002(3)	34(2)
C43	14377(6)	-4965(3)	1634(3)	30(2)
C44	13337(6)	-4441(3)	1819(3)	21(1)
C45	13797(6)	-4966(3)	2948(3)	30(2)
C46	15442(6)	-4781(3)	2914(3)	39(2)
C47	12838(7)	-4943(3)	3549(2)	36(2)
C48	9300(6)	-2739(3)	2452(3)	21(1)
C49	6927(6)	-1951(3)	2232(2)	29(2)
C50	6896(6)	-2345(3)	2931(3)	28(2)
C51	9194(6)	-2954(3)	3615(3)	24(1)
C52	10273(6)	-2569(3)	3732(2)	25(1)
C53	10914(7)	-2818(3)	4315(3)	35(2)
C54	10495(7)	-3425(3)	4770(3)	39(2)
C55	9377(7)	-3782(3)	4662(3)	37(2)
C56	8698(6)	-3564(3)	4082(3)	27(1)
C57	10713(7)	-1867(3)	3248(3)	31(2)
C58	9412(7)	-1233(3)	3239(3)	44(2)
C59	12272(7)	-1668(3)	3360(3)	44(2)
C60	7396(7)	-3955(3)	3993(3)	32(2)
C61	5823(7)	-3729(3)	4327(3)	47(2)
C62	7824(7)	-4780(3)	4252(3)	41(2)
C63	8762(6)	-2069(3)	1324(3)	22(1)
C64	9603(6)	-1475(3)	1073(3)	23(1)
C65	9945(7)	-1246(3)	422(3)	35(2)
C66	9428(7)	-1557(3)	37(3)	36(2)
C67	8568(7)	-2126(3)	299(3)	35(2)
C68	8219(7)	-2397(3)	947(3)	28(2)
C69	10157(7)	-1102(3)	1483(3)	33(2)
C70	9545(8)	-292(3)	1264(3)	48(2)

C71	11975(7)	-1227(3)	1487(3)	52(2)
C72	7258(7)	-3012(3)	1220(3)	33(2)
C73	5547(7)	-2765(3)	1032(3)	62(2)
C74	7972(8)	-3664(3)	1012(3)	50(2)
Cl5	15585(3)	-629(1)	483(1)	115(1)
C75	13903(14)	21(7)	7(7)	60(5)

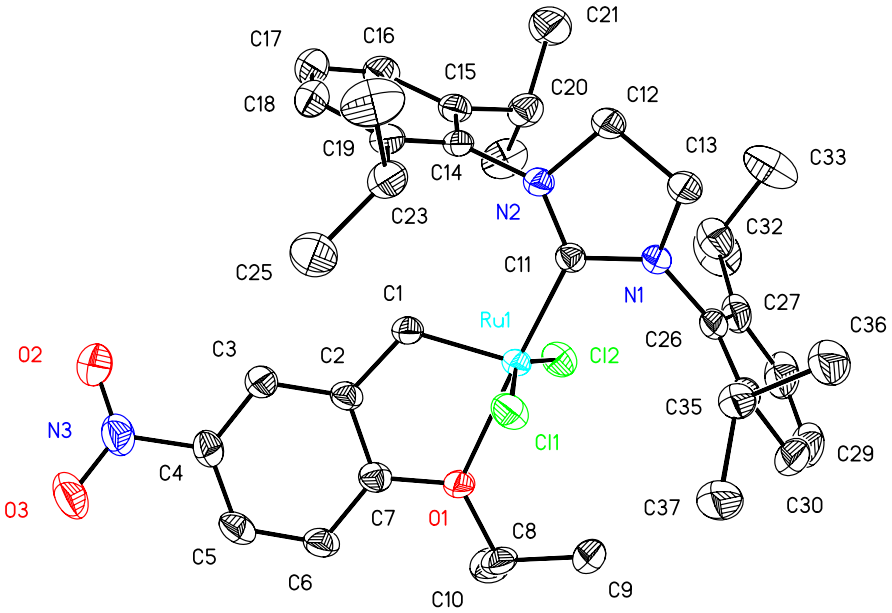

Figure A-2. Crystal structure for **[Ru]13**, $(H_2IPr)(Cl)_2Ru{=}CH(2\text{-}i\text{PrO})(5\text{-}NO_2)C_6H_3$

Table A-3. Crystal data and structure refinement for [Ru]13.

Empirical formula	C37 H49 Cl2 N3 O3 Ru	
Formula weight	755.76	
Temperature	173(2) K	
Wavelength	0.71073 Å	
Crystal system	Monoclinic	
Space group	I2/a	
Unit cell dimensions	a = 27.1836(18) Å	α= 90°.
	b = 12.0491(8) Å	β= 95.811(2)°.
	c = 22.2557(15) Å	γ = 90°.
Volume	7252.1(8) $Å^3$	
Z	8	
Density (calculated)	1.384 Mg/m^3	
Absorption coefficient	0.619 mm^{-1}	
F(000)	3152	
Crystal size	0.28 x 0.16 x 0.08 mm^3	
Theta range for data collection	1.51 to 27.49°.	
Index ranges	$-35\leq h\leq 35$, $-15\leq k\leq 15$, $-28\leq l\leq 28$	
Reflections collected	30787	
Independent reflections	8204 [R(int) = 0.0477]	
Completeness to theta = 27.49°	98.5 %	
Absorption correction	Integration	
Max. and min. transmission	0.9539 and 0.8601	
Refinement method	Full-matrix least-squares on F^2	
Data / restraints / parameters	8204 / 0 / 426	
Goodness-of-fit on F^2	1.059	
Final R indices [I>2sigma(I)]	R1 = 0.0319, wR2 = 0.0723 [7198]	
R indices (all data)	R1 = 0.0393, wR2 = 0.0757	
Largest diff. peak and hole	0.338 and -0.543 $e.Å^{-3}$	

$R1 = \sum(||F_o| - |F_c||) / \sum|F_o|$

$wR2 = [\sum[w(F_o^2 - F_c^2)^2] / \sum[w(F_o^2)^2]]^{1/2}$

$S = [\sum[w(F_o^2 - F_c^2)^2] / (n-p)]^{1/2}$

$w= 1/[\sigma^2(F_o^2)+(m*p)^2+n*p]$, $p = [\max(F_o^2,0)+ 2* F_c^2]/3$, m & n are constants.

Table A-4. Atomic coordinates (x 10^4) and equivalent isotropic displacement parameters ($Å^2$x 10^3) for **[Ru]13**.

	x	y	z	U(eq)
Ru1	8745(1)	1535(1)	9232(1)	23(1)
Cl2	9381(1)	2275(1)	9889(1)	35(1)
Cl1	7979(1)	1476(1)	8657(1)	32(1)
O1	8320(1)	1460(1)	10046(1)	30(1)
O2	8354(1)	-3683(2)	10321(1)	65(1)
O3	7689(1)	-3314(2)	10737(1)	52(1)
N1	9031(1)	2623(1)	8169(1)	25(1)
N2	9159(1)	851(1)	8057(1)	24(1)
N3	8053(1)	-3034(2)	10488(1)	42(1)
C1	8802(1)	52(2)	9409(1)	26(1)
C2	8502(1)	-382(2)	9863(1)	26(1)
C3	8445(1)	-1511(2)	9971(1)	31(1)
C4	8129(1)	-1844(2)	10389(1)	32(1)
C5	7878(1)	-1092(2)	10715(1)	34(1)
C6	7940(1)	34(2)	10625(1)	32(1)
C7	8245(1)	381(2)	10197(1)	27(1)
C8	8141(1)	2376(2)	10409(1)	33(1)
C9	8162(1)	3419(2)	10032(1)	38(1)
C10	8461(1)	2451(2)	11005(1)	44(1)
C11	9037(1)	1628(2)	8455(1)	23(1)
C12	9281(1)	1349(2)	7485(1)	30(1)
C13	9062(1)	2500(2)	7514(1)	33(1)
C14	9323(1)	-271(2)	8190(1)	26(1)
C15	9811(1)	-437(2)	8453(1)	29(1)
C16	9964(1)	-1532(2)	8571(1)	35(1)
C17	9654(1)	-2410(2)	8416(1)	40(1)
C18	9181(1)	-2232(2)	8142(1)	37(1)
C19	9004(1)	-1154(2)	8022(1)	30(1)
C20	10168(1)	506(2)	8619(1)	34(1)
C21	10633(1)	416(2)	8289(1)	52(1)
C22	10311(1)	557(2)	9299(1)	50(1)
C23	8478(1)	-989(2)	7729(1)	34(1)
C24	8412(1)	-1494(3)	7093(1)	57(1)
C25	8101(1)	-1486(2)	8119(1)	49(1)
C26	8978(1)	3677(2)	8469(1)	29(1)
C27	9399(1)	4115(2)	8807(1)	37(1)
C28	9337(1)	5080(2)	9137(1)	51(1)
C29	8884(1)	5591(2)	9121(1)	58(1)
C30	8484(1)	5198(2)	8757(1)	50(1)
C31	8521(1)	4237(2)	8408(1)	37(1)
C32	9910(1)	3599(2)	8801(1)	41(1)

Table A-4. continued

	x	y	z	U(eq)
C33	10132(1)	3874(3)	8220(1)	65(1)
C34	10282(1)	3909(3)	9334(1)	65(1)
C35	8096(1)	3917(2)	7946(1)	39(1)
C36	8131(1)	4624(2)	7375(1)	47(1)
C37	7584(1)	4060(2)	8164(1)	57(1)

U(eq) is defined as one third of the trace of the orthogonalized U^{ij} tensor.

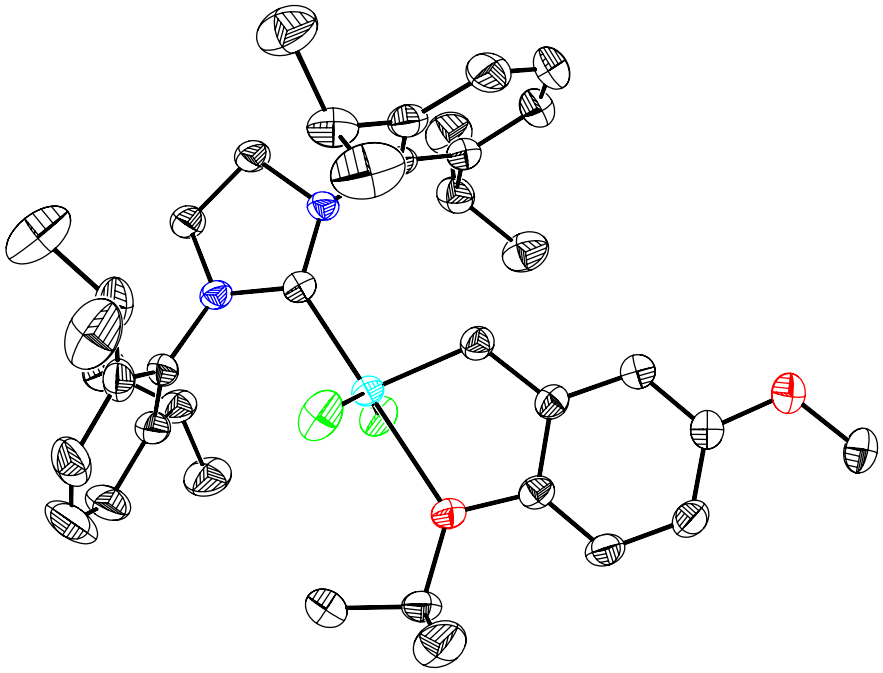

Figure A-3. Crystal structure for **[Ru]16**, $(H_2IPr)(Cl)_2Ru{=}CH(2\text{-}i\text{PrO})(5\text{-}OCH_3)C_6H_3$

Table A-5. Crystal data and structure refinement for **[Ru]16**.

Empirical formula	C38 H52 Cl2 N2 O2 Ru	
Formula weight	740.79	
Temperature	173(2) K	
Wavelength	0.71073 Å	
Crystal system	Monoclinic	
Space group	P2(1)/c	
Unit cell dimensions	a = 11.5767(8) Å	α= 90°.
	b = 12.1545(9) Å	β= 96.174(1)°.
	c = 26.1769(19) Å	γ = 90°.
Volume	3662.0(5) $Å^3$	
Z	4	
Density (calculated)	1.344 Mg/m^3	
Absorption coefficient	0.608 mm^{-1}	
F(000)	1552	
Crystal size	0.14 x 0.08 x 0.06 mm^3	
Theta range for data collection	1.77 to 27.50°.	
Index ranges	-14≤h≤15, -15≤k≤15, -16≤l≤34	
Reflections collected	23595	
Independent reflections	8270 [R(int) = 0.0436]	
Completeness to theta = 27.50°	98.6 %	
Absorption correction	Integration	
Max. and min. transmission	0.9470 and 0.8869	
Refinement method	Full-matrix least-squares on F^2	
Data / restraints / parameters	8270 / 0 / 406	
Goodness-of-fit on F^2	0.891	
Final R indices [I>2sigma(I)]	R1 = 0.0385, wR2 = 0.1146 [6677]	
R indices (all data)	R1 = 0.0521, wR2 = 0.1228	
Largest diff. peak and hole	1.835 and -0.648 $e.Å^{-3}$	

$R1 = \Sigma(||F_o| - |F_c||) / \Sigma|F_o|$

$wR2 = [\Sigma[w(F_o^2 - F_c^2)^2] / \Sigma[w(F_o^2)^2]]^{1/2}$

$S = [\Sigma[w(F_o^2 - F_c^2)^2] / (n-p)]^{1/2}$

$w= 1/[\sigma^2(F_o^2)+(m*p)^2+n*p]$, $p = [\max(F_o^2,0)+ 2* F_c^2]/3$, m & n are constants.

Table A-6. Atomic coordinates (x 10^4) and equivalent isotropic displacement parameters ($Å^2$x 10^3) for **[Ru]16**.

	x	y	z	U(eq)
Ru1	8479(1)	1373(1)	1272(1)	23(1)
Cl1	7500(1)	1327(1)	445(1)	37(1)
Cl2	9717(1)	770(1)	1978(1)	42(1)
O1	10089(2)	1569(2)	870(1)	30(1)
C11	6964(2)	1205(2)	1548(1)	23(1)
C14	6381(2)	3082(2)	1821(1)	28(1)
C5	11223(2)	4244(2)	462(1)	36(1)
C12	5101(2)	1431(2)	1806(1)	34(1)
C31	6936(3)	-1366(2)	1012(1)	38(1)
C6	11111(2)	3105(2)	504(1)	34(1)
C23	5532(3)	3640(2)	912(1)	39(1)
C27	7721(2)	-1261(2)	1929(1)	37(1)
C2	9573(2)	3361(2)	1046(1)	28(1)
C19	6033(2)	3904(2)	1455(1)	34(1)
C18	6208(3)	4995(3)	1610(1)	46(1)
C7	10302(2)	2671(2)	796(1)	28(1)
C26	7051(2)	-827(2)	1490(1)	30(1)
C1	8703(2)	2866(2)	1331(1)	28(1)
C13	5203(2)	280(2)	1609(1)	36(1)
C4	10515(2)	4942(2)	710(1)	34(1)
C15	6872(2)	3328(2)	2317(1)	33(1)
C16	7035(3)	4449(3)	2444(1)	46(1)
C35	7649(3)	-804(3)	2460(1)	43(1)
C3	9696(3)	4496(2)	1003(1)	35(1)
C32	6014(3)	-1064(3)	589(1)	41(1)
C30	7630(3)	-2293(3)	967(2)	55(1)
C28	8383(3)	-2195(3)	1853(2)	52(1)
C10	12009(3)	771(3)	1077(2)	60(1)
C29	8371(3)	-2655(3)	1379(2)	69(1)
C8	10902(3)	744(2)	715(1)	38(1)
C17	6706(3)	5259(3)	2093(1)	53(1)
C9	10273(3)	-338(3)	715(2)	56(1)
C38	11440(3)	6547(3)	426(1)	49(1)
C34	4925(3)	-1774(3)	635(1)	51(1)
C33	6387(4)	-1204(3)	43(1)	60(1)
C37	8715(4)	-1049(4)	2844(2)	71(1)
C22	6520(4)	2484(4)	3163(1)	65(1)
C36	6578(4)	-1249(4)	2683(2)	76(1)
C21	8540(3)	2545(4)	2913(2)	71(1)
N1	6176(2)	1947(2)	1677(1)	25(1)
N2	6445(2)	201(2)	1550(1)	25(1)

Table A-6. continued

	x	y	z	U(eq)
O2	10584(2)	6064(2)	705(1)	48(1)
C24	6248(3)	4157(3)	512(1)	52(1)
C25	4259(3)	4010(4)	811(2)	56(1)
C20	7263(3)	2450(3)	2713(1)	40(1)

U(eq) is defined as one third of the trace of the orthogonalized U^{ij} tensor.

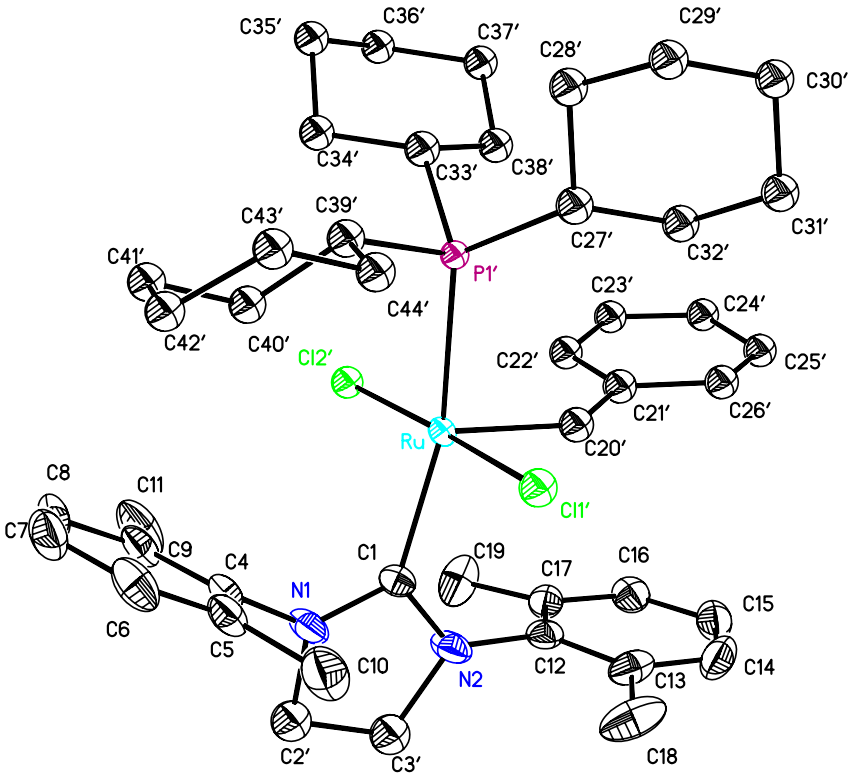

Figure A-4. Crystal structure for **[Ru]23**, $(H_2IPr)PCy_3(Cl)_2Ru{=}CHPh$

Table A-7. Crystal data and structure refinement for **[Ru]23**

Empirical formula	C44 H61 Cl2 N2 P Ru	
Formula weight	820.89	
Temperature	173(2) K	
Wavelength	0.71073 Å	
Crystal system	Triclinic	
Space group	P-1	
Unit cell dimensions	a = 11.7056(18) Å	α= 87.768(3)°.
	b = 12.3160(19) Å	β= 70.834(2)°.
	c = 16.042(3) Å	γ = 70.927(3)°.
Volume	2058.5(6) $Å^3$	
Z	2	
Density (calculated)	1.324 Mg/m^3	
Absorption coefficient	0.582 mm^{-1}	
F(000)	864	
Crystal size	0.20 x 0.11 x 0.06 mm^3	
Theta range for data collection	1.35 to 27.50°.	
Index ranges	$-13\leq h\leq 14$, $-12\leq k\leq 15$, $-20\leq l\leq 18$	
Reflections collected	13498	
Independent reflections	8977 [R(int) = 0.0287]	
Completeness to theta = 27.50°	95.1 %	
Absorption correction	Integration	
Max. and min. transmission	0.9530 and 0.8215	
Refinement method	Full-matrix least-squares on F^2	
Data / restraints / parameters	8977 / 48 / 539	
Goodness-of-fit on F^2	1.084	
Final R indices [I>2sigma(I)]	R1 = 0.0377, wR2 = 0.0840 [7550]	
R indices (all data)	R1 = 0.0496, wR2 = 0.0895	
Largest diff. peak and hole	0.775 and -0.792 $e.Å^{-3}$	

$R1 = \sum(||F_o| - |F_c||) / \sum|F_o|$

$wR2 = [\sum[w(F_o^2 - F_c^2)^2] / \sum[w(F_o^2)^2]]^{1/2}$

$S = [\sum[w(F_o^2 - F_c^2)^2] / (n-p)]^{1/2}$

$w= 1/[\sigma^2(F_o^2)+(m*p)^2+n*p]$, $p = [\max(F_o^2,0)+ 2* F_c^2]/3$, m & n are constants.

Table A-8. Atomic coordinates (x 10^4) and equivalent isotropic displacement parameters ($Å^2$x 10^3) for **[Ru]23**.

	x	y	z	U(eq)
Ru	-89(1)	7168(1)	2493(1)	25(1)
N1	1025(2)	4545(2)	1978(2)	47(1)
N2	2500(2)	5347(2)	1581(2)	49(1)
C1	1239(3)	5549(2)	2000(2)	34(1)
C2	2289(8)	3536(7)	1691(9)	48(3)
C3	3297(8)	4094(7)	1418(8)	44(2)
C2'	2111(6)	3621(5)	1372(6)	51(2)
C3'	3149(6)	4169(6)	1092(6)	52(2)
C4	-110(3)	4270(2)	2425(2)	37(1)
C5	-307(3)	3931(2)	3283(2)	45(1)
C6	-1378(4)	3603(3)	3685(2)	59(1)
C7	-2195(4)	3590(3)	3248(3)	65(1)
C8	-1974(4)	3902(3)	2404(3)	61(1)
C9	-920(3)	4241(2)	1955(2)	47(1)
C10	610(4)	3921(3)	3761(3)	73(1)
C11	-681(5)	4558(3)	1018(2)	77(1)
C12	3196(3)	6137(2)	1417(2)	39(1)
C13	3819(3)	6248(3)	2000(2)	52(1)
C14	4550(3)	6992(4)	1783(3)	63(1)
C15	4661(3)	7562(3)	1023(3)	58(1)
C16	4081(3)	7399(3)	453(2)	47(1)
C17	3356(3)	6670(3)	627(2)	40(1)
C18	3771(4)	5571(4)	2806(3)	83(1)
C19	2833(3)	6436(4)	-60(2)	67(1)
Cl1	603(1)	7049(1)	3733(1)	32(1)
Cl2	-397(1)	7433(1)	1063(1)	34(1)
P1	-1140(1)	9239(1)	2789(1)	24(1)
C20	-1549(3)	6761(2)	2874(2)	28(1)
C21	-2409(3)	6577(2)	3731(2)	30(1)
C22	-3588(3)	6513(3)	3747(2)	38(1)
C23	-4458(3)	6337(3)	4526(3)	47(1)
C24	-4172(4)	6222(4)	5287(3)	56(1)
C25	-3024(4)	6285(4)	5292(3)	58(1)
C26	-2145(3)	6463(3)	4520(2)	43(1)
C27	-1672(3)	9694(3)	3988(2)	36(1)
C28	-2896(4)	9446(3)	4508(2)	44(1)
C29	-3150(5)	9548(4)	5502(2)	65(1)
C30	-3190(7)	10719(9)	5799(4)	65(2)
C31	-2027(5)	11018(4)	5263(3)	58(1)
C32	-1766(4)	10899(3)	4271(2)	51(1)
C33	-2458(3)	9892(3)	2337(2)	29(1)

Table A-8. continued

	x	y	z	U(eq)
C34	-3480(3)	9326(3)	2523(3)	37(1)
C35	-4329(4)	9806(3)	1948(3)	43(1)
C36	-4942(3)	11108(3)	2098(3)	50(1)
C37	-3940(4)	11680(3)	1965(3)	51(1)
C38	-3088(3)	11204(3)	2529(2)	40(1)
C39	-25(3)	10039(2)	2251(2)	28(1)
C40	284(3)	10109(3)	1245(2)	43(1)
C41	1077(4)	10911(3)	913(3)	45(1)
C42	2319(3)	10493(3)	1133(3)	44(1)
C43	2033(4)	10360(4)	2118(3)	52(1)
C44	1229(3)	9571(3)	2452(2)	40(1)
Cl1'	334(6)	6815(6)	3982(4)	39(2)
Cl2'	-738(6)	7348(5)	1345(4)	33(2)
P1'	-2101(4)	8630(4)	3482(3)	23(1)
C20'	882(18)	8175(16)	2390(13)	37(1)
C21'	1129(17)	9065(15)	1838(11)	37(1)
C22'	757(18)	9305(16)	1085(11)	37(1)
C23'	978(17)	10209(15)	603(12)	37(1)
C24'	1590(20)	10847(19)	829(14)	37(1)
C25'	2040(20)	10593(18)	1524(14)	37(1)
C26'	1750(20)	9749(16)	2075(12)	37(1)
C27'	-2124(17)	9518(16)	4403(14)	37(1)
C28'	-3457(15)	10324(16)	4980(12)	37(1)
C29'	-3380(40)	10800(40)	5813(18)	37(1)
C30'	-2419(17)	11456(17)	5549(13)	37(1)
C31'	-1121(17)	10718(16)	4987(11)	37(1)
C32'	-1136(17)	10151(17)	4178(11)	37(1)
C33'	-3112(18)	9671(15)	2918(12)	37(1)
C34'	-3840(20)	9294(18)	2441(18)	37(1)
C35'	-4736(18)	10340(20)	2151(13)	37(1)
C36'	-4000(17)	10999(16)	1544(12)	37(1)
C37'	-3225(19)	11387(15)	1989(13)	37(1)
C38'	-2430(19)	10446(19)	2396(13)	37(1)
C39'	-3223(18)	7860(14)	4096(10)	37(1)
C40'	-3070(20)	6805(16)	3544(12)	37(1)
C41'	-4090(20)	6260(18)	4001(14)	37(1)
C42'	-4020(20)	5873(17)	4894(13)	37(1)
C43'	-4085(18)	6868(16)	5453(11)	37(1)
C44'	-3079(17)	7432(16)	4986(10)	37(1)

U(eq) is defined as one third of the trace of the orthogonalized U^{ij} tensor.

LIST OF REFERENCES

1. For olefin metathesis reviews, see: (a) R.H. Grubbs, Handbook of Metathesis, Wiley-VCH: Weinheim, Germany, 2003.

2. (b) K.J. Ivin, J.C. Mol, Olefin Metathesis and Metathesis Polymerization, Academic Press, London, 1997.

3. Eleuterio, H.S. *J. Mol. Cat.* **1991**, *65*, 55-61.

4. Anderson, A.W.; Merkling, N.G. (1955) US Patent 2, 721, 189

5. Calderon, N. *Tetrahedron. Lett.* **1967**, *8*, 3327-3329.

6. Calderon, N. *Acc. Chem. Res.* **1972**, *5*, 127-132.

7. Fürstner, A. *Angew. Chem. Int. Edit.* **2000**, *39*, 3013. A. Fürstner, *Angew. Chem. Int. Edit.* **2000**, *39*, 3012-3043.

8. Grubbs, R.H.; Chang, S. *Tetrahedron* **1998**, *54*, 4413-4450.

9. Schuster, M.; Blechert, S. *Angew.Chem. Int. Edit.* **1997**, *36*, 2036-2056.

10. Armstrong, S.K. *J. Chem. Soc. Perk. Trans. 1* **1998**, 371-388.

11. Wright, D. L. *Curr. Org. Chem.* **1999**, *3*, 211-240.

12. Chatterjee, A. K.; Choi, T.-L.; Sanders, D. P.; Grubbs, R. H. *J. Am. Chem. Soc.* **2003**, *125*, 10103-10109.

13. Blackwell, H. E.; O'Leary, D. J.; Chatterjee, A. K.; Washenfelder, R. A.; Bussmann, D. A.; Grubbs, R. H. *J. Am. Chem. Soc.* **2000**, 122, 58-71.

14. Chatterjee, A. K.; Grubbs, R. H. *Org. Lett.* **1999**, *1*, 1751-1753.

15. Seshadri, H.; Lovely, C. J. *Org. Lett.* **2000**, *2*, 327-330.

16. Morgan, J.P.; Morrill, C.; Grubbs, R.H. *Org Lett.* **2002**, 4, 67-70.

17. La, D.S.; Ford, J.G.; Sately, E.S.; Bonitatebus, P.J.; Schrock, R.R.; Hoveyda, A.H. *J. Am. Chem. Soc.* **1999**, *121*, 11603-11604.

18. Snapper, M.L.; Tallarico, J.A.; Randall, M.L. *J. Am. Chem. Soc.* **1997**, *119*, 1478-1479.

19. Buchmeiser, M. R. *Chem. Rev.* **2000**, *100*, 1565-1604.

20. Frenzel, U.; Nuyken, O. *J. Polym. Sci. Chem.* **2002**, *40*, 2895-2916.

21. Lehman, S. E.; Wagener, K. B. in *Handbook of Metathesis*; Grubbs, R. H., Ed.; Wiley-VCH: Weinheim, Germany, 2003; Vol. 3, pp 283-353.

22. Baughman, T. W.; Wagener, K. B. *Adv. Poly. Sci.* **2005**, *176*, 1-42.

23. Hérisson, J-L.; Chauvin, Y. *Makromol. Chem.* **1971**, *141*, 161-167.

24. Schrock, R.R. *J. Am. Chem. Soc.* **1974**, *96*, 6796-6797.

25. Wallace, K.C.; Liu, A. H.; Dewan, J. C.; Schrock, R.R. *J. Am. Chem. Soc.* **1988**, *110*, 4964-4977.

26. Grubbs, R.H.; Tumas, W. *Science* **1989**, *243*, 907-915.

27. Schrock, R.R.; Murdzek, J.S.; Bazan, G.C.; Robbins, M.; Dimare, M.; O'Regan, M. *J. Am. Chem. Soc.* **1990**, *112*, 3875-3886.

28. For a review on Schrock-type catalysts: (a) Schrock, R.R. *Tetrahedron* **1999**,*55*, 8141-8153. (b) R.R. Schrock, *Acc. Chem. Res.* **1990**, *23*, 158-165.

29. Kirkland, T.A.; Grubbs, R.H. *J.Org.Chem.* **1997**, *62*, 7310-7318.

30. Grubbs, R.H.; Miller, S.J.; Fu, G.C. *Acc. Chem. Res.* **1995**, 28, 446-452.

31. Trnka, T.M., Grubbs, R.H., *Acc. Chem. Res*. **2001**, *34*, 18-29

32. Novak, B.M.; Grubbs, R.H. *J. Am. Chem. Soc.* **1988**, *110*, 960-961.

33. Novak, B.M.; Grubbs, R.H. *J. Am. Chem. Soc.* **1988**, *110*, 7542-7543.

34. Nguyen, S.T.; Johnson, L.K.; Grubbs, R.H.; Ziller, J.W. *J. Am. Chem. Soc.* **1992**, *114*, 3974-3975.

35. Nguyen, S.T.; Grubbs, R.H.; Ziller, J.W. *J. Am. Chem. Soc.* **1993**, *115*, 9858-9859.

36. Schwab, P.; France M.B.; Ziller, J.W.; Grubbs, R.H. *Angew. Chem. Int. Edit.* **1995**, *34*, 2039-2041.

37. Schwab, P.; Grubbs, R.H.; Ziller, J.W. *J. Am. Chem. Soc.* **1996**, *118*, 100-110.

38. Lynn, D.M.; Mohr, B.; Grubbs, R.H.; Henling, L.M.; Day, M.W. *J. Am. Chem. Soc.* **2000**, *122*, 6601-6609.

39. Mohr, B.; Lynn, D.M.; Grubbs, R.H. *Organometallics* **1996**, *15*, 4317-4325.

40. Kirkland, T.A.; Lynn, D.M.; Grubbs, R.H. *J. Org. Chem.* **1998**, *63*, 9904-9909.

41. Nguyen, S.T.; Grubbs, R.H. *J. Organomet. Chem.* **1995**, *497*, 195-200.

42. Barrett, A.G.M.; Cramp, S.M.; Roberts, R.S. *Org. Lett.* **1999**, *7*, 1083-1086.

43. Ahmed, M.; Barrett, A.G.M.; Braddock, D.C.; Cramp, S.M.; Procopiou, P.A. *Tetrahedron Lett.* **1999**, *40*, 8657-8662.

44. Nieczypor, P.; Buchowicz, W.; Meester, W.J.N.; Rutjes, F.P.J.T.; Mol, J.C. *Tetrahedron Lett.* **2001**, *42*, 7103-7105.

45. Jafarpour, L.; Nolan, S.P. *Org. Lett.* **2000**, *25*, 4075-4078.

46. Dias, E.L.; Grubbs, R.H. *Organometallics* **1998**, *17*, 2758-2767

47. Chang, S.; Jones, L.; Wang, C.; Henling, L.M.; Grubbs, R.H. *Organometallics* **1988**, *17*, 3460-3465

48. DeClercq, B.; Verpoort, F. *Adv. Synth, Catal.* **2003**, *344*, 639-648.

49. Picquet, M.; Bruneau, C.; Dixneuf, P.H. *Chem. Commun.* **1998**, 2249-2250.

50. Fürstner, A.; Picquet, M.; Bruneau, C.; Dixneuf, P.H. *Chem. Commun.* **1998**, 1315-1316.

51. Jafarpour, L.; Huang, J.; Stevens, E.D.; Nolan, S.P. *Organometallics* **1999**, *18*, 3760-3763.

52. Fürstner, A.; Liebi, M.; Lehmann, C.W.; Picquet, M.; Bruneau, C.; Touchard, D.; Dixneuf, P.H. *Chem. Eur. J.* **2000**, *6*, 1847-1857.

53. Hansen, S.M.; Volland, M.A.O.; Rominger, F.; Eisentrager, F.; Hofmann, P. *Angew.Chem. Int. Edit.* **1999**, *38*, 1273-1276.

54. Hansen, S.M.; Rominger, F.; Metz, M.; Hofmann, P. *Chem. Eur. J.* **1999**, *5*, 557-566.

55. Dias, E.L., Ph.D. Thesis, California Institute of Technology, 1998.

56. Kingsbury, J.S.; Harrity, J.P.A.; Bonitatebus, P.J.; Hoveyda, A.H. *J. Am. Chem. Soc.* **1999**, *121*, 791-799.

57. Dias, E.L.; Nguyen, S.T.; Grubbs, R.H. *J. Am. Chem. Soc.* **1997**, *119*, 3887-3897.

58. Maughon, B.R.; Grubbs, R.H.; *Macromolecules* **1997**, *30*, 3459-3469.

59. Wu, Z.; Nguyen, S.T.; Grubbs, R.H.; Ziller, J.W. *J. Am. Chem. Soc.* **1995**, *117*, 5503-5511.

60. Tallarico, J.A.; Bonitatebus, P.J.; Snapper, M.L. *J. Am. Chem. Soc.* **1997**, *119*, 7157-7158.

61. Aldhart, C.; Hinderling, C.; Baumann, H.; Chen, P. *J. Am. Chem. Soc.* **2000**, *122*, 8204-8214.

62. Hinderling, C.; Aldhart, C.; Chen, P. *Angew.Chem. Int. Edit.* **1998**, *37*, 2685-2689.

63. Aagaard, O.M.; Meier, R.J.; Buda, F. *J. Am. Chem. Soc.* **1998**, *120*, 7174-7182.

64. Weskamp, T.; Shattenmann, W.C.; Spiegler, M.; Herrmann, W.A. *Angew.Chem. Int. Edit.* **1998**, *38*, 2490-2493. Westkamp, T.; Shattenmann, W.C.; Spiegler, M.; Herrmann, W.A. *Angew.Chem. Int. Edit.* **1998**, *38*, 262-265.

65. Arduengo III, A.J.; Harlow, R.L.; Kline, M. *J. Am. Chem. Soc.* **1991**, *113*, 361-363.

66. Arduengo III, A.J.; Rasika Dias, H.V.; Harlow, R.L.; Kline, M. *J. Am. Chem. Soc.* **1992**, *114*, 5530-5534.

67. Arduengo III, A.J.; Krafczyk, R.; Schmutzler, R.; Craig, H.A.; Goerlich, J.R.; Marshall, W.J.; Unverzagt, M. *Tetrahedron* **1999**, *55*, 14523-14534.

68. Arduengo III, A.J. *Acc. Chem. Res*. **1999**, *32*, 913-921.

69. Scholl, M.; Trnka, T.M.; Morgan, J.P.; Grubbs, R.H. *Tetrahedron Lett.* **1999**, *40*, 2247-2250.

70. Huang, J.; Stevens, E.D.; Nolan, S.P.; Petersen, J.L. *J. Am. Chem. Soc.* **1999**, *121*, 2674-2678.

71. Scholl, M.; Ding, S.; Lee, C.; Grubbs, R.H. *Org. Lett.* **1999**, *1*, 953-956.

72. Trnka, T. M.; Morgan, J. P.; Sanford, M. S.; Wilhelm, T. E.; Scholl, M.; Choi, T.-L.; Ding, S.; Day, M. W.; Grubbs, R. H.; *J. Am. Chem. Soc.*; **2003**; *125*; 2546-2558.

73. Jafarpour, L.; Nolan, S. *J. Organomet. Chem.* **2001**, *617-618*, 17-27.

74. Sanford, M. S.; Ulman, M.; Grubbs, R. H. *J. Am. Chem. Soc.* **2001**, *123*, 749-750.

75. Sanford, M. S.; Love, J. A.; Grubbs, R. H. *J. Am. Chem. Soc.* **2001**, *123*, 6543-6554.

76. McGuinness, D.S.; Cavell, K.J.; Skeleton, B.W.; White, A.H. *Organometallics* **1999**, *18*,1596-1605.

77. Bielawski, C.W.; Grubbs, R.H. *Angew.Chem. Int. Edit.* **2000**, *39*, 2903-2906.

78. Huang, J.; Schanz, H.J.; Stevens, E.D.; Nolan, S.P. *Organometallics.* **1999**, *18*, 2370-2375.

79. Cucullu, M.E.; Li, C.; Nolan, S.P.; Nguyen, S.T.; Grubbs, R.H. *Organometallics.* **1998**, *17*, 5565-5568.

80. Ulman, M.; Grubbs, R.H. *Organometallics* **1998**, *17*, 2484-2489.

81. Cavallo, L. *J. Am. Chem. Soc.* **2002**, *124*, 8965-8973.

82. Bernardi, F.; Bottoni, A.; Miscione, G.P. *Organometallics* **2003**, *22*, 940-947.

83. Aldhart, C.; Chen, P. *J. Am. Chem. Soc.* **2004**, *126*, 3496-3510.

84. Romero, P.E.; Piers, W.E. *J. Am. Chem. Soc.* **2005**, *127*, 5032-5033.

85. Trnka, T. M.; Day, M. W.; Grubbs, R. H. *Organometallics* **2001**, *20*, 3845-3847.

86. Seiders, T. J.; Ward, D. W.; Grubbs, R. H. *Org. Lett.* **2001**, *3*, 3225-3228.

87. Ulman, M.; Grubbs, R.H. *J.Org. Chem.* **1999**, *64*, 7202-7207.

88. Huang, J.; Schanz, H.J.; Stevens, E.D.; Nolan, S.P.; *Organometallics.* **1999**, *18*, 5375-5380.

89. Hong, S. H.; Day, M. W.; Grubbs, R. H. *J. Am. Chem. Soc.* **2004**, *126*, 7414-7415.

90. Wu, Z.; Nguyen, S. T.; Grubbs, R. H.; Ziller, J. W. *J. Am. Chem. Soc.* **1995**, *117*, 5503-5511.

91. Louie, J.; Grubbs, R. H. *Organometallics* **2002**, *21*, 2153-2164.

92. Dinger, M. B.; Mol, J. C. *Organometallics* **2003**, *22*, 1089-1095.

93. Dinger, M. B.; Mol, J. C. *Eur. J. Inorg. Chem.* **2003**, 2827-2833.

94. Banti, D.; Mol, J. C. *J. Organomet. Chem.* **2004**, *689*, 3113-3116.

95. Garber, S.B.; Kingsbury, J.S.; Gray, B.L.; Hoveyda, A.H. *J. Am. Chem. Soc.* **2000**, *122*, 8168-8179.

96. Randl, S.; Gessler, S.; Wakamatsu, H.; Blechert, S. *Synlett* **2001**, *3*, 430-433.

97. Gessler, S.; Randl, S.; Blechert, S. *Tetrahedron Lett.* **2000**, *41*, 9973-9976.

98. Imbhof, S.; Randl, S.; Blechert, S. *Chem. Commun.* **2001**, 1692-1693.

99. Love, J.A.; Morgan, J.P.; Trnka, T.M. *Angew. Chem. Int. Ed.* **2002**, *41* , 4035-4037.

100. Fürstner, A.; Ackermann, L.; Gabor, B.; Goddard, R.; Lehman, C.W.; Mynott, R.; Stelzer, F.; Thiel, O.R. *Chem. Eur. J.* **2001**, *7*, 3236-3253.

101. Dinger, M. B.; Mol, J. C. *Adv. Synth. Catal*. **2002**, *344*, 671-677.

102. Kingsbury, J. S.; Garber, S. B.; Giftos, J. M.; Gray, B. L.; Okamoto, M. M.; Farrer, M. A.; Fourkas, J. T.; Hoveyda, A. H. *Angew.Chem. Int. Edit.* **2001**, *40*, 4251-4255.

103. Connon, S. J.; Dunne, A. M.; Blechert, S. *Angew.Chem. Int. Edit.* **2002**, *41*, 3835.

104. Grela, K.; Tryznowski, M.; Bienik, M. *Tet. Lett.* **2002**, *43*, 9055-9059.

105. Zarka, M. T.; Nuyken, O.; Weberskirch, R. *Macromol. Rapid Commun.* **2004**, *25*, 858-862.

106. Yao, Q.; Motta, A. R. *Tetrahedron Lett.* **2004**, *45*, 2447-2451.

107. Dowden, J.; Savovic, J. *Chem. Comm.* **2001**, 37-38.

108. Zaja, M.; Connon, S. J.; Dunne, A. M.; Rivard, M.; Buschmann, N.; Jiricek, J.; Blechert, S. *Tetrahedron* **2003**, *59*, 6545-6558.

109. Michrowska, A.; Bujok, R.; Harutyunyan, S.; Sashuk, V.; Dolgonos, G.; Grela, K. *J. Am. Chem. Soc.* **2004**, *126*, 9318-9325.

110. Odian, G. Principles of Polymerization; John Wiley & Sons: New York, NY, 1991, Ch.2.

111. *Ibid.* pp.91-105

112. *Ibid.* pp.73-77

113. Wagener, K.B.; Smith, Jr, D.W. *Macromolecules* **1991**, *24*, 6073-6078.

114. Fürstner, A.; Thiel, O.R.; Ackermann, L.; Schanz, H.J.; Nolan, S.P. *J. Org. Chem.* **2000**, *65*, 2204-2207.

115. Odian, G. Principles of Polymerization; John Wiley & Sons: New York, NY, 1991, p.87.

116. Wagener, K.B.; Nel, J.G.; Konzelman, J.; Boncella, J.M. *Macromolecules* **1990**, *23*, 5155-5157.

117. Odian, G. "Principles of Polymerization", John Wiley & Sons: New York, NY, 1991, pp.83-90.

118. Flory, P.J. "Principles of Polymer Chemistry", Cornell University Press, Ithaca, N.Y., 1953, Chap. 3, 8, 9.

119. Brzezinska, K.; Wolfe, P. S.; Watson, M. D.; Wagener, K. B. *Macromol. Chem. Phys.* **1996**, *197*, 2065-2074.

120. Steiger, D.; Tervoort, T.; Weder, C.; Smith, P. *Macromol. Rapid Commun.* 2000, *21*, 405-422.

121. Watson, M. D.; Wagener, K. B. *Macromolecules* **2000**, *33*, 3196-3201.

122. Watson, M. D.; Wagener, K. B. *Macromolecules* **2000**, *33*, 5411-5417.

123. Wagener, K.B; Brzezinska, K.; *Macromolecules* **1991**, 24, 5273-5277.

124. Wolfe, P. S.; Wagener, K. B. *Macromolecules* **1999**, *32*, 7961-7967.

125. Gómez, F. J.; Wagener, K. B. *J. Organomet. Chem.* **1999**, *592*, 271-277.

126. Brzezinska, K.; Wagener, K.B; Burns, G.T. *J. Polym. Sci. A.: Chem.* **1999**, 37, 849-856.

127. Wagener, K.B; Valenti, D.J.; Hahn, S.F. *Macromolecules* **1997**, *30*, 6688-6690.

128. Smith, J. A.; Brzezinska, K. R.; Valenti, D. J.; Wagener, K. B. *Macromolecules* **2000**, *33*, 3781-3794.

129. Sworen, J. C., Smith, J. A., Baugh, L. S., Rucker, S. P., Wagener, K. B *J. Am. Chem. Soc.* **2003**, *125*, 2228-2240.

130. Sworen, J.C.; Smith, J. A.; Berg, J. M.; Wagener, K.W. *J. Am. Chem. Soc.* **2004**, *126*, 11238-11246.

131. Hopkins, T.E.; Ph.D. Dissertation, University of Florida, 2003.

132. Baughman, T.W.; Wagener, K.B. Unpublished results.

133. Watson, M. D.; Wagener, K. B. *Macromolecules* **2000**, *33*, 8963-8970.

134. Allcock, H.R.; Kellam, E.C.; Hofmann, M.A. *Macromolecules.* **2001**, *34*, 5140-5146.

135. Allcock, H.R.; Kellam, E.C.; *Macromolecules.* **2002**, *35*, 40-47.

136. Joo, S.H.; Yun, Y-K.; Jin, J-I.; Kim, D.C.; Zin, W-C. *Macromolecules.* **2000**, *33*, 6704-6712.

137. Tamura, H.; Nakayama, A. *J. Macromol. Sci. Pure App. Chem.* **2002**, *39*, 745-758.

138. Brzezinska, K.R.; Deming, T.J. *Macromolecules.* **2001**, *34*, 4348-4354.

139. Schultz, G.O.; Milkovich, J.R. *J. Appli. Polym. Sci.* **1982,** *27*, 4773-4786.

140. Mecerreyes, D.; Dubois, P.; Hedrick, J.L.; Jerome, R. *Macromol. Chem. Phys.* **1999**, *200*, 156-165.

141. O'Donnell, P. M.; Brzezinska, K. R.; Powell, D.;Wagener, K. B.; *Macromolecules.* **2001**, *34*, 6845-6849.

142. Watson, M.D.; Wagener, K.B *J. Polym. Sci. A.: Chem.* **1999**, 37, 1857-1861.

143. Watson, M.D.; Wagener, K.B *Macromolecules.* **2000**, 33, 1494-1496.

144. Lehman, S. E.; Wagener, K. B. *Macromolecules* **2002**, *35*, 48-53.

145. Smith, J. A.; Ph.D. Dissertation, University of Florida, 2002

146. Hopkins, T. E.; Pawlow, J. H.; Deters, K. H.; Solivan, S. M.; Davis, J. A.; Koren, D. L.; Gomez, F. J.; Wagener, K. B. *Macromolecules* **2001**, *34*, 7920-7922.

147. Hopkins, T. E.; Wagener, K. B. *Macromolecules* **2004**, *37*, 1180-1189.

148. O'Donnell, P. M.;Wagener, K. B. *J. Polym. Sci. Pol. Chem.* **2003**, *41*, 2816-2827.

149. Bielawski, C.W.; Morita, T.; Grubbs, R.H. *Macromolecules* **2000**, *33*, 678-680.

150. Bielawski, C.W.; Louie, J.; Grubbs, R.H. *J. Am. Chem. Soc.* **2000**, *122*, 12872-12873.

151. Oakley, G.W.; Ph.D. Dissertation, University of Florida, 2004

152. Craig, S.W.; Manzer, J.A.; Coughlin, E.B. *Macromolecules.* **2001**, 34, 7929-7931.

153. Fürstner, A.; Thiel, O.R.; Lehmann, C.W. *Organometallics* **2002**, *21*, 331-335.

154. Haigh, D. M.; Kenwright, A. M.; Khosravi, E. *Macromolecules* **2005**, 38, 7571-7579.

155. Wagener, K.B; Brzezinska, K.; Anderson, J.D.; Younkin, T.R.; Steppe, K.; DeBoer, W. *Macromolecules* **1997**, *30*, 7363-7369.

156. Christ, M. L.; Sabo-Etienne, S.; Chaudret, B. *Organometallics* **1994**, *13*, 3800-3804.

157. Drouin, S.D.; Zamanian, F.; Fogg, D.E. *Organometallics* **2001**, *20*, 5495-5497.

158. Drouin, S. D.; Yap, G. P. A.; Fogg, D. E. *Inorg. Chem.* **2000**, *39*, 5412-5414.

159. Louie, J.; Bielawski, C.W.; Grubbs, R.H. *J. Am. Chem. Soc.* **2001**, *123*, 11312-11313.

160. For a review on non-metathetic behavior of Ru-carbene see: Alcaide, B.; Almendros, P. *Chem. Eur. J.* **2003** , *9*, 1258-1262.

161. Schmidt, B.; Pohler, M.; Costisella, B. *J. Org. Chem.* **2004**, *69*, 1421-1424.

162. Faulkner, J.; Edlin, C. D.; Fengas, D.; Preece, I.; Quayle, P.; Richards, S. N. *Tetrahedron Lett.* **2005**, *46*, 2381-2385.

163. Edlin, C. D.; Faulkner, J.; Fengas, D.; Knight, C. K.; Parker, J.; Preece, I.; Quayle, P.; Richards, S. N. *Synlett* **2005**, *4*, 572-577.

164. Hoye, T. R.; Zhao, H. *Org. Lett.* **1999**, *1*, 169-171.

165. Gurjar, M. K.; Yakambram, P. *Tetrahedron Lett.* **2001** , *42* , 3633-3636.

166. For a short review on isomerization behavior of ruthenium carbene: Schmidt, B. *Eur. J. Org. Chem.* **2004**, *9*, 1865-1880.

167. Miller, S. J.; Blackwell, H. E.; Grubbs, R.H. *J. Am. Chem. Soc.* **1996**, *118*, 9606-9614.

168. Maynard, H. D; Grubbs, R. H. *Tetrahedron Lett.* **1999** , *40* , 4137-4140.

169. Bourgeois, D.; Pancrazi, A.; Ricard, L; Prunet, J. *Angew. Chem.* **2000**, *112*, 742-744; *Angew. Chem. Int. Ed.* **2000** , *39* , 725-728.

170. Edwards, S. D.; Lewis, T.; Taylor, R. J. K. *Tetrahedron Lett.* **1999** , *40* , 4267-4270.

171. Schmidt, B.; Wildemann, H. *J. Org. Chem.* **2000** , *65* , 5817-5822.

172. Cadot, C; Dalko, P. I.; Cossy, J. *Tetrahedron Lett.* **2002**, *43*, 1839-1841.

173. Sutton, A. E.; Seigal, B. A.; Finnegan, D. F.; Snapper, M. L. *J. Am. Chem. Soc.* **2002**, *124*, 13390-13391.

174. Bourgeois, D.; Pancrazi, A.; Nolan, S. P.; Prunet, J. *J. Organomet. Chem.* **2002**, *643-644*, 247-252.

175. Sworen, J. C.; Pawlow, J. H.; Case, W.; Lever, J.; Wagener, K. B. *J. Mol. Cat.* **2002**, *194*, 69-78.

176. Lehman, S. E.; Schwendeman, J. E.; O'Donnell, P. M.; Wagener, K. B. *Inorg. Chim. Acta* **2002**, *345*, 190-198.

177. Petkovska, V.; Hopkins, T.H.; Powell, D.; Wagener, K.B. *Macromolecules* **2005**, *38*, 5878-5885.

178. Crabtree, R. H. *The Organometallic Chemistry of the Transition Metals*, 2nd ed. Wiley, New York, 1994.

179. For relevant reviews on the reactivity of ruthenium hydride complexes see: (a) T. Naota , H. Takaya , S. Murahashi , *Chem. Rev.* 1998 , **98** , 2599-2660.

180. (b) B. M. Trost , F. D. Toste , A. B. Pinkerton , *Chem. Rev.* 2001 , **101** , 2067-2096.

181. Kraus, J.O.; Nuyken, O.; Wusrt, K.; Buchmeiser, M.R. *Chem. Eur. J.* **2004**, *10*, 777-784.

182. For a review on C-H activation see: Shilov, A.E.; Shul'pin, G.B. *Chem. Rev.* **1997**, *97*, 2879-2932.

183. Jazzar, R. F. R.; Macgregor, S. A.; Mahon, M. F.; Richards, S. P.; Whittlesey, M. K. *J. Am. Chem. Soc.* **2002**, *124*, 4944-4945.

184. Oakley, G. W.; Lehman, S. E.; Smith, J. A.; Van Gerven, P.; Wagener, K. B. *Macromolecules* **2003**, *36*, 539-542.

185. Arisawa, M.; Terada, Y.; Nakagawa, M.; Nishida, A. *Angew. Chem., Int. Edit.* **2002**, *41*, 4732-4734.

186. For a review on Ru bearing bidentate carbenes: Hoveyda, A. H.; Gillingham, D. G.; Van Veldhuizen, J. J.; Kataoka, O.; Garber, S. B.; Kingsbury, J. S.; Harrity, J. P. A. *Org. Biomol. Chem.* **2004**, *2*, 8-23.

187. Blechert, S.; Wakamatsu, H. *Angew.Chem. Int. Edit.* **2002**, *41*, 794-796.

188. Blechert, S.; Wakamatsu, H. *Angew.Chem. Int. Edit.* **2002**, *41*, 2403-2405.

189. Connon, S. J.; Rivard, M.; Zaja, M.; Blechert, S. *Adv. Synth. Catal.* **2003**, *345*, 572-575.

190. Grela, K.; Kim, M. *Eur. J. Org. Chem.* **2003**, 963-966.

191. Audic, N.; Clavier, H.; Mauduit, M.; Guillemin, J-C. *J. Am. Chem. Soc.* **2003**, *125*, 9248-9249.

192. Courchay, F. C.; Sworen, J. C.; Wagener, K. B. *Macromolecules* **2003**, *36*, 8231-8239.

193. Wagener, K.B; Brzezinska, K.; Anderson, J.D.; Younkin, T.R.; Steppe, K.; DeBoer, W. *Macromolecules* **1997**, *30*, 7363-7369.

194. For studies on the dissociative mechanism of Hoveyda-type complexes see also: Love, J. A.; Sanford, M. S.; Day, M. W.; Grubbs, R. H. *J. Am. Chem. Soc.* **2003**, *125*, 10103-10109.

195. Grela, K.; Harutyunyan, S.; Michrowska, A. *Angew. Chem., Int. Edit.* **2002**, *41*, 4038-4040.

196. Van Veldhuizen, J. J.; Gillingham, D. G.; Garber, S. B.; Kataoka, O.; Hoveyda, A. H. *J. Am. Chem. Soc.* **2003**, *125*, 12502-12508.

197. Hansch, C.; Leo, A.; Taft, R. W. *Chem. Rev.* **1991**, *91*, 165-195.

198. Slugovc, C.; Burtscher, D.; Stelzer, F.; Mereiter, K. *Organometallics* **2005**, *24*, 2255-2258.

199. Hoye, T. R.; Zhao, H. *Org. Lett.* **1999**, *1*, 1123-1125.

200. Alcaide, B.; Almendros, P.; Alonso, J.M.; Aly, M.F. *Org. Lett.* **2001***, 3,*3781-3784.

201. Schmidt, B. *J. Org. Chem.* **2004**, *69*, 7672-7687.

202. Lehman, S.E; Ph.D. Dissertation, University of Florida, 2003.

203. Chatterjee, A. K.; Morgan, J.P.; Scholl, M.; Grubbs, R. H. *J. Am. Chem. Soc.* **2000**, *122*, 3783-3784.

204. Sanford, M. S.; Love, J. A.; Grubbs, R. H. *Organometallics* **2001**, *20*, 5314-5318.

205. McGrath, D. V.; Grubbs, R. H. *Organometallics* **1994**, *13*, 224-235.

206. Abdur-Rashid, K.; Fedorkiw, T.; Lough, A.J.; Morris, R.H. *Organometallics* **2004**, *23*, 86-94.

207. Burtling, S.; Mahon, M. F.; Paine, B. M.; Whittlesey, M. K.; Williams, J. M. J. *Organometallics* **2004**, *23*, 4537-4539.

208. Owen, M.A.; Pye, P.L.; Piggott, B.;Capparelli, M.V. *J. Organomet. Chem.* **1992**, *434*, 351-362.

209. Hitchcock, P.B.; Lappert, M.F.; Pye, P.L.; Thomas, S. *J. Chem. Soc., Dalton Trans.* **1979**, *88*, 1929-1942.

210. Hendrix, W. T.; Cowherd, F. G.; von Rosenberg, J. L. *Chem. Comm* **1968**, 97-99.

211. Bergens, S. H.; Bosnich, B. *J. Am. Chem. Soc.* **1991**, *113*, 958-967.

212. Baudry, D.; Ephritikhine, M.; Felkin, H. *J. C. S. Chem. Comm.* **1978**, 694-695.

213. Clark, H. C.; Kurosawa, H. *Inorg. Chem.* **1973**, *12*, 1566-1569.

214. Casey, C. P.; Cyr, C. R. *J. Am. Chem. Soc.* **1973**, *95*, 2248-2253.

215. Fogg, D.E.; Drouin, S.D.; Zamanian, F. US. Pat. Appl. 60/192394, priority date March 26, 2000.

216. Beatty, R.P.; Paciello, R.A. U.S. Patent 5,554,778, 1996.

217. Yi, C. S.; Lee, D. W. *Organometallics* **1999**, *18*, 5152-5156.

218. Yi, C. S.; Lee, D. W.; He, Z.; Rheingold, A. L.; Lam, K.-C.; Concolino, T. E. *Organometallics* **2000**, *19*, 2909-2915.

219. Lee, H. M.; Smith, D. C.; Zhengjie, H.; Stevens, E. D.; Yi, C. S.; Nolan, S. P. *Organometallics* **2001**, *20*, 794-797.

220. Dharmasena, U. L.; Foucault, H. M.; dos Santos, E. N.; Fogg, D. E.; Nolan, S. P. *Organometallics* **2005**, *24*, 1056-1058.

221. Esteruelas, M. A.; Werner, H. *J. Organomet. Chem.* **1986**, *303*, 221-231.

222. Werner, H.; Grunwald, C.; Stuer, W.; Wolf, J. *Organometallics* **2003**, *22*, 1558-1560.

223. Cramer, R. *J. Am. Chem. Soc.* **1966**, *88*, 2272-2282.

224. Krompiec, S.; Antoszczyszyn, M.; Urbala, M.; Bieg, T. *Pol. J. Chem.* **2000**, *74*, 737-741.

225. Giunta, D; Hölsher, M.; Lehmann, C. W.; Mynott, R.; Wirtz, C.; Leitner, W. *Adv. Synth. Catal.* **2003**, *345*, 1139-1145.

226. van Rensburg, W.J.; Steynberg, P.J.; Meyer, W.H.; Kirk, M.M.; Forman, G.S. *J. Am. Chem. Soc.* **2004**, *126*, 14332-14333.

227. Rankin, M.A.; McDonald, R.; Ferguson, M.J.; Stradiotto, M. *Angew. Chem. Int. Ed.* **2005**, *44*, 3603-3606.

228. Hansen, S.M.; Rominger, F.; Metz, M.; Hofmann, P. *Chem. Eur. J.* **1999**, *5*, 557-566.

229. Nishiyama, K.; Tanaka, N. *J. Chem. Soc., Chem. Comm.* **1983**, *22*, 1322-1323.

230. Fieser, L. F.; Fieser, M. *Reagents for Organic Synthesis*; Wiley; New York, 1967; Vol. 1, pp 581-585.

231. Fox, H.H.; Lee, J.-K.; Park, L.Y.; Schrock, R.R. *Organometallics* **1993**, *12*, 759-768.

232. Gallivan, J.P.; Jordan, J.P.; Grubbs, R.H. *Tetrahedron Lett.* **2005**, *46,* 2577-2580.

233. Saoud, M.; Romerosa, A.; Peruzzini, M. *Organometallics* **2000**, *19,* 4005-4007.

234. Robbins, J.; Bazan, G.C.; Murdzek, J.S.; O'Regan, M.B.; Schrock, R.R. *Organometallics* **1991**, *10*, 2902-2907.

235. Schrock, R. R.; Jamieson, J. Y.; Araujo, J. P.; Bonitatebus, Jr., P. J.; Sinha, A.; Lopez L. P. H. *J. Organomet. Chem.* **2003**, *684,* 56-67.

236. Gadwood, R.C.; Lett, R.M.; Wissinger, J.E. *J. Am. Chem. Soc.* **1986**, *108*, 6343-6363.

BIOGRAPHICAL SKETCH

Florence Catherine Courchay was born on May 26th 1978 in Nice, France. After receiving her baccalaureat in 1996, she spent 2 years in preparatory classes at the International Center of Valbonne (France), where she majored in mathematics, physics and chemistry. In September 1998, she entered ESCPE Lyon (National School of Chemistry and Electronics) and studied chemistry and chemical engineering for 2 years. During this time, she worked as an undergraduate research assistant in the Laboratory of Surface Organometallic Chemistry, on a supported chromium catalyst for ethylene polymerization under the supervision of Mrs. Anne Baudoin and Prof. Jean-Marie Basset.

Then, in July 2000 she relocated to Rheinmünster, in southwest Germany, to work for Dow Deutschland as an intern in the R&D department, Drytech division of superabsorbent polymers. There, she researched optimal conditions for the continuous process of superabsorbent polymer manufacture, under the supervision of Dr. Herbert Gartner. Finally in August 2001, she arrived at the University of Florida, to start graduate school in chemistry. She immediately joined the group of Prof. Ken Wagener, where her research project focused on the design of ruthenium carbene catalyst for acyclic diene metathesis (ADMET) polymerization. In May 2003, she defended her master's degree with ESCPE Lyon and obtained her "Engineer Diploma". She is currently finishing her Ph.D. studies and plans to return to Europe to work for industry, upon completion of her degree in December 2005.